2003

Identification and Characterization of the DNA Damage Response Function of Human Rif1 and a Search For Human Rap1 Interacting Factors

Joshua Silverman

Identification and characterization of the DNA damage response function of human Rif1 and a search for human Rap1 interacting factors

A thesis presented to the faculty of the Rockefeller University in partial fulfillment of the requirements for the degree of Doctor of Philosophy

By
Joshua Silverman

Advisor
Titia de Lange

October 2003
The Rockefeller University
New York, New York

Identification and characterization of the DNA damage response function of human Rif1 and a search for human Rap1 interacting factors

A thesis presented to the faculty of the Rockefeller University in partial fulfillment of the requirements for the degree of Doctor of Philosophy

By
Joshua Silverman

Advisor
Titia de Lange

October 2003
The Rockefeller University
New York, New York

In honor of my family and friends.

In loving memory of my grandfather, Abraham Simon.

Acknowledgements

This work could simply not be possible without the sage advice and steady guidance of Titia de Lange. Her passion for science and life, depth of knowledge and standard of excellence have made it an inspiration to work for her over the past several years. Starting out as a boss and advisor, she has become a mentor, colleague, role model, and friend. Titia defines what mentorship is all about.

I would like to thank all of the present and past members of the lab for their advice and support. A special thanks goes to Jeffrey Ye, my bench partner over the past several years, for discussion, advice and friendship. Diego Loayza spent at least an hour (often more) a day during my first year in the lab teaching me the basics of laboratory technique and experimental design. Thank you for your help. Hiro Takai has been immensely helpful with his background and interest in the DNA damage response field. Giulia Celli has been both a great friend and advisor over the years. It has been great to discuss science with Sara Buonomo, who has the wisdom to continue to study Rif1. Richard Wang, my partner-in-crime and fellow MD-PhD student in the lab, has been inspiring to work with. His scientific vision has inspired many innovative experiments and discussions with him always lead to new insights. I would also like to thank the cadre of other graduate students that I have worked with: Jill Donigian, Dirk Hockemeyer, Kristina Hoke, Agata Smogorzewska, and Megan van Overbeek. I would also like to thank the postdocs who I worked with: Jacqueline Jacobs, Jan Karlseder, Bibo Li, Susan Smith, and Xu-Dong Zhu.

I would like to thank the following individuals for their technical support: Stephanie Blackwood, Amy Himelblau, Sara Hooper, Vanessa Marrero, and Rita Rodney. I particularly thank Heidi Moss, my former bench partner, who managed to sing opera and conduct science in a manner of excellence.

I thank Stew Barnes. His assistance in all issues related to computers and administration has been critical to the completion of this thesis.

I would like to express my gratitude to members of the scientific community who have provided valuable advice and reagents. I especially thank John Petrini and members of the Petrini lab (Carrie, Dennis, Jan, and Travis) for advice, discussion and reagents. Additionally, I would like to thank Thanos Halazonetis who has provided copious amounts of 53BP1 monoclonal antibody. Additional thanks to David Cortez, Steven Elledge, Michael Kastan, and David Livingston for providing reagents and protocols.

A great thanks to my PhD Thesis Committee members Robert Darnell, Scott Keeney, and Michael Young, and Titia de Lange for their guidance, patience, service and flexibility over the years. A special thanks is extended to my outside committee member, Thanos Halazonetis, for serving on my thesis committee.

I must thank the faculty and staff of the Tri-Instituional MD-PhD program. In particular, I would like to single out Olaf Andersen and Tom Sakmar for their guidance and support. Both have provided assistance when I switched labs and in discussing career options. The Tri-Institutional MD-PhD program and Rockefeller University Dean's Office staff deserve my thanks and gratitude.

I thank the scientific mentors I have had before I joined Titia's laboratory who provided guidance and motivation when I at the onset of my scientific career. I thank Daniel Kahne, my undergraduate thesis advisor in the Department of Chemistry at Princeton University. I would also like to thank Sandy Simon, Howard Petrie ("Pete"), and Markus Stoffel whose labs I rotated through in the Tri-Institutional MD-PhD program.

This thesis would not be possible without the support of friends and family. I would like to begin by thanking my friends in New York City and elsewhere who make my life fun and exciting. I particularly like to thank Edward Yang, a fellow MD-PhD student and

former roommate, for his friendship and discussions about science and everything else. A special thanks to Melissa Nussbaum, who has been supportive during the bad times and understanding of the long hours spent in the lab. She has taught me a great deal about life that could not be learned at the bench. Finally, I thank my family. My parents, Marc, and Alison are supportive in good and bad times. My mother and grandmother are always my biggest fans. Thank you.

Table of Contents

Acknowledgements iv

Table of Contents vii

List of Figures viii

List of Abbreviations x

Abstract 1

Introduction 3

Chapter 1: Identification of human Rif1 51

- Introduction 52
- Results 57
- Discussion 82

Chapter 2: The role of human Rif1 in the DNA damage response 84

- Introduction 85
- Results 87
- Discussion 122

Chapter 3: Identification of novel Rap-1 interacting factors using yeast two-hybrid screening 124

- Introduction 125
- Results and discussion 127

Conclusions 144

Appendix: Investigating how the Mre11 complex interacts with the TRF2 complex 154

- Introduction 155
- Results and Discussion 156

Materials and Methods 170

References 187

List of Tables and Figures

Figure I-1	Mechanisms of cell cycle arrest in response to double-stranded breaks.	6
Figure I-2	Factors that bind to mammalian telomeres.	34
Figure I-3	Domain stucture and sequence alignments of human Rap1.	44
Figure 1-1	Evolution of the telomere complex.	56
Figure 1-2	Alignment of human Rif1 with mouse Rif1 and fugu Rif1.	58
Figure 1-3	Alignment of conserved regions I and II of Rif1 in human and *S. cerevisiae*.	60
Figure 1-4	Alignment of conserved region III of Rif1 in human and *S. cerevisiae*.	61
Figure 1-5	Antibodies generated against human Rif1.	63
Figure 1-6	Antibodies recognize human Rif1.	68
Figure 1-7	Human Rif1 is expressed ubiquitously.	69
Figure 1-8	Rif1 does not accumulate at telomeres.	72
Figure 1-9	Cell-cycle distribution of Rif1 dots.	73
Figure 1-10	Rif1 dots do not co-localize with Cajal bodies.	75
Figure 1-11	Localization of Rif1 to the mid-body and Golgi complex.	76
Figure 1-12	Co-immunoprecipitation of human Rif1 and known telomeric proteins.	79
Figure 1-13	Rif1 is found at APBs in ALT cells.	81
Table 1-1	Characteristics of antibodies against human Rif1	64
Figure 2-1	Human Rif1 forms foci in cells exposed to ionizing radiation.	88
Figure 2-2	Multiple Rif1 antibodies recognize Rif1 IRIF.	90
Figure 2-3	Rif1 IRIF do not co-localize with human telomeres.	92
Figure 2-4	Rif1 forms foci following exposure to clastogenic drugs and UV treatment.	94
Figure 2-5	Rif1 IRIF co-localize with other known DNA damage response proteins.	97
Figure 2-6	Rif1 localizes to dysfunctional telomeres.	101
Figure 2-7	The PIKK inhibitors caffeine and wortmannin inhibit Rif1 IRIF formation.	102
Figure 2-8	Absence of Rif1 foci in A-T cells.	104
Figure 2-9	Rif1 immunoblot following ionizing radiation.	106
Figure 2-10	ATRIP siRNA treatment does not inhibit UV-induced Rif1 foci.	107
Figure 2-11	Deficiency of Chk2, Nbs1, Mre11 or Nbs1 does not affect Rif1 IRIF.	108
Figure 2-12	Rif1 IR-induced foci are dependent on 53BP1.	109
Figure 2-13	Rif1 siRNA.	114
Figure 2-14	Metaphase spreads of cells treated with Rif1 siRNA.	116
Figure 2-15	ATM-dependent phosphorylation of targets and p53 IR response in cells treated with Rif1 siRNAs.	117
Figure 2-16	Cells deficient in Rif1 are radiosensitive.	119

Figure 3-1	Quantitative β-galactosidase results for yeast two-hybrid screen.	129
Figure 3-2	C144, a novel CCHC-type zinc finger protein.	131
Figure 3-3	The conservation of the CCHC zinc fingers of C144.	133
Figure 3-4	Protein expression of C144.	134
Figure 3-5	Co-immunoprecipitation of C144 and telomere proteins.	136
Figure 3-6	Alignment of C144 and yeast orthologs.	137
Figure 3-7	Telomere blot of *S. cerevisiae* C144 delete.	140
Figure 3-8	IF of FLASH and telomere proteins	142

Figure 4-1	Baculovirus-derived Mre11 and Mre11 complex.	157
Figure 4-2	Preparation of GST and GST-Rap1 proteins.	160
Figure 4-3	GST-hRap1 pulldown of the Mre11 complex, TRF1 and TRF2.	162
Figure 4-4	Gel shift analysis to determine if Mre11 complex can supershift a TRF2-DNA complex.	166
Figure 4-5	Gel shift analysis to determine if Mre11 complex can supershift a Rap1-TRF2-DNA complex.	168

List of Abbreviations

3-AT	3-aminotiazole
ALT	alternative lengthening of telomeres
APB	ALT-associated PML bodies
A-T	ataxia-telangiectasia
ATLD	ataxia-telangiectasia like disorder
ATM	ataxia-telangiectasia mutated
ATR	ATM- and rad3- related
ATRIP	ATR interacting protein
BASC	BRCA1 associated surveillance complex
BRCA1	breast cancer 1
BRCT	BRCA1 carboxy terminus domain
C144	candidate gene 144
ChIP	chromatin immunoprecipitation
DAPI	4,6-diamidino-2-phenylindole
DBD	DNA-binding domain
DKC	dyskeratosis congenita
DSB	double-strand break
EMSA	electromobility shift assay
EST	ever shorter telomeres or expressed sequence tag
FLASH	FLICE-associated huge protein
GCR	gross chromosomal rearrangement

GFP	green fluorescent protein
CKI	cyclin-dependent kinase inhibitor
HR	homologous recombination
HU	hydroxyurea
IF	immunofluorescence
IP	immunoprecipitation
IR	ionizing radiation
IVTT	in vitro transcription / translation
IRIF	ionizing radiation induced foci
MDC1	mediator of damage checkpoint 1
NBS	Nijmegen breakage syndrome
NHEJ	non-homologous end joining
NLS	nuclear localization sequence
ORF	open reading frame
PARP	poly(ADP-ribose) polymerase
PCNA	proliferating cell nuclear antigen
PIKK	PI3-related kinases
PML	promyelocytic leukemia
RAP1	repressor and activator protein 1
RDS	radioresistant DNA synthesis
RFC	replication factor C
RIF	Rap1-interacting factor
SCE	sister chromatid exchange

SIR	Silent information regulator
TERT	telomerase reverse transcriptase
TIF	telomere dysfunction-induced focus
TPE	telomere position effect
TR	telomerase RNA
TRF	TTAGGG repeat binding factor
TRFH	TRF homology domain
TRD	telomere rapid deletion
UV	ultraviolet

Abstract

Human Rif1, the ortholog of the yeast Rap1 interacting factor 1, a telomere length regulator was identified. Immunofluorescence did not reveal an association of human Rif1 with telomeres. Preliminary co-immunoprecipitation with known telomeric proteins and chromatin immunoprecipitation failed to show an interaction of human Rif1 with telomeric protein complexes or with telomeric DNA. Unexpectedly, Rif1 responded to ionizing radiation (IR), UV light, and clastogens, forming foci that co-localized with other DNA damage response factors such as 53BP1, ATM, BRCA1, Chk1, Nbs1, and Rad17. Furthermore, Rif1 localized to uncapped telomeres, as do other DNA damage response factors. Among DNA damage response proteins, Rif1 showed a unique dependence on the ATM kinase. Whereas inhibition of ATR signaling did not suppress the Rif1 response, ATM deficient cells treated with IR or UV lacked Rif1 foci even after prolonged incubation or high radiation dose. Therefore, IR-induced Rif1 foci constitute an assay for ATM status. The Rif1 response also depended on the presence of 53BP1 but was not affected by reduced function of BRCA1, Chk2, Nbs1, and Mre11. RNAi-mediated Rif1 inhibition resulted in increased radiosensitivity, indicating that Rif1 contributes to ATM-mediated protection against exposure to ionizing radiation.

In order to more fully understand telomere length regulation in mammalian cells and the evolutionary history of telomere-binding complexes, a search for novel hRap1-binding proteins and studies of the Rap1 telomere complex at human telomeres were performed. Both genetic and biochemical methods were used in order to better understand the role of the Rap1 complex, consisting of hRap1, TRF2, and the Mre11

complex, in human telomere biology. A yeast two-hybrid screen was carried out using hRap1 as a bait and two genes were identified. The first gene, called candidate 144 (C144), encodes a novel zinc-finger containing protein. Immunofluorescence and co-immunoprecipitation failed to reveal an association of C144 with telomeres. Deletion of the open-reading frame YDL175c in *S. cerevisiae*, the ortholog of C144, did not result in detectable changes in telomere length. The second gene, called FLASH, was previously identified to play a role as an adaptor in ligand-mediated apoptosis. In immunofluorescence experiments, FLASH did not co-localize with known telomeric proteins.

Introduction

Part 1: The DNA damage response

The viability of both cells and organisms depends on the transmission of genetic information in an accurate manner. In order to facilitate this process, cells must maintain genomic stability and prevent an excess of potentially harmful heritable mutations. Eukaryotes have evolved a variety of checkpoints in order to verify that a proper sequence of events occurs at each stage of the cell cycle prior to the next. Such events include replication of genomic DNA once and only once, proper chromsome attachment to the mitotic spindle, and the presence of necessary growth conditions in the environment. The classic definition of a checkpoint is a pathway where progress through the cell cycle can be stopped until conditions are suitable for the cell to proceed to the next stage (Hartwell and Weinert 1989).

Genomic DNA can be damaged by both endogenous and exogenous stimuli. Failure to properly repair this damage is catastrophic and can lead to genomic instability and cell death. A number of specialized checkpoint mechanisms, collectively referred to as the DNA damage response, have evolved to recognize DNA damage. The ability of mammalian cells to survive chromosomal damage depends on the coordinated activity of DNA response pathways that halt cell cycle progression and facilitate DNA repair prior to DNA replication or mitosis. The DNA damage response extends beyond the classical definition of the checkpoint pathway because the DNA damage response links cell cycle arrest mechanisms with diverse processes including the recruitment of protein complexes to sites of DNA damage, DNA repair, apoptosis and transcription (Zhou and Elledge 2000).

The DNA damage response is a complex and overlapping set of molecular pathways that detects damage and triggers cellular responses. The ability of cells to detect double-stranded breaks (DSBs) is exquisitely sensitive and rapid. Studies in which a single break is generated with the HO endonuclease in yeast indicate that one DSB is sufficient to generate a DNA damage response and cell death (Weiffenbach and Haber 1981). The detection of DNA damage then initiates the effector arms of the DNA damage response.

The execution phase of the DNA damage response involves the establishment and maintenance of cell cycle arrest, repair processes, and the decision to re-enter the cell cycle or undergo apoptosis. Following the recognition of DNA damage, eukaryotic cells will halt their cell cycle progression until the DNA damage is repaired. Cells are capable of undergoing arrest in S and M phases as well as at the G1/S and G2/M transitions of the cell cycle through a number of molecular pathways (Figure I-1). Cells also initiate repair processes to correct the specific DNA lesion detected (see below). If the DNA damage is repaired, then cells can re-enter the cell cycle and continue to grow. In certain cases, such as overwhelming quantities of DNA damage or inability to properly execute repair, the damaged cell will undergo apoptosis. The exact signals involved in cell-cycle re-entry and apoptosis are not currently known.

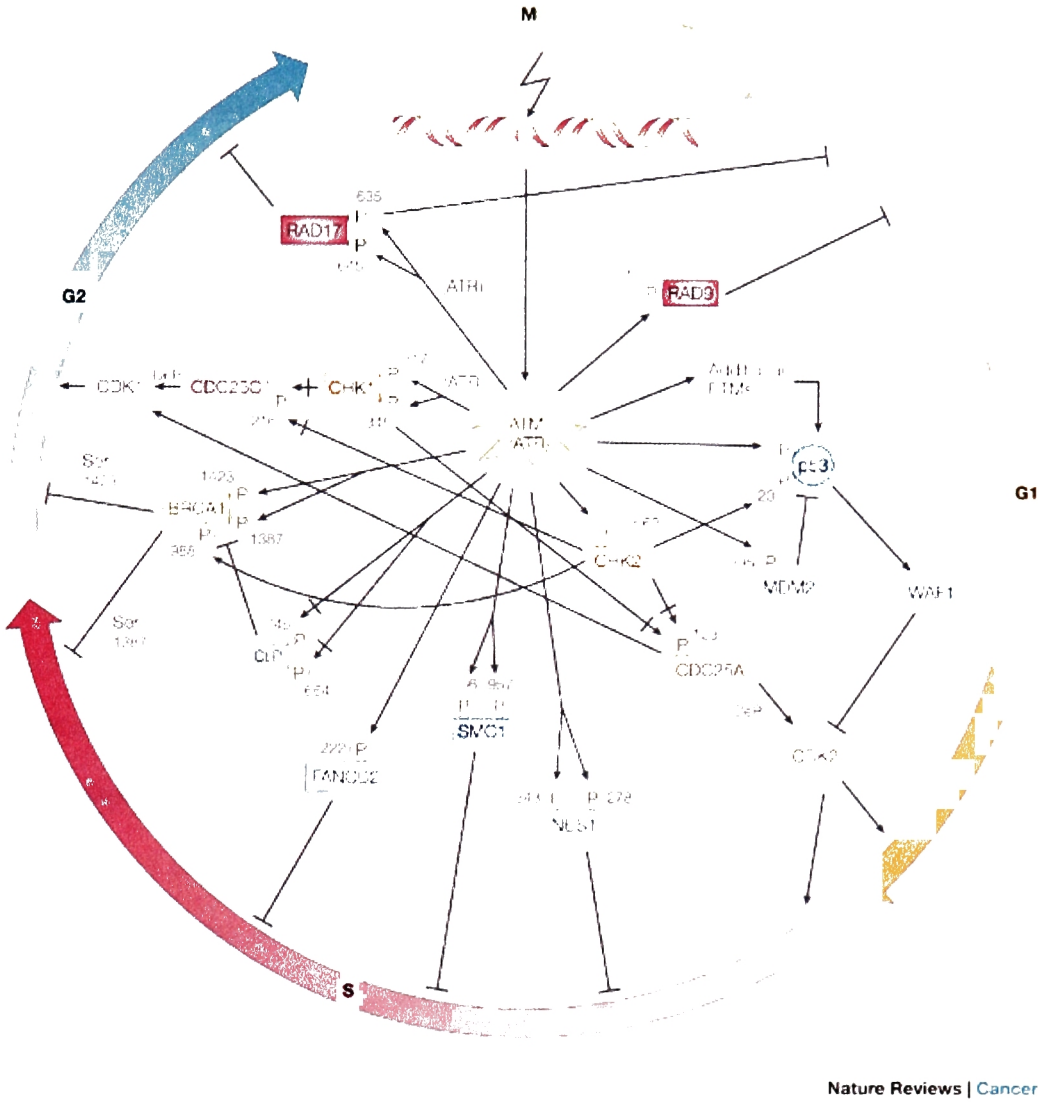

Figure I-1. Mechanisms of cell cycle arrest in response to double-stranded breaks. Many of the known factors involved in the DNA damage response are shown along with their ability to activate (arrows) or inhibit (t-shaped arrow) one another. Figure taken directly from Shiloh 2003.

The causes and types of DNA damage and repair

DNA can be damaged through a number of mechanisms that each leave signature alterations in DNA structure. DNA damage can arise from either endogenous or exogenous means. The three primary ways in which DNA damage occurs are the exposure of cells to exogenous radiation (including ultraviolet (UV) and ionizing radiation (IR)) or chemicals (including compounds found in cigarette smoke and cancer chemotherapy agents), the products of normal cellular metabolism (including reactive oxygen species and products of lipid peroxidation), and spontaneous chemical changes in DNA bases (including hydrolysis of nucleotide bases that result in abasic sites and spontaneous deamination) (reviewed in (Hoeijmakers 2001)). In addition to this list, normal replication can lead to stalled replication forks which can be processed into single-stranded and double-stranded DNA breaks. The inability of cells to properly repair damaged DNA leads to gross chromosome rearrangements (GCRs), a proposed source of genomic instability (Kolodner et al. 2002). Genes involved in the processes of maintaining S-phase checkpoints, recombinational repair and telomere maintenance act to suppress GCR in *S. cerevisiae* and these genes likely perform similar functions in mammalian cells (Myung et al. 2001; Kolodner et al. 2002).

Different DNA damage response pathways are capable of detecting and repairing the various types of DNA damage that occur. These pathways include the mismatch repair, base-excision repair, transcription-coupled repair, and the repair pathways for single- and double- stranded breaks. Cells can also replicate directly though certain types of DNA damage in an error-prone process termed damage tolerance (Friedberg 2003).

The Y-family DNA polymerases are capable of replicating damaged DNA (Goodman 2002). Double-stranded DNA breaks (DSBs) are particularly harmful to the cell because it is unable to properly progress through mitosis. When DSBs occur as a result of DNA damage, a rapid DNA damage response begins within minutes in order to facilitate repair and prevent either replication or mitosis, which would be fatal to the damaged cell (Khanna and Jackson 2001; van Gent et al. 2001; Jackson 2002).

In mammalian cells, DSBs are repaired with high fidelity by homologous recombination (HR) or they are processed through the error-prone non-homologous end-joining (NHEJ) pathway. It is unclear exactly how mammalian cells decide whether to repair DSBs via HR or NHEJ. Since HR is more accurate, it is assumed that this is the preferred mechanism of DSB repair. However, DSBs that occur in repetitive sequences should be repaired by NHEJ since HR may lead to inappropriate recombination with an incorrect locus (Lieber et al. 2003). In *S. cerevisiae*, DSBs are repaired primarily through HR (Haber 1995) and loss of NHEJ components do not lead to radiosensitivity in diploid strains. In vertebrate cells, HR seems to occur preferentially after replication when a sister is present, whereas NHEJ takes place in G1 (Takata et al. 1998). DSBs also occur under physiologic conditions including meiotic recombination, V(D)J recombination in the formation of the T cell receptor and immunoglobulin genes, and isotype class switching. Factors involved in NHEJ, including Ku70/Ku86, Artemis, DNA-PK_{cs}, XRCC4 and DNA ligase IV, and in HR, including the Mre11 complex, Rad51, Rad52, Rad54, Rad55, Rad57, BRCA1, and BRCA2, play a role in the processing of DNA breaks.

ATM and ATR: master regulators of the DNA damage response

Ataxia-telangiectasia mutated (ATM) and ATM- and rad3- related (ATR) play a central role in the response of mammalian cells to IR, UV and replication stress. ATM was identified in 1995 as the gene mutated in the disease ataxia-telangiectasia (A-T) (Savitsky et al. 1995). A-T is an autosomal recessive, pleiotropic genetic disorder characterized by cerebellar degeneration at an early age leading to progressive motor dysfunction, immunodeficiency, genomic instability, gonadal and thymic atrophy and cancer predisposition (reviewed in (Shiloh 1995; Lavin and Shiloh 1997; Crawford 1998; Becker-Catania and Gatti 2001)). The initial observation that A-T patients were particularly sensitive to the radiotherapy used to treat their lymphoreticular tumors suggested that A-T was a disorder involving an improper response to DNA damage (Gotoff et al. 1967; Morgan et al. 1968). At the cellular level, cells from A-T patients are hypersensitive to IR and other agents that cause DSBs (Agarwal et al. 1977). In response to IR, these cells have diminished ability to undergo G1 and G2 arrest and reduce their level of DNA synthesis (Painter and Young 1980; Kastan et al. 1992; Paules et al. 1995). The ATM cDNA was cloned by two groups and could complement many of the cellular defects of A-T cells (Zhang et al. 1997; Ziv et al. 1997). Heterozygous carriers of ATM mutations have an elevated risk of developing breast cancer (Swift et al. 1991; Athma et al. 1996; Inskip et al. 1999; Olsen et al. 2001). The effect of diminished ATM function on this finding was recently substantiated in a murine model that also is cancer-prone (Spring et al. 2002).

ATM and ATR contain a C-terminal domain similar to the protein PI3 kinase domain. Whereas PI3 kinase phosphorylates lipids, many other members of the PIKK family, including ATM, ATR, DNA-PK, ATX/SMG-1, mTOR/FRAP, and TRRAP, have protein targets. DNA-PK plays an accessory role in the NHEJ pathway. TOR proteins play a role in monitoring nutrient levels and TRRAP, which does not have a functional kinase domain, plays a role in histone acetylation (Grant et al. 1998; McMahon et al. 1998; Schmelzle and Hall 2000). Members of this family also contain a FAT domain adjacent to the kinase domain and the exact role of this domain is unclear. PIKK family members are large proteins with molecular weights ranging from 270 – 450 kilodaltons and the kinase domain and the FAT domain together make up only a small portion of the total protein. Members of the PIKK family have been shown to contain numerous HEAT repeat sequence motifs, which suggests an relationship between PIKKs that extends beyond the kinase domain (Perry and Kleckner 2003).

ATM and ATR play a central role in the DNA damage response by phosphorylating target proteins that act as mediators and effectors of the DNA damage response. ATM has a number of direct targets, including the Nbs1 component of the Mre11 complex, a proposed DNA damage sensor that is also involved in recombinational repair ((Gatei et al. 2000b; Lim et al. 2000; Zhao et al. 2000), reviewed in (Petrini and Stracker 2003)). Additional ATM targets include Chk1 and Chk2, Mdm2, p53 and 53BP1, BRCA1, Rad9, Rad17, Smc1, and H2AX (reviewed in (Kastan and Lim 2000; Shiloh 2003)). ATM and ATR, serine/threonine kinases that are often referred to as (S/T)-Q kinases because the glutamine residue is almost invariably found after either a serine or threonine residue in phosphorylation sites. A broader consensus sequence was

identified for ATM by changing the known target sequences and monitoring the effect in in vitro ATM kinase assays (Kim et al. 1999). A similar approach yielded an optimal target sequence of LSQE for ATM when a library of peptides was tested (O'Neill et al. 2000).

ATM and ATR phosphorylate overlapping targets. An example of the overlapping specificity of ATM and ATR is the phosphorylation of p53 on serine 15. Both ATM and ATR phosphorylate this site both in vitro and in vivo (Banin et al. 1998; Canman et al. 1998; Lakin et al. 1999; Tibbetts et al. 1999). The phosphorylation of BRCA1 on residues 1423 and 1524 is another example of a single target that can be modified by both ATM and ATR (Scully et al. 1997b; Cortez et al. 1999). Even though ATM and ATR have overlapping target specificities, the kinetics and extent to which they participate in the phosphorylation of a given target in response to different DNA damage stimuli often differs. For example, ATM phosphorylates p53 on serine 15 almost immediately after exposure of cells to IR, whereas ATR phosphorylation of p53 serine 15 occurs only at late stage following IR. Additionally, ATR phosphorylates p53 on serine 15 in a time-independent manner when cells are exposed to UV (Tibbetts et al. 1999).

One basic difference between ATM and ATR signaling is that ATM is more strongly activated by IR, whereas ATR is more strongly activated by UV and drugs that cause replication stress such as hydroxyurea (HU). This division is not strict. Targets of ATM are still phosphorylated in A-T cells in response to IR, albeit with slower kinetics and to a lesser extent. Furthermore, ectopic expression of ATR can complement the radioresistant DNA synthesis phenotype in A-T cells (Cliby et al. 1998).

The detection of double-stranded breaks

The actual detection of DSBs and other DNA lesions is the first step in the initiation of the DNA damage response. A longstanding question in the DNA damage field involves the mechanism(s) by which DSBs are detected. It is clear from immunofluorescence (IF) studies that DNA damage proteins associate with presumptive sites of DNA damage within minutes (and possibly shorter) after exposure of cells to IR. A variety of mechanisms have been proposed to explain the rapid and sensitive detection of DNA damage. It is currently unclear if a single proposed mechanism dominates or if multiple mechanisms act either simultaneously or in concert. Studies in bacteria and yeast indicate that lesions such as mismatched bases or abasic sites can be recognized by specific proteins. Thus, the most obvious mechanism of DSB detection involves one or more proteins that are able to detect DSBs. Two early candidates as the sensors of DSBs were poly(ADP-ribose) polymerase (PARP) and DNA-protein kinase (DNA-PK) because they could recognize abberant DNA structures in vitro. However, genetic evidence has failed to substantiate these claims and cells deficient in these proteins can still form ionizing radiation induced foci (IRIF) (Wang et al. 1995; Jimenez et al. 1999). Ionizing radiation induced foci represent the accumulation of DNA damage response factors on DNA lesion and these can be visualized with IF microscopy. Thus, these molecules are either not functioning as sensors or there is considerable redundancy in their function.

ATM and/or ATR have been proposed as direct sensors of DNA damage since ATM and ATR play a critical role in the cellular response to IR. The question of whether ATM and ATR can directly recognize DSBs and other abberant DNA structures in vitro

and in vivo is controversial. Following the generation of DSBs by IR or clastogens, inactive ATM kinase dimers are converted into active monomers through autophosphorylation on serine 1981 (Bakkenist and Kastan 2003). This phosphorylation event takes place at IR doses as low as 0.1 Gy and occurs almost immediately after DNA damage. The suggested stimulus for this mechanism of ATM activation is a gross change in chromatin based on the effects of chloroquine and altering salt conditions (Bakkenist and Kastan 2003). Although the exact mechanism of ATM activation has not been conclusively established, it is clear that the phosphorylation of ATM at serine 1981 is an early and critical event in the cellular response to IR. ATR requires a signaling partner, ATR-interacting protein (ATRIP), in order to respond to DNA damage (Cortez et al. 2001). ATRIP is phosphorylated by ATR and is required for the stability of ATR and ATR signaling following DNA damage.

Recent studies have provided significant insight into possible mechanisms by which ATM and ATR could be sensors of DNA damage. A heterotrimeric complex of Rad9, Rad 1, and Hus 1, often termed the 9-1-1 complex, may act as a sensor. ATM phosphorylates Rad9 on Serine 272 and Hus1 is also an ATM target (Chen et al. 2001; Foray et al. 2003). These proteins are thought to form a structure related to proliferating cell nuclear antigen (PCNA) (Thelen et al. 1999). Another DNA damage response, Rad17, is phosphorylated at multiple sites by ATM after IR exposure and is proposed to have structural homology with replication factor C (RFC) (Green et al. 2000). During DNA replication, the clamp loader, RFC, loads the heterotrimeric PCNA ring onto the product of primase and PCNA subsequently facilitates polymerase recruitment and replication. By analogy, Rad17 may act to recruit and load the 9-1-1 complex onto DSBs

and other DNA lesions (Bermudez et al. 2003). It is unclear whether Rad17 phosphorylation by ATM is required for this recruitment event. Alternatively, the 9-1-1 complex may act as a surveillance complex to constantly monitor the genome for DSBs based on its presumptive ability to slide along the DNA.

Finally, another important complex in the DNA damage response, the Mre11 complex, which consists of Mre11, Nbs1 and Rad50, acts as a sensor of DNA damage. The criteria for a DNA sensor are as follows: the sensor should physically associate with DNA after damage; the sensor should be associated with DNA damage in a manner independent of activating modifications such as ATM phosphorylation; mutations that affect the ability of the sensor to bind damaged DNA should correlate with failure to activate DNA damage cell cycle checkpoints; and it should be possible to identify mutations that result in a constituitively active damage signal or a sharply up-regulated signal. Thus far, the Mre11 complex fits all of these criteria (Petrini and Stracker 2003). RPA may also act as a sensor of DNA damage. Recent evidence suggests that RPA interacts with ATRIP and recruits the ATR-ATRIP complex to ssDNA after DNA damage (Zou and Elledge 2003). The binding of RPA to damaged DNA in yeast had previously been demonstrated (Carr 2003).

DNA damage induced cell cycle arrest

The ATM-dependent DNA damage response pathway can affect progression through the cell cycle before, during, and after DNA replication. ATR also plays a role in the ability of cells to halt cell cycle progression following DNA damage.

Cells with DNA damage undergo an arrest at the G1/S transition that presumably prevents the cell from replicating damaged DNA until the damage is properly repaired. The central player in G1/S arrest of cells after DNA damage is p53, a target of ATM (Canman et al. 1994; Siliciano et al. 1997; Banin et al. 1998; Canman et al. 1998; Khanna et al. 1998). p53 functions as a transcriptional activator of the cyclin-dependent kinase inhibitor (CKI), p21 (el-Deiry et al. 1993; Canman et al. 1994; Dulic et al. 1994; Deng et al. 1995). p21 directly inhibits the kinase activities of both cylinA-cdk2 and cyclinE-cdk2 complexes which facilitate the G1-S transition. ATM phosphorylates p53 on a number of residues and it was assumed that this modification is the molecular event that leads to p53 accumulation and, hence, p21 transcriptional activation. Initial attention went to p53 serine 15 modification because this residue is in the region of p53 that binds its inhibitor MDM2. The release of MDM2 from p53 as a result of serine 15 phosphorylation would lead to p53 accumulation. The actual situation, however, is more complicated. First, serine 15 modification does not affect the p53-MDM2 interaction (Dumaz and Meek 1999). Second, ATM also phosphorylates MDM2 on residue serine 395 and there is evidence to suggest that this event results in the disruption of the p53-MDM2 complex (Maya et al. 2001). Finally, another ATM target, Chk2, is itself a kinase and phosphorylates p53 on serine 20 (Chehab et al. 2000; Hirao et al. 2000; Shieh et al. 2000). Serine 20 phosphorylation interferes with the p53-MDM2 interaction. In addition to the various mechanisms by which p53 accumulates after DNA damage, G1 arrest to DNA damage is more complicated than p53 transcriptional activation of p21. More specifically, G1 arrest following DNA damage is at least a two-step process with an initial p53-independent process mediated by cyclin D1 proteolysis followed by a slower

arrest maintenance mediated by p53-dependent p21 transcription (Agami and Bernards 2000).

Cells also activate an intra S-phase checkpoint following DNA damage presumably in order to resolve stalled replication forks. A number of redundant molecular mechanisms underlie the intra S-phase checkpoint. The phenomenon of radioresistant DNA synthesis (RDS), which is the inappropriate replication of DNA following DNA damage, was first observed in A-T cells (Painter and Young 1980). ATM phosphorylates Chk2, which has a role in G1/S arrest but also plays a role in the intra S-phase checkpoint. ATM and Chk2 are responsible for the phosphorylation of Cdc25A, resulting in its degradation (Falck et al. 2001). The destruction of Cdc25A prevents the dephosphorylation of Cdk2 which leads to intra S-phase arrest. Cdk2 is necessary for DNA replication because it loads Cdc45, which recruits the MCM complex to cellular origins of replication (Walter and Newport 2000). The intra S-phase checkpoint is due in part to phosphorylation of Nbs1, Smc1, FANCD2, and BRCA1 by ATM (reviewed in (Shiloh 2003)). The phosphorylation of Nbs1 and Chk2 by ATM act as separate and parallel pathways in the intra S-phase checkpoint (Falck et al. 2002).

Finally, cells with DNA damage undergo an arrest at the G2/M transition, presumably to prevent the cells from undergoing mitosis and segregating defective or broken chromosomes. Similar to the other checkpoint responses to DNA damage, the G2/M arrest following damage results from an overlapping series of mechanisms. Both ATM and ATR play a role in the G2 arrest pathway through their phosphorylation of Chk1 and Chk2, respectively. Chk1 and Chk2 subsequently phosphorylate Cdc25C, which leads to the dephosphorylation of Cdk1 (reviewed in (Shiloh 2003)). It has been

proposed that phosphorylated Cdc25C binds 14-3-3 proteins which render Cdc25C inactive and unable to activate the mitotic cyclin B/Cdc2 kinase (Abraham 2001).

The DNA damage response signal transduction network

The DNA damage response is often described as a signal transduction network with one or more DNA damage signals detected by sensors which signal to effectors through a series of mediators and transducers. Signal amplification is a common property of transduction pathways. The phosphorylation cascade that results from ATM and ATR activation described above acts to modify and mobilize multiple cellular proteins in response to even a single DSB. Redundancy and cross-talk are two additional hallmarks of signal transduction which apply to the DNA damage response. The redundancy and cross-talk of ATM and ATR have been described above. Redundancy and cross-talk complicate the study of the DNA damage response just as they complicate the study of other signaling networks.

An appreciation of the complexities of the DNA damage response provides a more realistic picture of what occurs in the cell following DNA damage. First, there is not always a sharp distinction between DNA damage sensor, transducer and effector. As discussed above, many of the proposed sensors also serve as transducers and effectors in response to DNA damage. Also, many proteins play a number of distinct roles in the DNA damage response. Several DNA damage response factors such as 53BP1, BRCA1, and the Mre11 complex have multiple toles in the DNA damage response. Additionally, traditional notions of upstream and downstream signaling relationships are not always

instructive and may be difficult to dissect in the rapid DNA damage response. As discussed below, the Mre11 complex appears to function both upstream and downstream of ATM. Finally, the effector functions of the DNA damage response occur simultaneously and involve common players. It is likely that the cell monitors the consequences of both cell-cycle arrest and repair in order to determine whether damage can be resolved or apoptosis should be initiated.

The following sections will feature a description of a number of key players in the mammalian DNA damage response. Their roles in various aspects of the DNA damage response, such as checkpoint arrest, phosphorylation, and repair will be discussed.

53BP1

53BP1 was originally identified as a protein that interacts through a yeast two-hybrid screen with p53 and was subsequently shown to be a co-activator of p53-dependent transcription (Iwabuchi et al. 1994; Iwabuchi et al. 1998). 53BP1 contains BRCA1 carboxy terminal (BRCT) domains that are often found in DNA damage response factors and, as a result, the hypothesis arose that 53BP1 functions in the DNA damage response. Indeed, both human and Xenopus 53BP1 formed IRIF rapidly which co-localized with other known DNA damage response proteins (Schultz et al. 2000; Anderson et al. 2001; Rappold et al. 2001). Although the exact details differed slightly in the original publications, it appears that 53BP1 responds more strongly to IR than to UV or replication stress; that 53BP1 is phosphorylated in vitro and in vivo by ATM; and that,

although 53BP1 is capable of forming IRIF in A-T cells, the kinetics and extent of IRIF formation depend on ATM (Schultz et al. 2000; Anderson et al. 2001). Numerous studies have attempted to elucidate the specific function of 53BP1 in the DNA damage response. 53BP1 is found at the kinetochore during mitosis and it is suggested that this may play a role in the mitotic checkpoint (Jullien et al. 2002). An siRNA approach that lowered levels of 53BP1 revealed that 53BP1 plays a role in p53 accumulation, the G2/M checkpoint, and the intra-S-phase checkpoint in response to IR (Wang et al. 2002). 53BP1 forms foci in cancer cell lines expressing mutant p53, which suggests that the DNA damage respsonse may be constuitively activated in human tumors lacking p53 (DiTullio et al. 2002). The exact role of 53BP1 in DNA damage response signal transduction is still under investigation.

BRCA1

Breast cancer 1 (BRCA1) plays an assortment of roles in the DNA damage response. Germline mutations of BRCA1 lead to a hereditary breast and ovarian cancer syndrome (Miki et al. 1994). BRCA1 is a large molecular weight protein that contains an N-terminal RING domain and two C-terminal BRCT domains (Wu et al. 1996; Bork et al. 1997; Callebaut and Mornon 1997). A large number of proteins with BRCT domains play a role in the DNA damage response and several factors, including TopBP1, MDC1 and 53BP1, have been identified as DNA damage response proteins because of the presence of one or more BRCT domains (Makiniemi et al. 2001; Yamane et al. 2002; Goldberg et al. 2003; Lou et al. 2003a; Lou et al. 2003b; Stewart et al. 2003; Xu and

Stern 2003). BRCA1 has many characterized cellular functions and it is difficult to identify which functions are critical for the DNA damage response. Early studies reveal that BRCA1 can function as a transcription factor with association to RNA pol II via RNA helicase A and that it can function in a complex with histone deacetylase activity (Scully et al. 1997a; Anderson et al. 1998; Yarden and Brody 1999). BRCA1 has a large number of proposed interacting partners, including BARD1 and CtIP. BRCA1 was shown to interact with the Mre11 complex and biochemical purification revealed a large molecular complex termed the BRCA1 genome surveillance complex (BASC) which contains a variety of DNA damage components (Zhong et al. 1999; Wang et al. 2000).

A large body of experimental evidence suggests that BRCA1 plays a role in the cellular response to DNA damage. BRCA1 forms nuclear foci during S phase and when exposed to DNA damaging stimuli such as UV, IR or mitomycin C (Scully et al. 1997b). A cell line termed HCC1937, deficient in BRCA1, was shown to be hypersensitive to IR (Scully et al. 1999). BRCA1 is a target of ATM and co-immunoprecipitates with ATM (Cortez et al. 1999). BRCA1 is directly phosphorylated by ATM on a number of residues, including serine residues 1387, 1423, 1457 and 1524 as shown by phospho-specific antibodies (Gatei et al. 2000a; Gatei et al. 2001). The ATM-dependent BRCA1 phosphorylation on serine 1387 is necessary for the ATM-mediated intra-S-phase checkpoint (Xu et al. 2002b). ATR can also phosphorylate BRCA1 (Tibbetts et al. 2000). BRCA1 is required for a subset of ATM- and ATR- dependent responses to DNA damage (Foray et al. 2003). Chk2 phosphorylates BRCA1 at serine 988 and this event is important for rescue of cell survival after damage in HCC1937 cells (Lee et al. 2000).

The exact mechanism by which BRCA1 deficiency leads to tissue-specific tumorigenesis is currently unknown. One possibility is the concept of redundancy in which tissues other than the breast and ovary are able to properly execute BRCA1's functions in its absence. Conversely, it has been suggested that only breast and ovary provide a suitable environment for cells that have lost BRCA1 to survive. This idea is termed the BRCA1 suppressor hypothesis (Elledge and Amon 2002). The finding that BRCA1 co-localizes with the inactive X chromosome in females provides another possible mechanism underlying tissue-specific tumorigenesis upon loss of BRCA1 (Ganesan et al. 2002). The authors propose that perturbations of the behavior of the inactive X resulting from BRCA1 loss may contriute to tumorigenesis in the breast and ovary.

The Mre11 complex

The Mre11 complex is a large molecular-weight complex consisting of Mre11, Nbs1 (originally termed p95), and Rad50 that plays a role in the DNA damage response as well as a diverse array of other biological activities. Mre11 complex components are evolutionarily related to the SbcCD proteins found in bacteriophage T4, bacteria, yeast, Drosophila, and vertebrates (Sharples and Leach 1995). The Mre11 complex has a structure resembling SMC proteins and have a 3' → 5' nuclease activity in vitro (Sharples and Leach 1995; Connelly et al. 1999). The Mre11 complex in yeast, consisting of Mre11, the Nbs1 ortholog Xrs2, and Rad50 has been extensively characterized. It is known to play a critical role in the following three biological

processes: the creation of meiotic DSBs through the removal of Spo11, homologous recombination, and the DNA damage response (reviewed in (Haber 1998; Petrini and Stracker 2003)). The identification of a human ortholog of Mre11 began the study of the human Mre11 complex and human orthologs of Rad50 and Nbs1 were subsequently identified (Petrini et al. 1995; Dolganov et al. 1996; Carney et al. 1998). The Mre11 complex is essential in chicken and mouse cells, but it is unclear which function is responsible for this property.

The known biochemical functions and interaction partners of the Mre11 complex may contribute to its biological function(s). Nbs1 has a 3' to 5' exonuclease activity in vitro (Trujillo et al. 1998). It has been suggested that this nuclease activity may work on DSBs and facilitate repair (Paull and Gellert 1998), although the exact mechanism is unknown. The Mre11 complex has a helicase activity as well which is potentiated by Nbs1 (Paull and Gellert 1999). A proposed zinc hook structure for Rad50 suggests that it might bridge multiple DNA molecules together and this may enable the Mre11 complex to properly carry out its roles in DSB repair and recombination (Hopfner et al. 2002). The Mre11 complex has been shown to co-immunoprecipitate with mediator of DNA damage checkpoint 1 (MDC1), an important DNA damage response factor (Stewart et al. 2003). Mre11 complex has also been found at human telomeres as part of the TRF2 complex (Zhu et al. 2000).

The components of the Mre11 complex play an important role in the reponse to DNA damage. Mre11 complex components were among the first proteins shown to form IRIF in response to DSBs (Maser et al. 1997). A special overlay technique using a layered grid placed over cells exposed to soft x-rays provides evidence that these IRIF

correspond to sites of DSBs (Nelms et al. 1998). Mre11 complex components were originally predicted targets of ATM phosphorylation (Kim et al. 1999). It was then subsequently shown that Mre11 and Nbs1 are targets of ATM. Nbs1 is necessary for Mre11 phosphorylation after damage (Dong et al. 1999). ATM phosphorylates Nbs1 and loss of this site leads to a defect in the intra-S-phase checkpoint (Gatei et al. 2000b; Lim et al. 2000; Zhao et al. 2000). The Mre11 complex also plays a role in the G2/M checkpoint following IR (Xu et al. 2002a). Nbs1 is required for Chk1 phosphorylation after IR (Gatei et al. 2003). Interestingly, ATM does not seem to be required to the localization of Mre11 to sites of DSBs (Mirzoeva and Petrini 2001). The Mre11 complex can still localize to dysfunctional telomeres in cells treated with caffeine, which inhibits both ATM and ATR (Takai et al. 2003), further indicating a role in the sensing of DNA damage. This requirement of the Mre11 complex for Atm function has been demonstrated by others (Carson et al. 2003; Uziel et al. 2003).

Deficiencies in the components of the Mre11 complex lead to human chromosome instability syndromes. Nbs1 is mutated in patients with Nijmegen breakage syndrome (NBS) (Varon et al. 1998). This rare, autosomal recessive genetic disease results in microencephaly, growth defects, immunodeficiency, and an increased risk of cancer. NBS has been classified as a disorder related to A-T based on the properties of cells from NBS patients and it is interesting that both Nbs1 and ATM play a role in the DNA damage response. The discovery that Mre11 is mutated in patients with an ataxia-telangiectasia-like disorder (ATLD) suggests an even closer link between the Mre11 complex and ATM (Stewart et al. 1999). ATLD is a disorder in which patients have a clinical syndrome resembling A-T, but have wild type ATM. Although Rad50 has not

currently been associated with a chromosome instability disorder, the growth defects and cancer predisposition of knockin mice expressing the Rad50S allele of Rad50 suggest that mutations in Rad50 could lead to human disease (Bender et al. 2002).

γ-H2AX

H2AX has been proposed to play an important role in the mammalian DNA damage response. Each nucleosome contains eight proteins with two proteins each from the families H2A, H2B, H3, and H4. H2AX is one of the H2A subfamilies (H2A1-H2A2 and H2AZ are the others) and H2AX represents 2 - 25% of cellular H2A in mammalian cells and virtually all of the H2A in yeast. The difference between H2AX and the other family members is a motif that contains residue serine 139, which is phosphorylated by ATM in response to IR (Rogakou et al. 1998; Burma et al. 2001). This response occurs within one minute of damage and it maximal after ten minutes post-IR. Calculations indicate that approximately 2 x 10^3 kilobases of DNA contain phosphorylated H2AX per DSB and points to models where large chromatin domains are formed at sites of DSBs (Rogakou et al. 1998; Rogakou et al. 1999).

The ATM pathway and DSB repair

A-T cells have a diminished ability to survive ionizing radiation (IR) and other genotoxic treatments that create double-strand breaks ((Taylor et al. 1975); reviewed in (Shiloh 2003)). This phenotype could be due to either checkpoint deficiency or

inadequate DNA repair or both. A-T patients are proficient in NHEJ as evidenced by their normal V(D)J recombination (Hsieh et al. 1993). However, A-T patients show aberrant interlocus recombination events in the T-cell receptor locus (Aurias et al. 1980; Lipkowitz et al. 1990), potentially leading to translocations that promote lymphomagenesis. A defect in the regulation of DNA repair pathways is also suggested by the fact that A-T cells show an error-prone hyperrecombination phenotype, have increased rates of chromosome mis-rejoining after damage, and have a high rate of spontaneous telomere fusions ((Luo et al. 1996), reviewed in (Kojis et al. 1991)). Furthermore, A-T cells have increased rates of intrachromosomal recombination (Meyn 1993) and several ATM targets have been implicated in homologous recombination (HR) (e.g. BRCA1, FANCD2, and the Mre11 complex (reviewed in (Petrini 2000; Jasin 2002; Moynahan 2002; D'Andrea and Grompe 2003)). However, in other settings, ATM deficient cells show impaired HR (Takao et al. 1999; Morrison et al. 2000) or have normal rates of sister chromatid exchanges (SCEs) (Galloway and Evans 1975; Galloway 1977), which are thought to be generated by HR (Sonoda et al. 1999). Thus, the exact role of ATM signaling in the regulation of NHEJ and HR is still poorly defined.

Part II: Rif1 and telomere biology

Telomeres: Discovery and Basic Structure

Telomeres are functional elements at the physical ends of eukaryotic chromosomes. Early observations hinted that telomeres play an important role in chromosomal stability and maintenance. In the late 1930's, H.J. Müller observed that terminal deletions and inversions were not recovered in the offspring of X-ray irradiated Drosophila males (Muller 1938). At about the same time, McClintock examined broken chromosomes in maize. She noticed the resulting formation of dicentric chromosomes and the subsequent loss breakage of these fused chromatids during cell division (McClintock 1941). McClintock suggested that telomeres act to prevent fusion and breakage events in intact, linear chromosomes. Taken together, these experiments laid the foundation for the protective role of telomeres in eukaryotic cells. It is now clear that telomeres serve to protect the ends of linear chromosomes from being recognized as DNA damage.

Telomeres consist of tandem, repetitive, G+C-rich sequences. The G-rich strand runs 5' – 3' towards the end of the chromosome. The actual telomeric repeat sequence varies between species and these repeats can be either homogeneous or heterogeneous. Telomere length ranges from 30 bp in *Euplotes* and *Oxytricha* to 250 – 400 bp in *Saccharomyces cerevisiae* to 2 – 30 kb in humans. Murine chromosomes contain even longer telomeres, but have the same TTAGGG double-stranded telomeric repeat as human chromosomes. Typically, telomeres also have a 3' overhang of the G-rich

telomeric strand, which is approximately 150 nucleotides at human chromosome ends. Telomeric repeats are occasionally found at interstitial sites in eukaryotic genomes where they may represent the remnants of ancestral chromosomal fusion events.

An early dilemma in the telomere field arose from the characterization of the strategy of DNA replication. The so-called "end-replication problem" results from the inadequacy of the replication machinery to complete lagging strand synthesis due to a requirement for an RNA primer (Watson 1972; Olovnikov 1973). This inability of the replication machinery to copy the ends of linear chromosomes results in a loss of sequence at the telomere in the absense of mechanisms to synthesize additional telomeric repeats (Levis 1989; Lundblad and Szostak 1989; Johnson et al. 2001). The loss of telomeric repeats ultimately leads to a critically short telomere that is unable to protect the end from DNA damage and other signaling pathways, which results in senescence or apoptosis (as discussed below).

One solution to this problem came with the discovery of telomerase. Blackburn and Greider identified a telomere synthesizing activity, now known as telomerase (Greider and Blackburn 1985). Telomerase is a ribonucleoprotein that uses its essential RNA component, called the telomerase RNA component (TERC, TR or TER), as a template for the synthesis of tandem repeats on the G-rich strand (Greider and Blackburn 1989; Shippen-Lentz and Blackburn 1990; Singer and Gottschling 1994; Feng et al. 1995). The protein component of core telomerase, called telomerase reverse transcriptase (TERT), uses the TERC template to synthesize additional telomeric repeats (Lingner et al. 1997; Meyerson et al. 1997; Nakamura et al. 1997). Telomerase provides a solution to the end-replication problem by adding additional telomeric sequences.

Although most unicellular organisms have constitutive telomerase activity, telomerase is tightly regulated in human cells. Human somatic cells have suppressed telomerase activity, whereas ovaries, testis, and various proliferating cell populations such as stem cells have telomerase activity (Kim et al. 1994; Meyerson et al. 1997; Nakamura et al. 1997). The protein component, TERT, rather than the RNA component, TERC, is the limiting component responsible for the suppression of telomerase in somatic cells (Feng et al. 1995). The transcriptional suppression of the protein component of telomerase occurs through a number of individual pathways, including Menin, the Mad/Myc pathway and the TGFβ target Sip1 (Lin and Elledge 2003). This ensures that the loss of any one pathway will not result in spurious telomerase activity. The exact regulation of telomerase in terms of the timing of telomere repeat addition is still being investigated. It is thought that telomere addition takes place during S phase. The observation that Est2p, the telomerase protein component in *S. cerevisiae*, is found in telomeric chromatin during S phase is consistent with S phase telomere repeat addition (Taggart et al. 2002). However, telomerase is competent to extend telomere-like substrates in mitosis (Diede and Gottschling 1999; Taggart et al. 2002). Est2p is also at telomeres in G1 (Taggart et al. 2002).

Exogenous expression of hTERT in primary human fibroblasts is sufficient to reconstitute telomerase activity and counter-act telomere erosion. The resulting telomere maintenance immortalizes most human cells types (Bodnar et al. 1998; Vaziri and Benchimol 1998; Ramirez et al. 2001). Like primary cells, tumor cells require a telomere maintenance system for long-term proliferation and in the majority of cases this is provided by upregulation of hTERT (reviewed in (Cong et al. 2002)). Other tumor cells

maintain their telomeres through telomerase-independent pathways. This mechanism is known as alternative lengthening of telomeres (ALT), although it is unclear whether there are one or more such pathways (discussed below). Telomerase activity per se does not induce transformation (Morales et al. 1999) and although telomerase is necessary for immortalization, hTERT is not an oncogene (Hahn et al. 1999; Hahn et al. 2002). Additionally, oncogenic transformation per se does not require telomerase activity and cells with very long telomeres can be fully transformed into a tumorigenic phenotype in vitro without a telomerase maintenance system (Seger et al. 2002). Similarly, certain childhood tumors that originate in young cells with long telomeres can be cancerous and metastatic even though they lack telomerase (Hiyama et al. 1995). However, the extensive proliferation of cells during the prolonged multi-step tumorigenesis pathways that leads to most adult human cancers is predicted to exhaust the telomere reserve, necessitating telomerase activation (Hiyama et al. 1995). Thus, telomere maintenance, particularly through telomerase activity, plays a critical role in facilitating tumorigenesis.

Telomerase and telomerase-binding factors

The telomerase RNA and reverse transciptase component of telomerase that together form the core telomerase enzyme required for catalysis in vitro are not the only components of the telomerase holoenzyme. In addition to core TLC1 and Est2p in *S. cerevisiae*, Est1p and Est3p are also part of the telomerase holoenzyme and both est1 and est3 strains display the progressive telomere shortening phenotype, known as ever shorter telomeres (est) (Lundblad and Szostak 1989; Lendvay et al. 1996; Hughes et al. 2000).

Additionally, TLC1 is also associated with Sm proteins in *S. cerevisiae* (Seto et al. 1999). The human telomerase holoenzyme also contains components other than the core RNA and reverse transcriptase. Two orthologs of EST1, EST1A and EST1B, have been identified and shown to be found in the telomerase holoenzyme (Reichenbach et al. 2003; Snow et al. 2003). Orthologs of Est3p in humans have not been identified and there is no data that Sm proteins bind TERC in humans.

Another component of the human telomerase holoenzyme is the protein dyskerin (Mitchell et al. 1999b). TERC contains an H/ACA motif which dyskerin is able to bind (Mitchell et al. 1999a). The X-linked form of dyskeratosis congenital, DKC, which includes abnormal skin pigmentation, nail dystrophy and mucosal leukoplakia, is due to a mutation in dyskerin while the autosomal dominant form is due to mutations in the hTERC gene (Mitchell et al. 1999b).

Telomerase-independent telomere maintenance pathways

Telomere length can be maintained through mechanisms that do not depend on telomerase. One type of telomerase-independent telomere maintenance pathway involves recombination. The majority of est1 *S. cerevisiae* cells die in culture, but a minor population of cells manages to survive (Lundblad and Blackburn 1993). The ability of est1 survivors to appear was critically dependent on RAD52 function, which implied a recombination-based mechanism to the *S. cerevisiae* survivor pathway (Lundblad and Blackburn 1993). It was subsequently shown that two types of survivors formed, termed type I and type II survivors, and that these survivors were dependent on RAD51 and

RAD52, respectively (Teng and Zakian 1999). Type I survivors are characterized by extensive amplification and dispersal of sub-telomeric Y' elements to most telomeres and type II survivors are characterized by a long telomeric tract (Teng and Zakian 1999). In competition experiments, telomerase-positive wild type cells outgrow telomerase-deficient survivors (Morris and Lundblad 1997).

Although the majority of immortalized and cancer cells in humans use up-regulation of telomerase for telomere maintenance (Shay 1997), a subset of immortalized cells lack detectable telomerase activity (Bryan et al. 1995; Bryan et al. 1997a; Bryan et al. 1997b; Bryan and Reddel 1997). These cells seem to maintain their telomeres through one or more recombination-mediated mechanisms similar to the survivor pathway in *S. cerevisiae*. ALT cells have long, heterogeneous telomeres and contain ALT-associated PML bodies (APBs) (Henson et al. 2002). APBs contain RAD51, RAD52, telomeric DNA and known telomere binding proteins (Yeager et al. 1999). The role of APBs in the ALT remains unclear.

Additional telomerase-independent mechanisms of telomere maintenance are present in certain circumstances. In the absence of telomerase, *S. pombe* is able to survive with three circularized chromosomes (Naito et al. 1998). This pathway is presumably not available to either *S. cerevisiae* or mammalian cells because of their higher number of chromosomes. Another mechanism of telomerase-independent telomere maintenance is the transposon-mediated telomere maintenance that occurs normally in Drosophila (Danilevskaya et al. 1994; Cenci et al. 1997; Danilevskaya et al. 1998).

The discovery of cis-acting telomere-binding factors

Studies of telomerase confirmed the idea that eukaryotic cells have proteins that bind specifically to telomeric DNA. Yu *et al.* mutated the RNA component of *Tetrahymena* telomerase *in vivo* and noticed a deprotected telomere phenotype due to the change in the sequence of the telomeric DNA, consistent with the requirement for a sequence specific telomere binding protein (Yu et al. 1990). A similar phenomenon was observed in the budding yeast *Kluyveromyces lactis* (McEachern and Blackburn 1995). A number of groups identified sequence-specific telomeric DNA binding proteins, including the α/β telomere binding proteins in *Oxytricha*, Rap1 in the budding yeasts *S. cerevisiae* and *K. lactis*, Taz1 in *S. pombe* (Berman et al. 1986; Price and Cech 1987; Larson et al. 1994; Cooper et al. 1997). The de Lange lab first discovered TRF1 (TTAGGG repeat binding factor 1) and TRF2, the telomeric DNA binding proteins in vertebrates (Chong et al. 1995; Broccoli et al. 1997b).

The discovery of TRF1 and TRF2 led to insights into how telomere length is maintained within given limits in telomerase positive cells (telomere length regulation) as well as how human chromosome ends are protected. TRF2 plays a critical role in the prevention of telomeric ends from being recognized by cells as double-stranded breaks. Expression of a dominant negative allele of TRF2 in cells leads to the loss of telomeric 3' overhangs, chromosome fusion, cell cycle arrest, p53/ATM-dependent apoptosis, or a senescence-like state (van Steensel et al. 1998; Karlseder et al. 1999). Thus, the TRFs seem to be essential for this important function of telomeres. The over-expresssion of TRF1 and TRF2 using the tetracycline-inducible system resulted in gradual telomeric

shortening (van Steensel and de Lange 1997; Smogorzewska et al. 2000). Expression of a dominant negative TRF1 allele results in telomere elongation. This allele does not affect the activity of telomerase in cell extracts, which suggests that TRF1 regulates telomere length in *cis*. A number of other factors have been identified as proteins that associated with telomeres (Figure I-2). The protein protector of telomeres 1 (POT1) was identified in human cells and initially shown to protect telomeric ends (Baumann and Cech 2001). POT1, which binds to single-stranded telomeric DNA, plays a role in telomere length regulation by acting as a telomerase-dependent positive regulator of telomere length (Loayza and De Lange 2003). Since POT1 binding can be affected by the TRF1 complex, POT1 may act as a transducer of TRF1 signalling to control telomere length (Loayza and De Lange 2003).

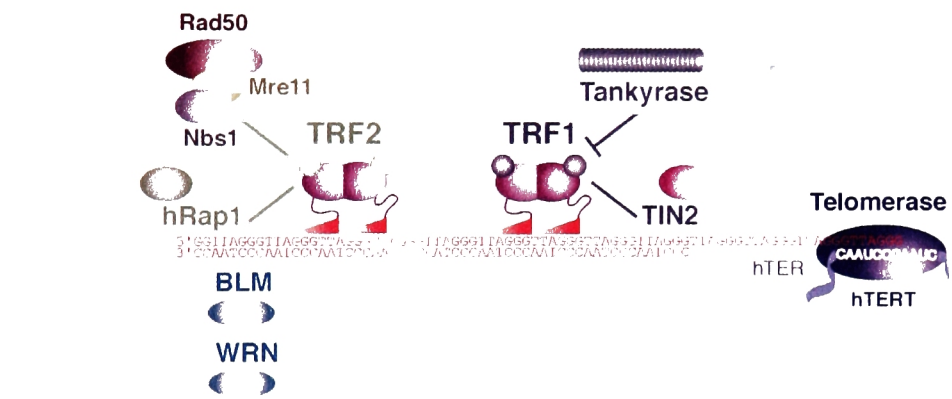

Figure I-2. Factors that bind to mammalian telomeres.

The following factors have been described as being found at telomeres in mammalian cells. This figure does not show POT1, which can bind to both the TRF1 complex and to the 3' G-rich overhang. Figure courtesy of Titia de Lange (de Lange 2003).

T-loops

Mammalian telomeres form structures termed t-loops that result from strand invasion of the 3' overhang into the telomeric duplex DNA (Griffith et al. 1999). A similar structure exists in the ciliate *Oxytricha*, in the typanosome *T. brucei*, and in the plant *A, thaliana* (Murti and Prescott 1999; Munoz-Jordan et al. 2001). Incubation of a telomeric model containing 3 kb of non-telomeric DNA followed by 0.5 kb of telomeric DNA with baculovirus-derived human TRF2 increases the rate of formation of t-loops (Griffith et al. 1999). T-loops are observed in isolated psoralen-crosslinked telomeric DNA (Griffith et al. 1999). A preliminary model predicts that TRF1 and TRF2 aid in the formation of t-loops *in vivo*. TRF1, because of its spatial and orientational flexibility in binding telomeric DNA, brings together regions of the duplex DNA array and TRF2 facilitates the invasion of the G-rich 3' overhang (Bianchi et al. 1999; Griffith et al. 1999).

The telomeric complex in *Saccharomyces cerevisiae*: Rap1 and its binding factors

Rap1p is the predominant telomeric binding protein in *S. cerevisiae*. Berman *et al.* first identified the presence of a yeast protein that could bind telomeric repeats (Berman et al. 1986). This factor turns out to be Rap1 (Repressor and Activator Protein 1) (Longtine et al. 1989). Different labs independently identified factors identical to Rap1 known as TBA, GRF1 or TUF1 that bound a number of DNA sequences and play a role in silencing at the mating-type loci, transcriptional activation of ribosomal protein

genes, and transcriptional regulation of other genes (Shore and Nasmyth 1987; Vignais et al. 1987; Buchman et al. 1988; Chambers et al. 1989). Rap1 is an essential gene in yeast that encodes an abundant 120 kD nuclear protein that is similar to the mammalian transcription/replication factor NF1 and the yeast ARS-binding protein ABF1 (Shore and Nasmyth 1987; Buchman et al. 1988; Santoro et al. 1988; Diffley and Stillman 1989)). The consensus binding site for Rap1 is 5'-AAYCCRYNCAYY-3' which occurs approximately every 18 bp within yeast telomeric DNA allowing approximately twenty copies of Rap1 to associate with each chromosome (Gilson et al. 1993).

Rap1 plays a significant role in yeast telomeric function. Rap1 is found in telomeric chromatin and is located at telomeres by indirect immunofluorescence (Conrad et al. 1990; Klein et al. 1992). Telomere shortening occurs when yeast cells with temperature-sensitive Rap1 mutations are grown at semipermissive temperature (Lustig et al. 1990). These mutations are recessive with respect to the wild type allele. Overexpression of full-length Rap1 results in a slight, dose-dependent telomere elongation, increased length heterogeneity, and increased rates of recombination and chromosome loss (Conrad et al. 1990). The expression of C-terminal truncation Rap1 mutants leads to telomere elongation, highly unstable telomeres susceptible to rapid deletion, and chromosome nondisjunction rates that are 15- to 30- fold higher than wild type levels (Kyrion et al. 1992).

Rap1 functions to recruit other proteins to the yeast telomere. Two-hybrid studies using the C-terminus of Rap1 were used to identify two sets of proteins, the SIRs (Sir3p and Sir4p) and the RIFs (Rif1p and Rif2p) (Hardy et al. 1992; Moretti et al. 1994; Cockell et al. 1995; Liu and Lustig 1996; Wotton and Shore 1997). SIR (Silent

Information Regulator) proteins are required for silencing at HM mating-type loci and telomeres. Sir3p and Sir4p colocalize with Rap1 at telomeres by indirect immunofluorescence and FISH using telomeric repeat probes (Gotta et al. 1996). Sir3p no longer colocalizes with Rap1p in *sir4*$^-$ cells and Sir4p no longer colocalizes in *sir3*$^-$ cells (Gotta and Gasser 1996). Sir3 and Sir4 are not required for telomere length regulation or telomere protection.

The Rifs (Rap1-Interacting Factors), Rif1 and Rif2, play a direct role in telomere length regulation. Overexpression of either Rif1 or Rif2 leads to telomere shortening and overexpression of Rif1 and Rif2 reverses the elongation seen with overexpression of the C-terminus of Rap1 (Wotton and Shore 1997). Thus, telomere length changes resulting from overexpression of wild type or mutant Rap1 alleles may result from titrating Rif1 and Rif2 away from the telomere. A more extensive introduction to Rif1 is given in the introduction sections of chapters 1 and 2. A major portion of this thesis focuses on the identification and characterization of the human ortholog of yeast Rif1.

Deletion analysis using gel shifts of telomeric oligonucleotides indicated that the minimal DNA-binding domain (DBD) of Rap1 lies between amino acids 361 and 596 (Henry et al. 1990). The crystal structure of the Rap1 DBD with an 18 nucleotide telomeric DNA fragment shows that Rap1 binds DNA with two myb-like HTH motifs (Konig et al. 1996). The vertebrate telomeric-binding proteins TRF1 and TRF2 and the *S. pombe* protein Taz1 also use myb domains to bind DNA (Bianchi et al. 1997; Broccoli et al. 1997a; Cooper et al. 1997). There are important differences in the way Rap1 and TRFs bind their consensus sequences. Rap1 binds to DNA with two myb-like motifs in a single polypeptide, whereas TRF1 and TRF2, each having only a single C-terminal Myb

domain, homodimerize in order to bind DNA with two Myb domains (Bianchi et al. 1997; Broccoli et al. 1997b). The existence of two nearly adjacent Myb domains within each Rap1 molecule confines the protein to recognize two tandem sites in yeast telomeric DNA. In contrast, the TRF1 homodimer is able to bind two 5'-YTAGGGTTR-3' half-sites with spatial and orientational flexibility (Bianchi et al. 1999). This flexibility may serve a tethering function in establishing higher order DNA structures.

The TRF1 complex: TRF1, Tankyrase, Tin2, and PinX1

In human cells, the TRF1 complex acts as a negative feedback control system in the regulation of telomere length. Telomerase-positive cells often have stably maintained telomere length. This telomere length "set-point" varies between cells lines and even between subclones of a given cell line. In order to initially study telomere length, individual clones were analyzed by using an inducible gene expression system to regulate the amount of TRF1 alleles in cells (van Steensel and de Lange 1997; Smogorzewska et al. 2000). The idea behind this negative feedback control system is that TRF1 binds along the length of duplex telomeric DNA and exerts a negative regulatory influence on telomerase. If the telomere shortens, less TRF1 will bind to the telomere and telomerase can more easily act to lengthen the telomere. Conversely, telomere lengthening results in increased TRF1 binding and diminished ability for telomerase to lengthen longer telomeres. The observations that the TRF1 IF signal increases with telomere length (Smogorzewska et al. 2000) and that a comparable percentage of telomeric chromatin is

immunoprecipitated with TRF1 in ChIP experiments regardless of telomere length (Loayza and De Lange 2003) are consistent with this model.

The binding of TRF1 to telomeres can be inhibited by two related enzymes, tankyrase 1 and 2 (Smith et al. 1998; Smith and de Lange 2000; Kaminker et al. 2001; Cook et al. 2002; Sbodio et al. 2002; Seimiya and Smith 2002). The takyrases are poly(ADP-ribose) polymerases (PARPs), that were originally identified as TRF1-interacting proteins. Tankyrases can ADP-ribosylate TRF1 in vitro and in vivo and this modification diminishes the ability of TRF1 to bind to telomeric DNA in vitro (Smith et al. 1998). Ectopic expression of tankyrase 1 in the nucleus results in the removal of TRF1 from telomeres in vivo (Smith and de Lange 2000; Cook et al. 2002; Loayza and De Lange 2003). Consistent with these findings, overexpression of tankyrase 1 leads to telomere elongation, the phenotype seen upon TRF1 inhibition. TRF1 also binds to Tin2 and PinX1. Tin2 is able to form a ternary complex with TRF1 and tankyrase (Ye, J. and de Lange, T., in press). PinX1 has been proposed to inhibit telomerase directly in order to participate in telomere length regulation (Zhou and Lu 2001). The proposed role of PinX1 differs dramatically from the cis-acting mechanisms proposed for TRF1, tankyrase and Tin2.

The end of the telomere: CDC13 and Pot1

The Cdc13 protein in *S. cerevisiae* plays a critical role in the regulation of telomere length maintenance and telomere protection through its actions at the most distal part of the telomere; namely, the telomere terminus. Although CDC13 was initially

identified as a gene essential for cell division cycle (Garvik et al. 1995), it was subsequently identified as one of several genes whose mutation leads to an ever shorter telomere (est) phenotype, similar to the loss of telomerase (Lendvay et al. 1996). Cdc13 is able to bind to the G-rich single-stranded overhang and acts by recruiting telomerase through an interaction with Est1 (Garvik et al. 1995; Nugent et al. 1996). Indeed, there is an allele specific suppression of the *cdc13-2^{est}* mutant (which is a loss-of-function mutant resulting in an est phenotype) by an *est1-60* mutant (which also displays an est phenotype), consistent with a physical interaction between Cdc13 and Est1 (Pennock et al. 2001). The proposed model underlying this genetic data is that a role of Cdc13 at the telomere is to recruit telomerase. In fact, a fusion between the DNA-binding domain of Cdc13 and Est2, the protein component of core telomerase, rescues the inability of *cdc13-2^{est}* and est1-Δ strains to maintain their telomeres (Evans and Lundblad 1999; Pennock et al. 2001).

In addition to the ability of Cdc13 to recruit telomerase to the telomere in *S. cerevisiae*, Cdc13 also recruits additional factors that limit telomere elongation. In particular, Cdc13 recruits the protein Stn1 and mutations in either CDC13 that fail to bind Stn1 or STN1 mutations result in telomere elongation (Chandra et al. 2001; Grandin et al. 2001). One such CDC13 mutant, cdc13-5, results in increased telomere length and excessive G-strand overhangs in late S phase that become duplex with delayed kinetics (Chandra et al. 2001). This suggests a defect in the co-ordination of lagging strand synthesis with telomere elongation. The observation that Stn1 suppresses both the telomere elongation and G-stand overhang phenotype points to Stn1 as the cause of these phenotypes.

POT1, a factor distantly related to Cdc13, binds to the telomere terminus in *S. pombe* and human cells. This gene was first discovered in the fission yeast *S. pombe* and was shown to bind to the G-rich strand of telomeric DNA in vitro (Baumann and Cech 2001). Pot1 binds to telomeric DNA through an OB fold that resembles that of the telomere binding protein Oxytricha α and Cdc13 (Baumann and Cech 2001; Mitton-Fry et al. 2002). The binding of Pot1 to the *S. pombe* telomeric DNA occurs in a cooperative fashion (Lei et al. 2002). Deletion of the pot1+ gene results in chromosome instability, as demonstrated by a mis-segregation phenotype, as well as the loss of telomeric DNA and subsequent circularization of chromosomes (Baumann and Cech 2001). Hence the name Pot1, protector of telomeres 1, was given because Pot1 plays a critical role in protecting telomeres.

A human ortholog of Pot1 was identified and characterized. Human Pot1 co-localizes with known telomere proteins in immunofluorescence experiments (Baumann et al. 2002). Additionally, human POT1 is also able to bind to telomeric DNA in vitro (Baumann et al. 2002) and is present at telomeres in vivo based on ChIP (Loayza and De Lange 2003). The amount of POT1 on telomeres was reduced when the quantity of single-stranded telomeric DNA was reduced (Loayza and De Lange 2003; Loayza et al. 2004). Furthermore, a deletion of the POT1 DNA-binding domain results in rapid telomere elongation (Loayza and De Lange 2003). Since POT1 interacts with the TRF1 complex, it has been proposed that TRF1 sends information about telomere length to POT1 at the telomere terminus, which regulates either the recruitment or access of telomerase to the telomere terminus (Loayza and De Lange 2003).

hRap1 and spRap1 as orthologs of scRap1

A search for TRF2-interacting proteins using a yeast two-hybrid approach has uncovered a factor, termed hRap, that has significant sequence identity to Rap1 in *S. cerevisiae* (Li et al. 2000). hRap1 encodes a 47-kD, 399-amino acid protein that contains an N-terminal BRCT domain, a Myb-type domain, and an acidic C-terminus (Figure I-3). These domains in hRap1 have approximately 25% sequence identity and 50% sequence homology to their respective domains in scRap1 (Figure I-3). Thus, hRap1 seems to be an ortholog of scRap1.

Further analysis reveals that hRap1 plays a role at human telomeres. Northern analysis reveals a 2.5 kb band that is widely expressed in human tissues. Indirect immunofluorescence using an anti-hRap1 antibody in HeLa cells, HT1080 cells, and IMR90 cells shows punctuate nuclear staining. hRap1 colocalizes with TRF2 and TRF1 in cells and immunofluorescence of metaphase chromosomes shows a signal only at chromosome ends. Using a tetracycline-inducible system in telomerase-positive HTC75 cells (derived from HT1080 cells), inducible overexpression of full-length FLAG-tagged hRap1 results in the gradual elongation of telomere length (Li et al. 2000). Surprisingly, hRap1 does not appear to bind directly to telomeric DNA, though it can supershift TRF2-telomeric DNA complexes (Li et al. 2000).

A more thorough discussion of the domain structure and the importance of hRap1 is found in the introductions to chapters 1 and 3 of this thesis. Since one of the projects in this thesis is the identification of novel Rap1-interacting factors, this topic is discussed in depth along with the data in chapter 3.

The TRF2 complex: TRF2, hRap1, and the Mre11 complex

The protein complex associated with TRF2 plays a critical role in telomere length regulation and end protection. Studies of the proteins found in TRF2 immunoprecipitate pellets resulted in the identification of the Mre11 complex, consisting of Mre11, Rad50, and Nbs1 (Zhu et al. 2000). As discussed earlier in this introduction, the Mre11 complex plays a role in a variety of biological functions including recombination and DNA damage repair. Components of the Mre11 complex co-localized with known telomere proteins (Zhu et al. 2000). Additional studies of TRF2-interacting factors resulted in the identification of ERCC1 and XPF in the TRF2 complex (Zhu, X, et al., submitted).

Human Rap1 and the evolution of the telomere complex

The identification of hRap1 raises important questions regarding the evolution of telomeric complexes. A contradiction seems to exist between the structure and function of Rap1 in vertebrates and budding yeast. *S. cerevisiae* utilizes Rap1 to bind directly to telomeric DNA while, in humans, Rap1 does not bind telomeric DNA and associates with the telomere via its interaction with TRF2. *S. cerevisiae* lacks a TRF-like component at their telomeres. What factors were contained in the "ancestral" telomeric complex? Further examination of known telomeric protein similarities suggests a possible resolution to this problem. The major binding factor in the fission yeast, *S. pombe*, is the protein Taz1. Although no ortholog of Rap1 is currently known in *S. pombe*, Taz1 can be

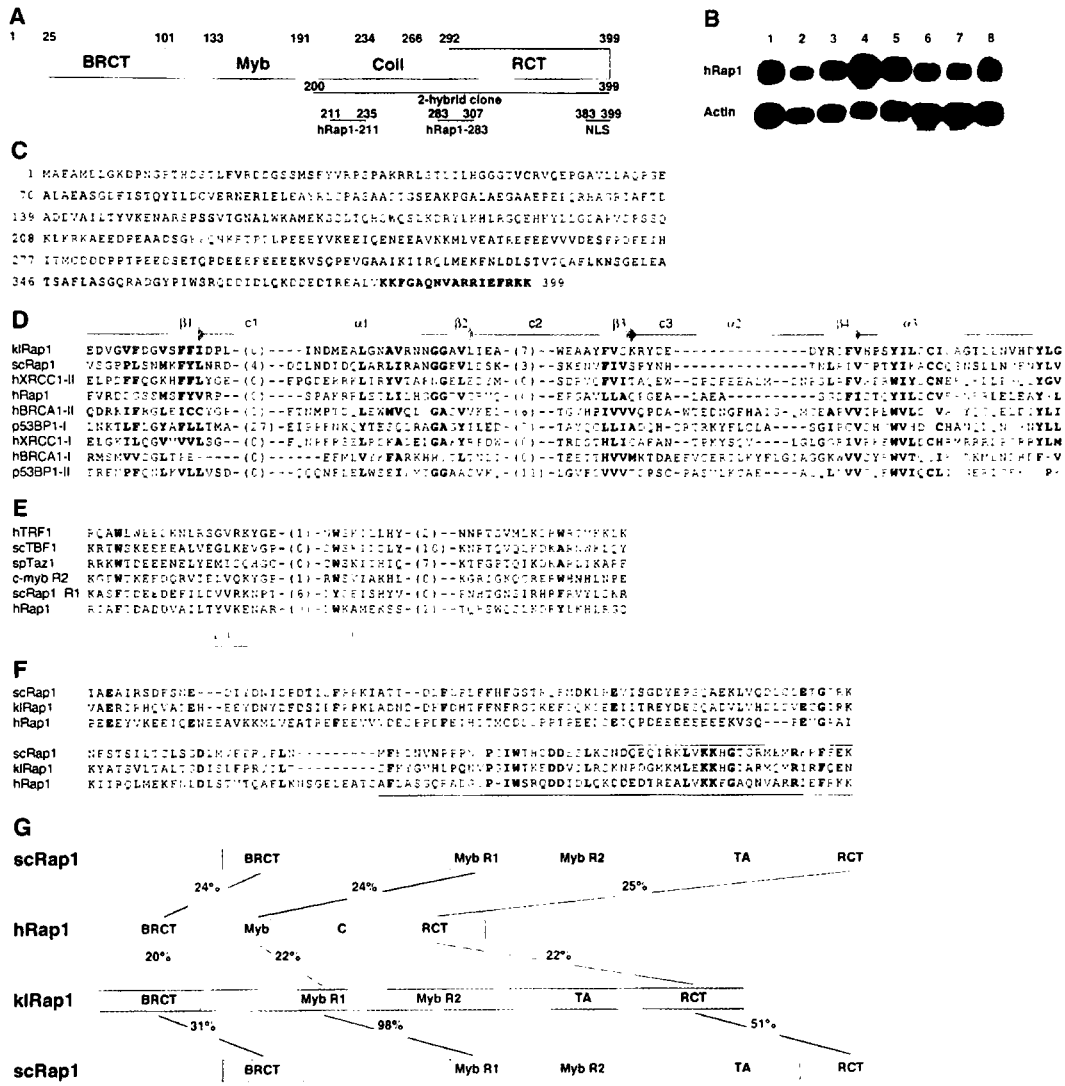

Figure I-3. Domain stucture and sequence alignments of human Rap1.

The domain stucture of hRap1 is given in A. The protein structure is given in C. D, E and F depict alignments of the BRCT domain, Myb domain, and RCT domains, respectively. G illustrates the conservation of the various domains between human Rap1 and yeast Rap1. Figure courtesy of Titia de Lange (Li et al. 2000).

classified as a member of the TRF family of proteins (Li et al. 2000). The Myb domain of Taz1 more closely resembles the Myb domains of the TRFs than the Myb domains of Rap1. Taz1 also contains a central TRFH (TRF homology) domain (Li et al. 2000). The TRFH domain acts as a dimerization domain in TRF1 and TRF2 (Bianchi et al. 1997; Broccoli et al. 1997b; Fairall et al. 2001) A model emerges in which the "ancestral" telomeric complex contains both a TRF-like component and a Rap1-like component. Budding yeast, including *C. albicans*, *K. lactis* and *S. cerevisiae*, seemed to have lost the TRF component. In support of this, the budding yeast has a more divergent telomeric repeat than the TTAGGG found in vertebrates (most lower organisms have telomeric repeats that very closely resemble TTAGGG). Possibly a mutation in the telomerase RNA template resulted in a change in the telomeric template and the ability of Rap1 to bind to this new telomeric repeat enabled the budding yeast to remain viable (Li et al. 2000). Further discussion of how the discovery and characterization of Rap1 and Rif1 in S. pombe add to this picture of evolution and the roles of these proteins in telomere biology is reserved for the introductions of later chapters.

DNA damage response factors and telomeres

A number of DNA damage response factors are involved in telomere length maintenance. Telomere maintenance and length control in *S. pombe* are influenced by the DNA damage response factors Rad17, Rad53, Mec3 and Ddc1 (Dahlen et al. 1998; Longhese et al. 2000; Nakamura et al. 2002). Additionally, in both *S. cerevisiae* and *S. pombe*, the deletion of the NHEJ factor Ku leads to very short, but stable, telomeres

(Porter et al. 1996; Boulton and Jackson 1998; Gravel et al. 1998; Nugent et al. 1998; Polotnianka et al. 1998; Baumann and Cech 2000). This phenotype is unrelated to the loss of NHEJ in cells, as the loss of DNA ligase IV, another factor involved in NHEJ, does not affect telomere length (Boulton and Jackson 1998; Baumann and Cech 2000).

Factors involved in the DNA damage response, including ATM, play a role in telomere length maintenance in mammalian cells. Peripheral blood lymphocytes from A-T patients show significant telomere shortening compared to age-matched donors (Metcalfe et al. 1996). Also, cells from ATM deficient mice and A-T patients have extrachromosomal telomeric DNA (Hande et al. 2001). The mechanism of ATM regulation of telomere length maintenance and telomere stability is unknown.

The mechanism is also unclear for the role of Ku70/80, DNA-PK_{cs}, and PARP-1 in telomere length maintenance. While DNA-PK_{cs} null mice have normal telomere length (Goytisolo et al. 2001; Espejel et al. 2002), mice with the DNA-PK_{cs} SCID mutation have been reported to have longer telomeres (Hande et al. 1999; Goytisolo et al. 2001). Perhaps the SCID mutation, while deficient in NHEJ, may be a gain of function mutation for the role of DNA-PK_{cs} in telomere length control. It is more difficult to explain discrepancies in reports on Ku80. Even though two groups measured telomere lengths in the same Ku86 null mouse strain, one report indicates shorter telomeres (d'Adda di Fagagna et al. 2001), while another found no change (Samper et al. 2000). Finally, mice lacking PARP-1 have shorter telomeres but this phenotype is only seen in the absence of p53 (d'Adda di Fagagna et al. 1999; Samper et al. 2001).

Consequences of telomere dysfunction and link to the DNA damage response

Telomeres prevent the ends of linear chromosomes from being recognized as damaged DNA. Dysfunctional telomeres, which fail to protect chromosome ends, are indeed recognized by the DNA damage response. The consequences of telomere dysfunction are disastrous and potentially lethal for cells. Model systems for telomere dysfunction can be generated by passaging primary cells, which lack telomerase, in culture. Primary fibroblasts undergo telomere attrition and will enter into a type of growth arrest known as senescence after a given number of passages in culture (Hayflick 1998). Senescence occurs when one or more telomeres have shortened to a certain critical length and are unable to properly protect chromosome ends. The ectopic expression of a dominant negative TRF2 allele lacking both the basic and Myb domains ($TRF2^{\Delta B \Delta M}$) also results in dysfunctional telomeres (van Steensel et al. 1998). The following discussion will briefly describe the consequences of telomere dysfunction, including apoptosis and senescence, and the recognition of dysfunctional telomeres by the DNA damage response.

Dysfunctional telomeres resulting from the ectopic expression of $TRF2^{\Delta B \Delta M}$ result in apoptosis and senescence, depending on cellular context. Telomere-telomere fusions and anaphase bridges occur as a result of $TRF2^{\Delta B \Delta M}$ over-expression (van Steensel et al. 1998). Additionally, cells can also enter senescence (van Steensel et al. 1998; Smogorzewska and de Lange 2002). Telomeric DNA is still detectable by Southern blot and IF, which is consistent with the idea that $TRF2^{\Delta B \Delta M}$ results in telomere dysfunction

because of structural changes in the telomere rather than loss of telomeric DNA. The telomere end-to-end fusions and anaphase bridges are consistent with dysfunctional telomeres being recognized as DNA damage and subsequently being fused together by the NHEJ repair pathway. The formation of telomere end-to-end fusions upon $TRF2^{\Delta B \Delta M}$ over-expression is dependent upon ligase IV, a critical component of the NHEJ pathway (Smogorzewska et al. 2002). Additionally, certain cells over-expressing $TRF2^{\Delta B \Delta M}$ can undergo apoptosis in a manner dependent on ATM and p53 (Karlseder et al. 1999). The formation of telomere dysfunction-induced foci (TIFs), wherein DNA damage response factors accumulate at dysfunctional telomeres, provides further evidence that deprotected telomeres induced by $TRF2^{\Delta B \Delta M}$ are interpreted by the cell as DNA damage (Takai et al. 2003).

Summary and Relevance

This thesis deals primarily with the identification and characterization of human Rif1, an ortholog of the telomere length regulator Rif1 in *S. cerevisiae* and *S. pombe*. Chapter 1 describes the identification of human Rif1 using a bioinformatics approach where sequences from *S. cerevisiae* Rif1 were used to query the human database. The generation of antibodies led to the initial characterization of human Rif1. Chapter 1 describes efforts to implicate Rif1 in human telomere biology. These efforts failed to discern a definitive role for human Rif1 in telomere biology. Immunofluorescence, co-immunoprecipitation and ChIP techniques were all used to determine if Rif1 localizes to telomeres, interacts with known telomeric proteins, or associates with telomeric chromatin. Chapter 2 reports on the most significant and surprising discovery in this thesis which is that Rif1 plays a role in the DNA damage response in human cells. The data demonstrate that Rif1 forms foci in response to DNA damage. Rif1 responded to ionizing radiation (IR), UV light, and clastogens, forming foci that co-localized with other DNA damage response factors such as 53BP1, ATM, BRCA1, Chk1, Nbs1, and Rad17. Furthermore, Rif1 localized to uncapped telomeres, as do other DNA damage response factors. Among DNA damage response proteins, Rif1 showed a unique dependence on the ATM kinase. Whereas inhibition of ATR signaling did not inhibit the Rif1 response, ATM deficient cells treated with IR or UV lacked Rif1 foci even after prolonged incubation or high radiation dose. Therefore, IR-induced Rif1 foci constitute an assay for ATM status. The Rif1 response also depended on the presence of 53BP1 but was not affected by reduced function of BRCA1, Chk2, Nbs1, and Mre11. RNAi-

mediated Rif1 inhibition resulted in increased radiosensitivity, indicating that Rif1 function contributes to the ATM-mediated protection against exposure to ionizing radiation.

This thesis also focuses on the human TRF2 complex, which includes Rap1 and the Mre11 complex. Chapter 3 describes a yeast two-hybrid screen conducted using Rap1 as a bait to identify novel Rap1-interacting factors in mammalian cells. Two genes, a novel gene called cDNA 144 and a previously identified gene called FLASH, were identified in this screen. Neither cDNA 144 nor FLASH were shown to have a role in human telomere biology.

Chapter 1 – Identification of human Rif1

Introduction

The importance of yeast Rif1 in telomere biology provided the impetus that led to the identifications of a Rif1 ortholog in human cells. Rif1 was first discovered through a yeast two-hybrid screen as a protein that binds to Rap1 (Hardy et al. 1992). Specifically, the C-terminal portion of Rif extending from amino acids 1614 to 1916 interacts wth the C-terminus of Rap1 extending from amino acids 667 to 827 (Hardy et al. 1992). The fact that there is allele-specific suppression of $rap1^{s}$ mutants, which have altered telomere length and do not bind Rif1, by the RIF1 allele rif1-1 confirms the biological significance of this interaction (Hardy et al. 1992).

Rif1 plays a role in telomere length regulation, transcriptional silencing at the yeast mating-type locus, and transcriptional silencing of telomere proximal genes, known as the telomere position effect (TPE) (Hardy et al. 1992; Kyrion et al. 1993). Yeast one-hybrid analysis suggests that *S. cerevisiae* (scRif1) associates with telomeric DNA in vivo (Bourns et al. 1998). Deletion of RIF1 leads to mild telomere elongation that is telomerase-dependent and RAD52-independent (Kyrion et al. 1993; Teng et al. 2000). Rif2, which is not related to Rif1, also binds to the C-terminus of Rap1 in *S. cerevisiae* (Wotton and Shore 1997). Like deletion of RIF1, deletion of RIF2 leads to telomere elongation and rif1 rif2 strains have telomeres longer than either rif1 or rif2 strains alone (Wotton and Shore 1997; Mishra and Shore 1999).

While most *S. cerevisiae* cells that lack telomerase will die after 50-100 generations, survivors arise spontaneously and fall into two types (Lundblad and Blackburn 1993). Type I survivors have a tandem repeat of the Y' element and very

short tracts of telomeric repeat DNA, and type II survivors have very long and heterogeneous tracts of telomeric repeat DNA. In culture, type I survivors frequently convert to type II survivors and type II survivor telomeres return to wild-type length with the re-introduction of telomerase (Teng and Zakian 1999). The distribution of type I and type II survivors after loss of telomerase is affected by Rif1, as rif1 tlc1 cells result in 18% type II survivors whereas tlc1 cells result in 6.5% type II survivors (Teng et al. 2000). The mechanism underlying the effect of Rif1 on the survivor pathway in *S. cerevisiae* is currently unknown.

The discovery of *S. pombe* Rif1 (spRif1) and analysis of its roles in telomere biology reveal that scRif1 and spRif1 behave similarly in terms of telomere length regulation. Deletion of spRif1 also results in telomere elongation (Kanoh and Ishikawa 2001). As mentioned in the introduction, spRif1 is recruited to telomeres through its interaction with Taz1, whereas scRif1 is recruited to telomeres through its interaction with Rap1 (Hardy et al. 1992; Kanoh and Ishikawa 2001).

Rif1, Rif2, Sir3 and Sir4 all compete for binding to the carboxy-terminus of Rap1 (Buck and Shore 1995; Mishra and Shore 1999). Furthermore, there is also competition between Ku and Rif1 in terms of telomeric silencing (Mishra and Shore 1999). This competition may be the reason underlying a decrease of telomeric silencing seen in cells lacking scRif1 (Kyrion et al. 1993). *S. pombe* Rif1 (spRif1) also plays a role in telomere length regulation and TPE (Kanoh and Ishikawa 2001). *S. pombe* rif1$^-$ strains have decreased spore viability and aberrant chromosome segregation which implies an additional role for rif1 in meiosis (Kanoh and Ishikawa 2001).

Based on these findings, the identification of human Rif1 was anticipated to provide insight into human telomere function. The role of human Rif1 (hRif1) could also address issues related to the evolution of telomere protein complexes. In *S. cerevisiae*, Rap1 is the predominant double-stranded telomeric binding protein. Rif1 is then recruited to *S. cerevisiae* telomeres through its interactions with Rap1. In *S. pombe*, Taz1 is the major protein that binds directly to telomeres. Rap1 is recruited to telomeres through its interaction with Taz1 (Chikashige and Hiraoka 2001; Kanoh and Ishikawa 2001). *S. pombe* Rif1 is also recruited to telomeres by Taz1, but this recruitment is Rap1 independent (Kanoh and Ishikawa 2001). Thus, the interactions of the telomere proteins differ in these two yeast species (Figure 1-1). The discovery of human Rap1 and the finding that Taz1 in *S. pombe* is similar to human TRF1 and TRF2 raises the question of what role human Rif1 may play in the human telomere complex (Li et al. 2000). Does the human telomere complex resemble the complex in *S. cerevisiae* where Rif1 is recruited to telomeres through Rap1 or the complex in *S. pombe* where Rif1 is brought to telomeres through the TRF-like Taz1?

This chapter focuses on the identification and initial characterization of a human ortholog of yeast Rif1. hRif1 was found using a bioinformatics approach where the human genome and expressed sequence tags (ESTs) were queried with scRif1 and spRif1. Antibodies were generated against human Rif1 in order to study this protein. Since Rif1 plays a role in telomere biology in both *S. cerevisiae* and *S. pombe*, a series of experiments were conducted to address whether or not Rif1 plays a role in human telomere biology. An indirect immunofluorescence (IF) approach was taken to address whether Rif1 co-localizes with previously known human telomere proteins such as TRF1,

TRF2, hRap1 and Tin2. Additionally, attempts were made to co-immunoprecipitate Rif1 with known telomere complexes. Rif1 was also found at other cellular locations in human cells.

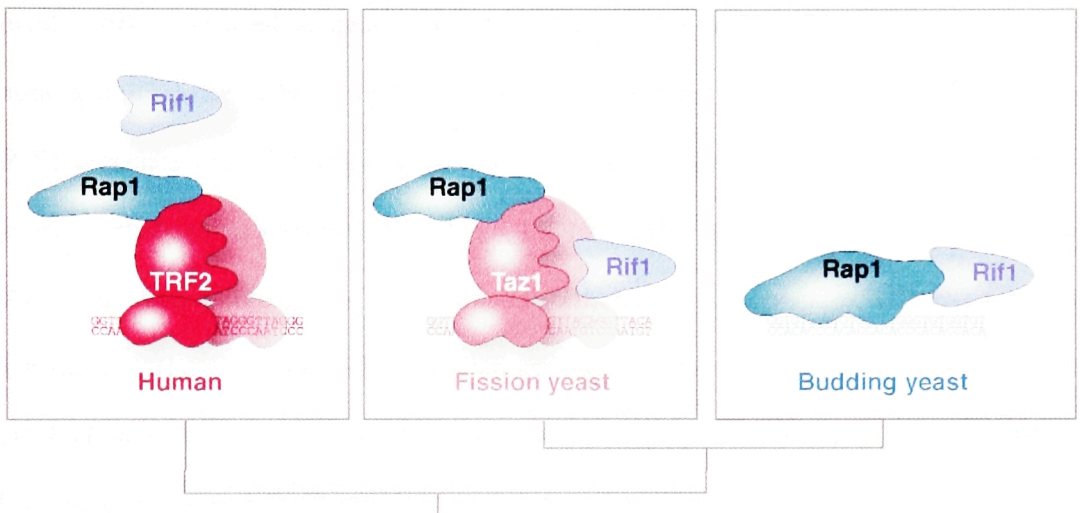

Figure 1-1. Evolution of the telomere complex.

The relationship among telomeric protein complexes in vertebrates, fission yeast, and budding yeast. TRF2 and Taz1 are structurally related. In budding yeast, Rap1 binds telomeric DNA whereas human and fission yeast Rap1 bind to telomeres via TRF2 and Taz1, respectively. Budding yeast Rif1 binds to Rap1, whereas fission yeast Rif1 binds to Taz1. The role of Rif1 at human telomeres is currently unclear. Figure courtesy of Agata Smogorzewska and Titia de Lange.

Results

A search for the human ortholog of yeast Rif1 was undertaken due to its importance in telomere biology. Initially, the *S. cerevisiae* Rif1 protein sequence (Hardy et al. 1992) was used to query the human database in a BLAST search. Using this approach, a human ortholog of *S. cerevisiae* RIF1 was not detected. Then, *S. cerevisiae* RIF1 sequence was used to query the *S. pombe* database using a BLAST search and an *S. pombe* ortholog was identified (P value = 1×10^{-7}). This gene was identical to *S. pombe* Rif1 gene later published as the functional ortholog of *S. cerevisiae* Rif1 (Kanoh and Ishikawa 2001). *S. pombe* Rif1 was then used to identify a human Rif1 ortholog using a BLAST search (P $=9 \times 10^{-5}$, Unigene hypothetical protein FLJ10599). The DNA sequence of human Rif1 was assembled from the following overlapping clones in Genbank: Homo sapiens cDNA FLJ12870 fis, clone NT2RP2003727 (Genbank accession number AK022932); Homo sapiens cDNA FLJ10599 fis, clone NT2RP2004959 (Genbank accession number AK001461); IMAGE clone 2187070 3' end (Genbank accession number AI537278); and cDNA DKFZp434D193 (Genbank accession number AL080129). The full DNA sequence of human Rif1 is given in Genbank accession number AY585745.

The predicted open reading frame of combined ESTs is 2472 amino acids encoding a protein with a pI of 5.46 and a predicted MW of 274 kilodaltons (Figure 1-2). The sequence similarity of hRif1 to scRif1 and spRif1 was low (15% and 18% sequence identity, respectively) but extended throughout the reading frame. The initial alignment of *S. cerevisiae*, *S. pombe* and human Rif1 using a CLUSTAL

Figure 1-2. Alignment of human Rif1 with mouse Rif1 and fugu Rif1.

The human Rif1 amino acid sequence is depicted and aligned with mouse Rif1 and fugu Rif1. Conserved amino acids are depicted in red and blue and a consensus sequence is given below. The protein product of human Rif1 is predicted to be 2472 amino acids. The full DNA sequence of human Rif1 is given in Genbank accession number AY585745.

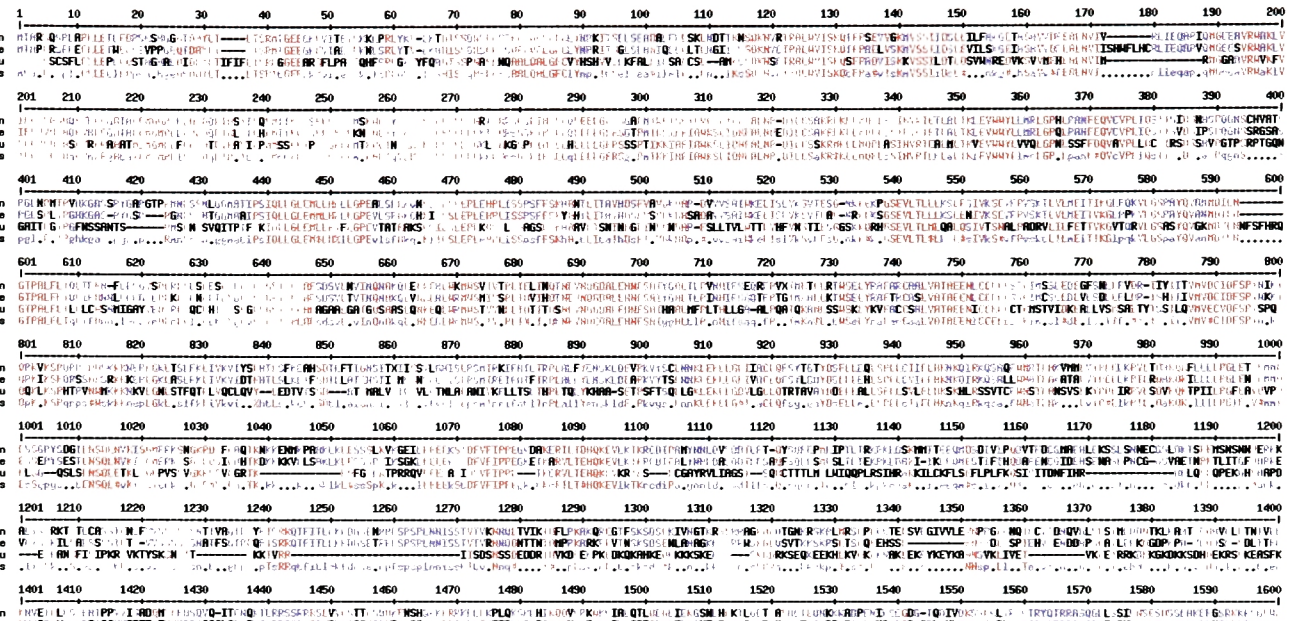
human
mouse
fugu
Consensus

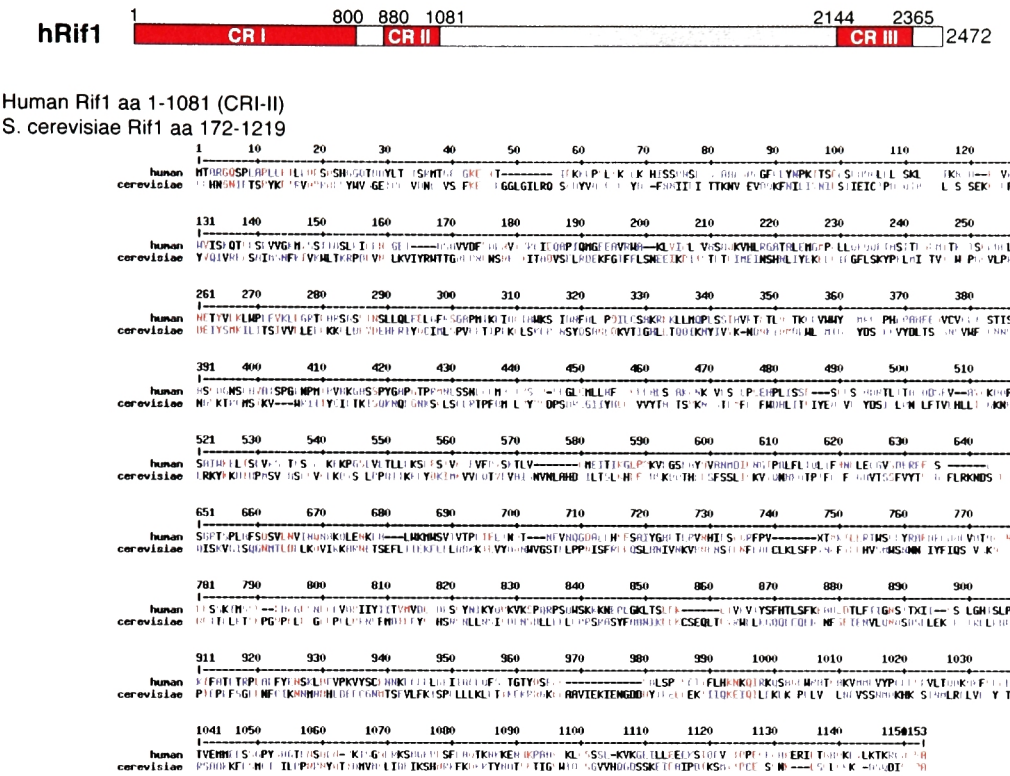

Figure 1-3. Alignment of conserved regions I and II of Rif1 in human and *S. cerevisiae*.

The CLUSTAL algorithm was used to align Rif1 in *S. cerevisiae* and human. A schematic of human Rif1 above depicts the three conserved regions of Rif1 with sequence conservation of 20-25%. The alignment shown depicts the first two conserved regions of Rif1.

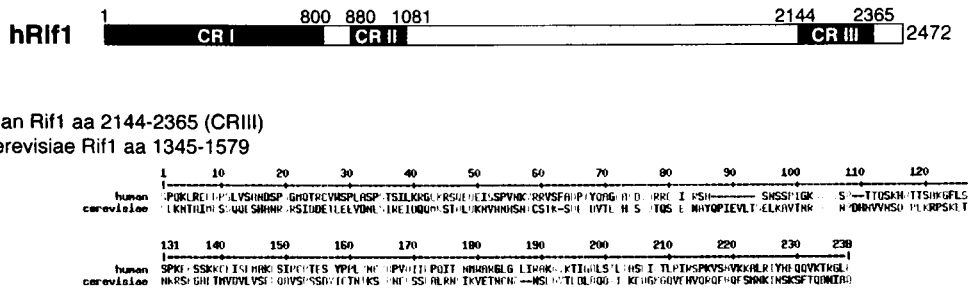

Figure 1-4. Alignment of conserved region III of Rif1 in human and *S. cerevisiae*. The CLUSTAL algorithm was used to align the C-terminal portions of Rif1 in *S. cerevisiae* and human. The alignment depicts conserved region III.

algorithm suggests more sequence similarity between the N-terminal regions and less similarity between the C-terminal regions. Further analysis reveals three conserved regions when human, mouse and fugu Rif1 are aligned (Figure 1-2). These conserved regions, designated CRI-III, have 20-25% conserved amino acids (Figures 1-3 and 1-4). Secondary structure analysis revealed a series of conserved predicted helices between *S. cerevisiae*, *S. pombe* and human Rif1 proteins. The mammalian Rif1 proteins are composed almost entirely of Armadillo repeats. ARM repeat folds, which are composed of three helices, often occur in long arrays and form an extended curved protein interaction surface (Huber et al. 1997; Conti et al. 1998). The open reading frame predicts a high density of helical segments in its N-terminal 800 amino acids, a putative bipartite NLS sequence at position 2188 and a serine-rich region from position 1149-1204 (Figure 1-4 and 1-5A).

In order to understand the role of Rif1 in human cells and determine whether or not Rif1 is associated with telomeres, antibodies were generated against hRif1. Two types of antigens, KLH-conjugated peptides and GST-fusion proteins, were used to produce antibodies (Figure 1-5A). The PROTEAN program in the Lasergene navigator software package was used to predict the optimal peptides for antibody generation based on the criteria of hydrophobicity and antigenicity (Figure 1-5B). Using the output, a total of four peptides individually containing amino acids 773-798 (YNIKYQPKVKSPQRPSDWSKKKNEPC), amino acids 1552-1587 (NH2 – NSESDSSEAKEEGSRKKRSGKWKNKC – COOH), amino acids 2077-2102 (NH2 – EEGIIDANKTETNTEYSKSEEKLDNC – COOH) or amino acids 2448-2473 (NH2 – LSCMANSVIKNLQSRWRSPSHENSIC – COOH) of hRif1 were synthesized in vitro

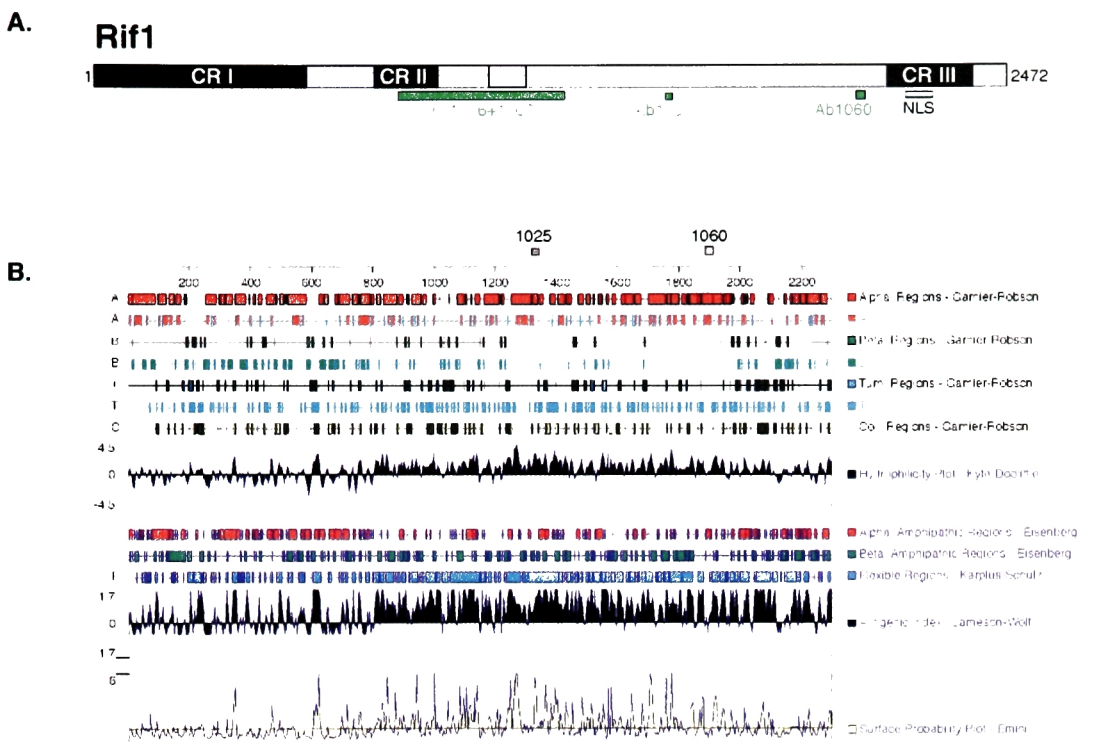

Figure 1-5. Antibodies generated against human Rif1.

A. A schematic of human Rif1 is shown. Conserved regions I-III (black), the serine-rich region (purple), and NLS (aqua) are shown. The positions of the antigens used in antibody generation are shown (green).

B. The biochemical properties of the amino acids in hRif1. The PROTEAN program in the Lasergene software package was used to generate the plots from the hRif1 protein primary sequence. A combination of the antigenic index and the surface probability plot was used to select the peptides that would be used as immunogens to generate antibodies against hRif1.

(Biosynthesis) and conjugated to keyhole limpet haemocyanin (KLH). Each KLH-conjugated peptide was used to immunize two rabbits (Covance) and the resulting sera were affinity-purified. A carboxy-terminal cysteine was added to each peptide to allow for conjugation to KLH. Table 1-1 below describes the various antibodies raised against Rif1, including the antigens used and their efficacy in Western blots.

Serum number	Antigen used	Peptide positions	Affinity-purified?	Detection of Rif1 in Western blot	Non-specific bands in Western
1023	KLH-conjugated peptide	773-798	Yes		
1024	KLH-conjugated peptide	773-798	Yes		
1025	KLH-conjugated peptide	1552-1577	Yes	++	+
1026	KLH-conjugated peptide	1552-1577	Yes	++	+
1060	KLH-conjugated peptide	2077-2102	Yes	+++	
1061	KLH-conjugated peptide	2077-2102	Yes	+	+/-
1062	KLH-conjugated peptide	2448-2472	No		+
1063	KLH-conjugated peptide	2448-2472	No	+ (weak)	+/-
1066	GST-Rif1 fragment fusion	1974-2472	No	+++	
1067	GST-Rif1 fragment fusion	1974-2472	No	+++	

Table 1-1. Characteristics of antibodies against human Rif1.

The antibodies designated 1025 and 1060 recognized a single large (>250 kDa) polypeptide in Western blots of HeLa cells, whereas preimmune serum did not recognize this polypeptide (Figure 1-6A). The 1060 peptide antigen was also injected into mice to generate a polyclonal mouse serum designated as mouse 1060. GST-fusion proteins were also used to generate anti-Rif1 antibodies. Proteins with an N-terminal GST fused to portions of hRif1 were made in order to generate antibodies. Four GST-fusion proteins were constructed. The first two, from amino acids 177-797 and 177-907, designated GST-hRif1$_{177\text{-}797}$ and GST-hRif1$_{177\text{-}907}$, respectively, did not yield protein products detectable by Coomassie staining. It is unclear if this was due to protein solubility, stability, or some other factor. A GST-Rif1 fusion containing amino acids 907-1327, designated GST-hRif1$_{907\text{-}1327}$, was used as an antigen to generate the rabbit polyclonal sera 1066 and 1067 (Figure 1-5A). This GST-fusion protein was expressed in BL21 strain E. coli and purified using glutathione-conjugated sepharose beads (Figure 1-6B). Another GST-hRif1 fusion containing Rif1 amino acids 1974-2472, designated GST-hRif1$_{1974\text{-}2472}$, was produced (Figure 1-6B), but sufficient quantities for antibody production were difficult to obtain. GST-hRif1$_{907\text{-}1327}$ was used to immunize two rabbits and the resulting crude sera, designated 1066 and 1067, reacted with the same large molecular weight polypeptide as the previously described 1025 and 1060 (Figure 1-6A). Cells treated with siRNAs corresponding to Rif1 diminished the abundance of this protein (see Chapter 2), confirming that this polypeptide is encoded by the Rif1 gene and establishing the specificity of the sera used in this study.

Human Rif1 mRNA is greater than nine kilobases and is present in a wide variety of tissues (Figure 1-7A). The Rif1 protein was detectable in different human cell lines

and strains (e.g. IMR90, GM847, VA-13, HeLa, U2OS) suggesting ubiquitous expression (Figure 1-7B, see also below and Chapter 2). Thus, Rif1 is found in all primary fibroblasts, including IMR90 and BJ cells, and tumor cells, including HeLa and HT1080 cells. It is interesting to note that Saos-2 cells have diminished levels of hRif1 whereas other ALT lines such as GM847, U2OS, and VA-13 cells have normal hRif1 levels (Figure 1-7B). It is unclear how and why this decrease in Rif1 protein is observed with these cell lines and it has not been determined if these cell lines have Rif1 mutations at the DNA level or if they fail to express Rif1 mRNA. The inability of the Rif1 antibodies to detect Rif1 in the murine NIH3T3 cells merely indicates that these antibodies do not cross-react with mouse Rif1. Mouse Rif1 does exist and studies to elucidate the role of mouse Rif1 in vivo are currently being performed (S. Buonomo, unpublished results, (Adams and McLaren 2004)). As mentioned in the introduction, ALT resembles the survivor pathways in yeast that lack telomerase. *S. cerevisiae* Rif1 affects the distribution between type I and type II survivors (Teng et al. 2000). The mechanism underlying this is unclear, but a similar mechanism may be occurring in human ALT cells where Rif1 can inhibit the initiation or maintenance of ALT. This proposed mechanism is still highly speculative. A subset of ALT cells, such as Saos-2, may actually require the loss of Rif1 in order to survive. The antibodies 1025 and 1067 fail to detect Rif1 in NIH 3T3 cells, indicating that they do not cross-react with mouse Rif1 (Figure 1-7B). HeLa cells in G1, S, or G2/M phase obtained by centrifugal elutriation contained similar amounts of Rif1 protein (Figure 1-7C). FACS analysis of the individual elutriation fractions which were pooled to generate the G1, G1/S, S and G2/M fractions is shown in figure 1-7C.

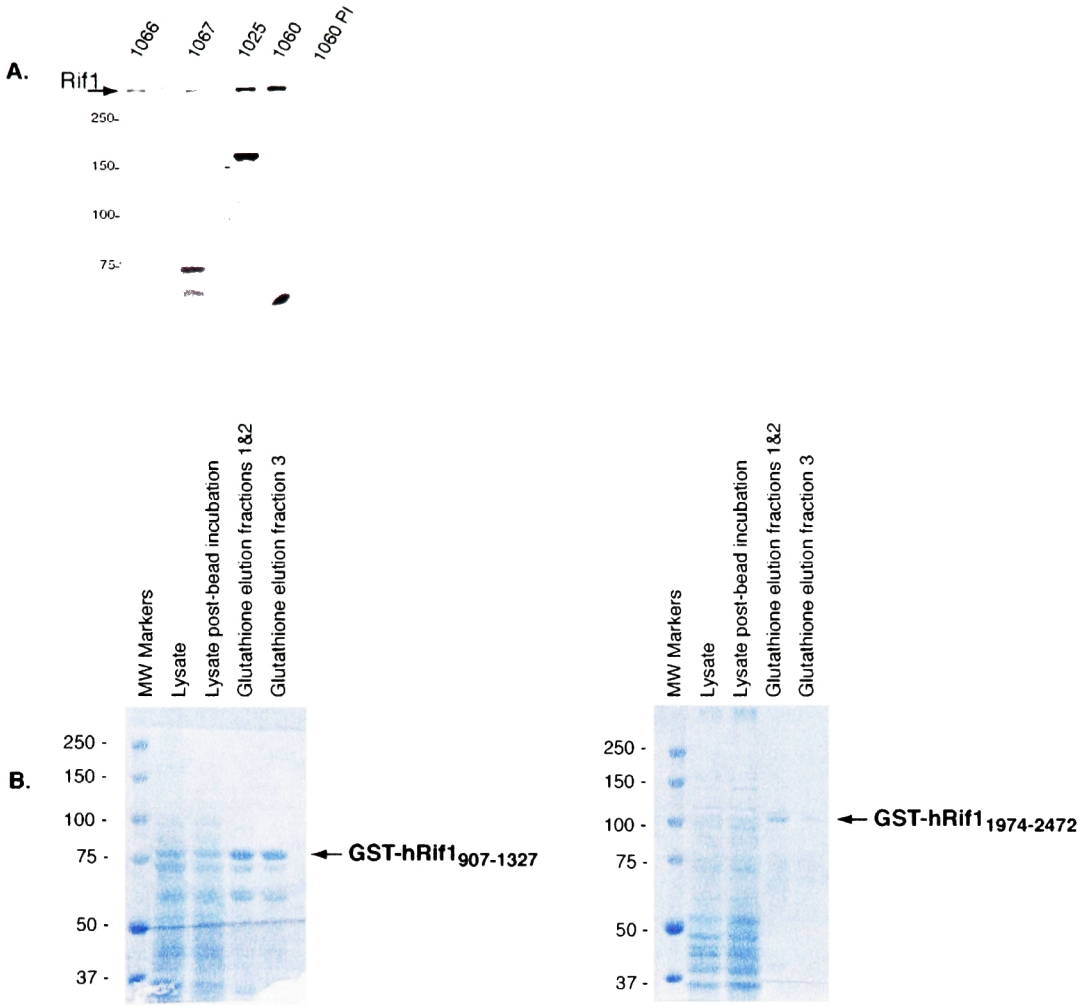

Figure 1-6. Antibodies to human Rif1.

A. Detection of human Rif1 protein. Immunoblots of HeLa whole cell extract probed with the indicated antibodies or a pre-immune serum (1060 PI).

B. GST fusion proteins. GST-fusion proteins containing GST fused to either hRif1 amino acids 907-1327 or hRif1 amino acids 1979-2296 were produced in BL21 strain *E. coli*.

Figure 1-7. Human Rif1 is expressed ubiquitously.

A. Rif1 RNA levels in human tissues. A Rif1-specific sequence was used to probe a multiple tissue northern blot (Clontech). RNA sources are indicated.

B. Immunoblotting of Rif1 in multiple cell lines. Whole cell lysates were made from HeLa1.2.11, VA-13, GM847, Saos-2 and NIH-3T3 cells. Immunoblots were performed using Rif antibodies 1025 and 1067. The tubulin immunoblot serves as a loading control.

C. Rif1 expression throughout the cell cycle. HeLa cells were subjected to elutriation. FACS analysis was performed on the resulting fractons. Whole cell lysates were then prepared from the pooled fractions as indicated. Immunoblotting was performed using antibodies recognizing Rif1 (1060) and tubulin. Elutriation and FACS analysis were performed by Jeffrey Ye and Lei Zheng. The drop in G2/M Rif1 level was not reproducible.

A.

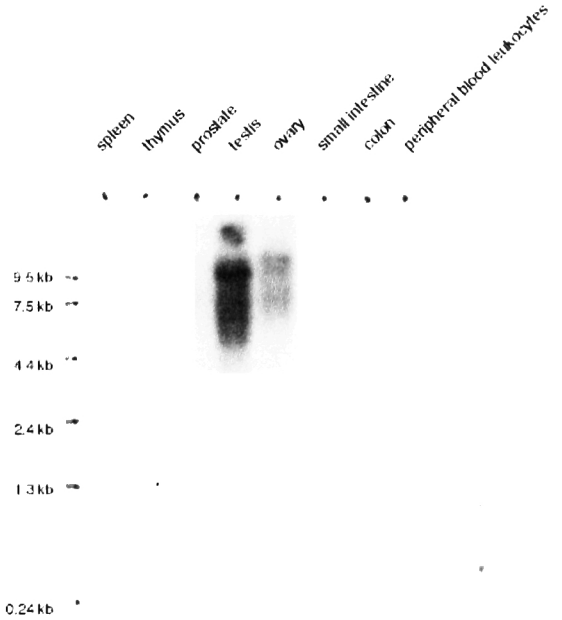
spleen
thymus
prostate
testis
ovary
small intestine
colon
peripheral blood leukocytes
9.5 kb
7.5 kb
4.4 kb
2.4 kb
1.3 kb
0.24 kb

B.

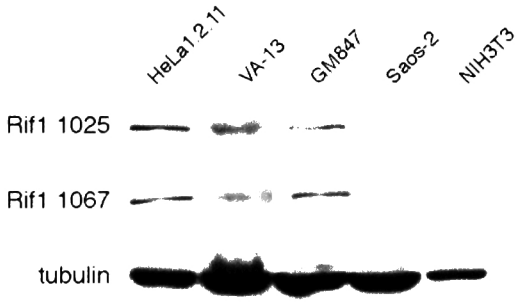
HeLa1.2.11
VA-13
GM847
Saos-2
NIH3T3
Rif1 1025
Rif1 1067
tubulin

C.

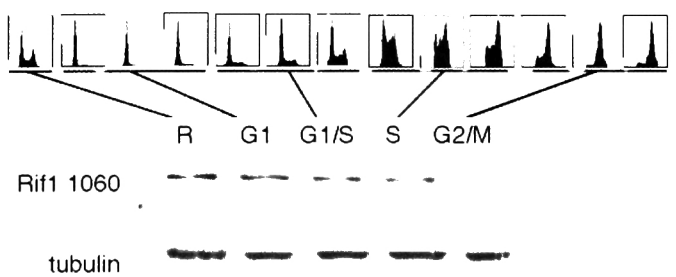
R
G1
G1/S
S
G2/M
Rif1 1060
tubulin

Indirect immunofluorescence (IF) with Rif1 antibodies revealed a nuclear staining pattern with most of the signal distributed in a fine granular pattern throughout the nucleus of interphase cells (Figure 1-8A). We also observed one or a few nuclear sites of more intense Rif1 staining with the Rif1 antibodies 1025, 1060, 1066, and 1067 (Figure 1-8A and Chapter 2). Cell cycle experiments using HeLa cells released from double thymidine block were conducted in order to determine if these Rif1 dots varied during the cell cycle. Almost no cells displayed the intense dot pattern after release from double thymidine block (Figure 1-9A and B). Between 50 and 70 percent of cells display one or more intense Rif1 foci after the 10 hr point (Figure 1-9A and B). This indicated that these Rif1 dots formed as cells exited mitosis and disappeared in S-phase. Rif1 dots did not co-localize with antibodies to coilin (a marker for Cajal bodies) and their nature remains to be determined (Figure 1-10). Rif1 was also found at the mid-body of the cell and in the Golgi complex. The mid-body is a structure that forms at the point of cell division as cells undergo cytokinesis and its exact role is unclear. The localization of Rif1 to the mid-body is seen with antibodies 1025 and 1060 (Figure 1-11A). Using anti-Rif1 antibody 1025, Rif1 co-localizes with the Golgi complex protein GM130 (Figure 1-11B). The localization of Rif1 to the Golgi is only observed with antibody 1025, so it is likely that this is actually an artifact or that 1025 cross-reacts with another protein that is

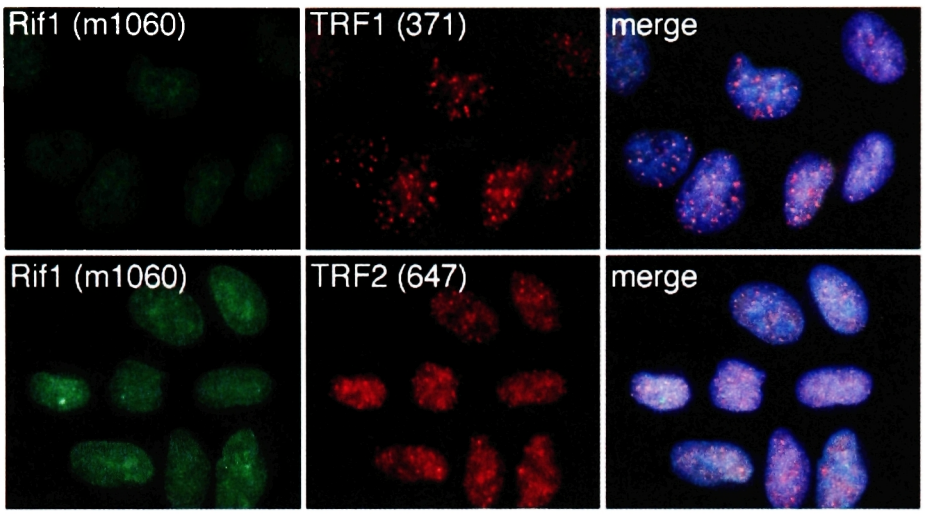

Figure 1-8. Rif1 does not accumulate at telomeres.

Rif1 is a nuclear protein. Immunofluorescence (IF) of paraformaldehyde-fixed HeLa1.2.11 cells with mouse serum raised against Rif1 antigen 1060 (green) and antibodies against TRF1 (371) and TRF2 (647) (both red) along with DAPI staining (blue).

Figure 1-9. Cell-cycle distribution of Rif1 dots.

A. HeLa1.2.11 cells were synchronized using a double-thymidine block. Cells were then released into media and fixed at the time points indicated. IF was performed on fixed cells. Cells were stained with Rif1 antibody (1060) and DAPI and the percentage of cells with at least one Rif1-intense focus was determined by counting 200 cells. Each color represents an independent count from the same experiment.

B. A micrograph of double thymidine arrested HeLa1.2.11 cells treated as in A at 0 and 10.5 hr post-release as indicated. Cells were stained with Rif1 1060 (green).

A

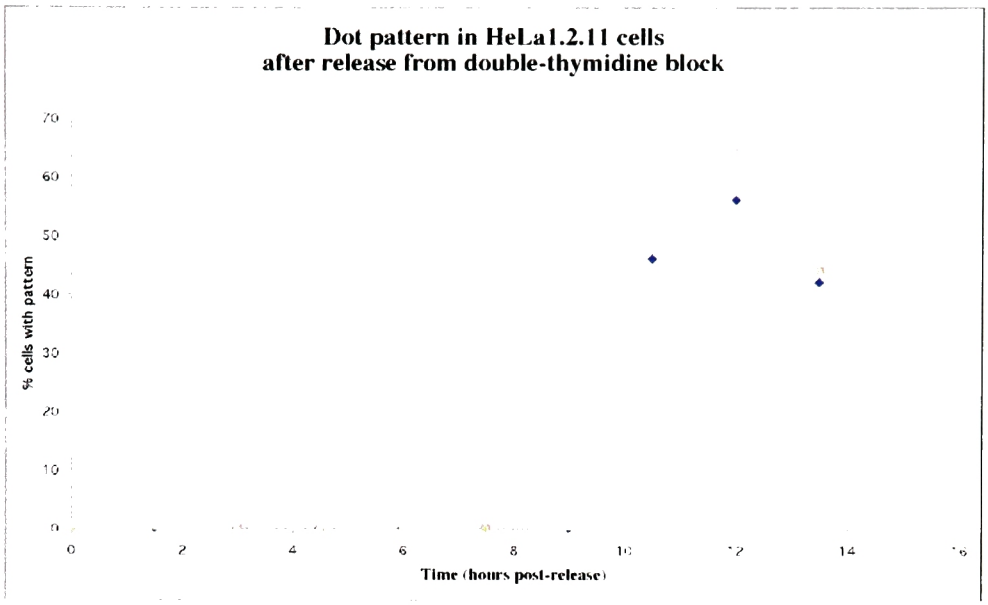
Dot pattern in HeLa1.2.11 cells
after release from double-thymidine block
% cells with pattern
70
60
50
40
30
20
10
0
0
2
4
6
8
10
12
14
Time (hours post-release)

B

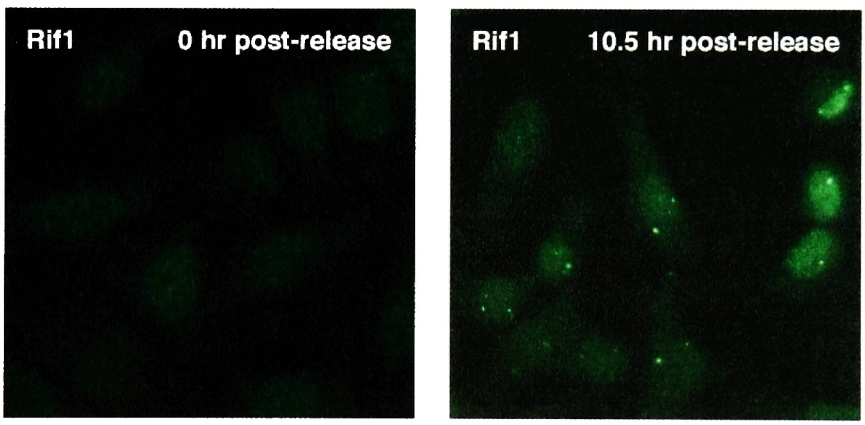
Rif1
0 hr post-release
Rif1
10.5 hr post-release

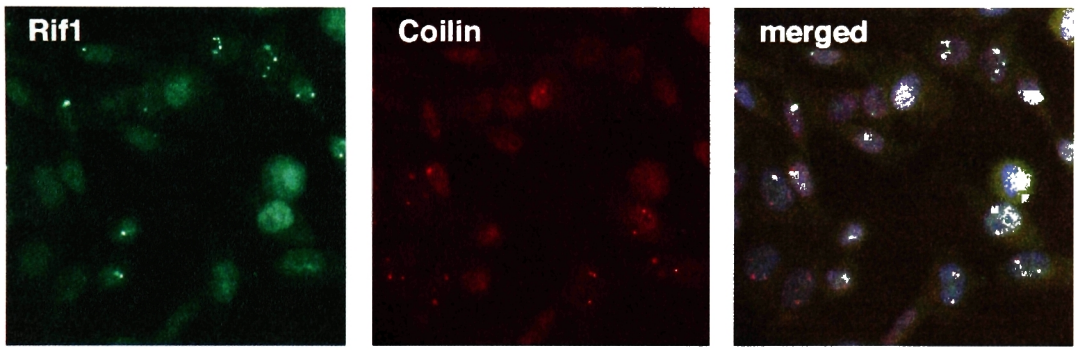

Figure 1-10. Rif1 dots do not co-localize with Cajal bodies.

IF performed on HeLa1.2.11 cells using antibodies against Rif1 (green) and coilin (red) along with DAPI (blue).

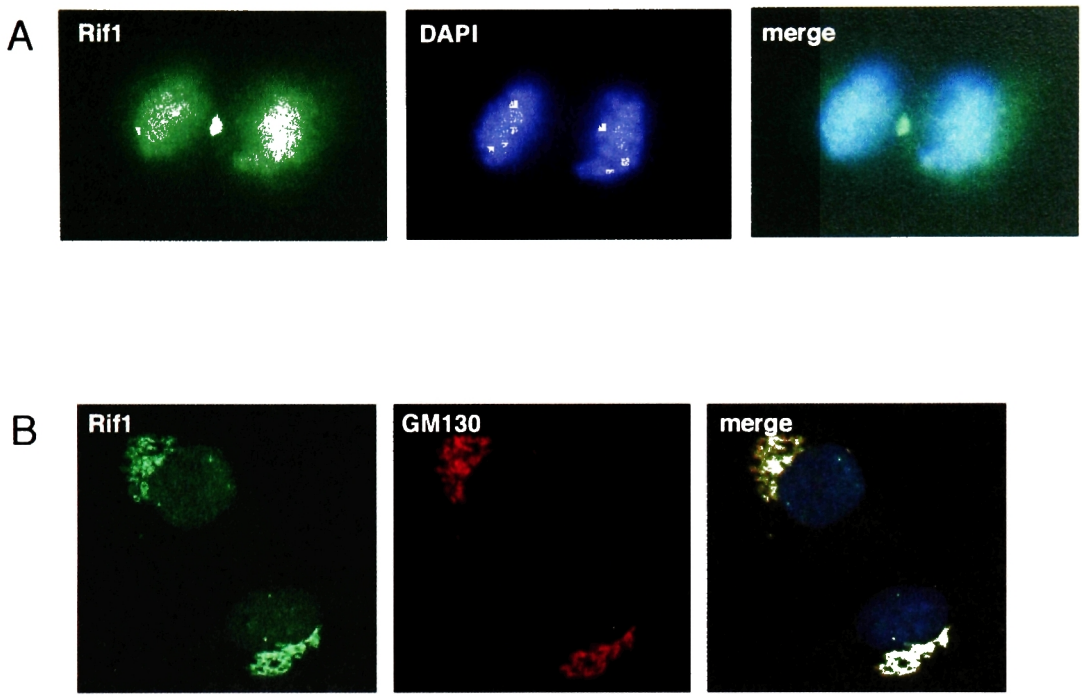

Figure 1-11. Localization of Rif1 to the mid-body and Golgi complex.

A. Rif1 at the mid-body during telophase. IF was performed on paraformaldehyde-fixed HeLa1.2.11 cells. Cells were stained with Rif1 1060 (green) and DAPI.

B. Rif1 in the Golgi complex. IF was performed on paraformaldehyde-fixed BJ/hTERT cells. Cells were stained with Rif1 1025 (green), GM130 (red) and DAPI. This localization is only observed by using Rif1 1025 antibody.

at the Golgi complex (Figure 1-11B). The possible role of Rif1 at both the mid-body and Golgi apparatus is currently unknown. The single dot pattern was not suppressed in cells treated with Rif1 siRNA. Whether the Golgi pattern disappears after Rif1 siRNA treatment was not determined.

Dual IF with markers for telomeric sites, including TRF1, TRF2, and Rap1, failed to reveal accumulation of Rif1 on chromosome ends (Figure 1-5 and Chapter 2). This failure of Rif1 to co-localize with telomeres occurs in HeLa, IMR90, and BJ cells. Negative results were also obtained using different methods for cell fixation (paraformaldehyde and methanol) or extraction of soluble nucleoplasmic proteins with Triton X-100. Co-immunoprecipitation (co-IP) experiments were performed in order to determine if hRif1 interacts with known telomere proteins. Co-IP failed to find an association of Rif1 with TRF1, TRF2, and Rap1 in HeLa1.2.11 cells. Antibodies against Rif1 are able to successfully immunoprecipitate Rif1 from HeLa1.2.11 whole cell extracts (Figure 1-12B). TRF1, TRF2 and Rap1 are not detected in Rif1 immunoprecipitates (Figure 1-12A, E, and F). Conversely, Rif1 is not detectable in TRF1 and TRF2 immunoprecipitates (Figre 1-12B). There is a small amount of Rif1 in the Rap1 immunoprecipitate shown, but this is not reproducible in other experiments (Figure 1-12B). The telomere complexes behaved as expected. As a positive control, TRF2 and Rap1 interact in this co-IP experiment (Figure 1-12A and E). Neither Rap1 nor TRF2 interact with TRF1 in this experiment (Figure 1-12A,E, and F).

Co-IP was also used to determine whether or not Rif1 interacts with components of the Mre11 complex. Using co-IP of endogenous complexes, Nbs1 is detected in Mre11 immunoprecipitate as expected (Figure 1-12C and D). In this experiment, the

Mre11 immunoprecipitate contains detectable levels of Rif1 (Figure 1-12B). Rif1 immunoprecipitates contain no more Mre11 than the beads alone control and only a small amount of additional Nbs1 (Figure 1-12C and D). It is unclear if these results indicate a true biochemical interaction between Rif1 and the Mre11 complex. It is likely that either the Mre11 antibody used cross-reacts with additional proteins or that only a small percentage of the Mre11 complex is engaged in a complex with Rif1.

Chromatin immunoprecipitations (ChIP) with Rif1 antiserum did not bring down telomeric DNA (data not shown; experiment performed by Jill Donigian with technical assistance from Diego Loayza). In this experiment, TRF1, TRF2, and Tin2 immunoprecipitates contained telomeric chromatin. These findings do not exclude a possible association of a minor fraction of Rif1 with telomeric sites or association of Rif1 with telomeres in specialized cells or in response to specific stimuli.

Interestingly, Rif1 associated with unusual telomeric loci present in certain ALT cell lines. As discussed in the introduction, these structures are referred to as ALT associated PML Bodies, or APBs. IF analysis showed that Rif1 associated with APBs in the ALT cell line GM847 (Figure 1-13). Rif1 co-localizes with APBs in only about 20% of cells and only a fraction of APBs contain Rif1 within many cells. This may indicate that APBs resemble DNA damage foci or that the telomeric DNA in the APBs represent a rare state of the telomeric complex in which Rif1 contributes to telomere function.

Figure 1-12. Co-immunoprecipitation of human Rif1 and known telomeric proteins. Buffer C extracts were prepared from HeLa1.2.11 cells and antibodies against Rif1 (1060), Rap1 (765), TRF1 (371) and TRF2 (647), Mre11 (874) and Nbs1 (16/9, gift of John Petrini) were used to immunoprecipitate endogenous complexes. Pellets were washed and Laemelli buffer was added. The indicated IP pellets were immunoblotted with antibodies against Rap1, Rif1, Mre11, Nbs1, TRF2 and TRF1 (A-F, respectively). 1% of the input whole cell extract and a sample pellet with no IP antibody (beads alone) were also immunoblotted. The lower bands in the immunoprecipitate lanes in Rap1 and TRF1 immunoblots represent the IgG band of the immunoprecipitating antibodies.

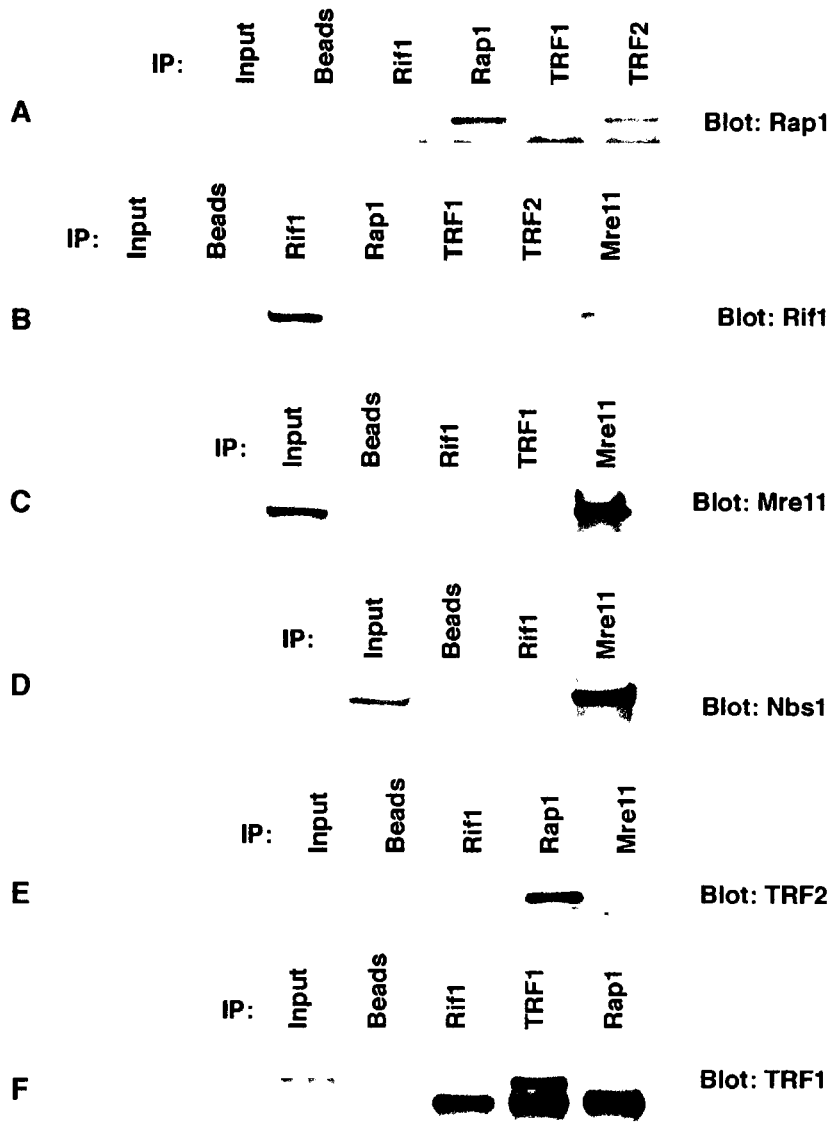
A
IP:
Input
Beads
Rif1
Rap1
TRF1
TRF2
Blot: Rap1
B
IP:
Input
Beads
Rif1
Rap1
TRF1
TRF2
Mre11
Blot: Rif1
C
IP:
Input
Beads
Rif1
TRF1
Mre11
Blot: Mre11
D
IP:
Input
Beads
Rif1
Mre11
Blot: Nbs1
E
IP:
Input
Beads
Rif1
Rap1
Mre11
Blot: TRF2
F
IP:
Input
Beads
Rif1
TRF1
Rap1
Blot: TRF1

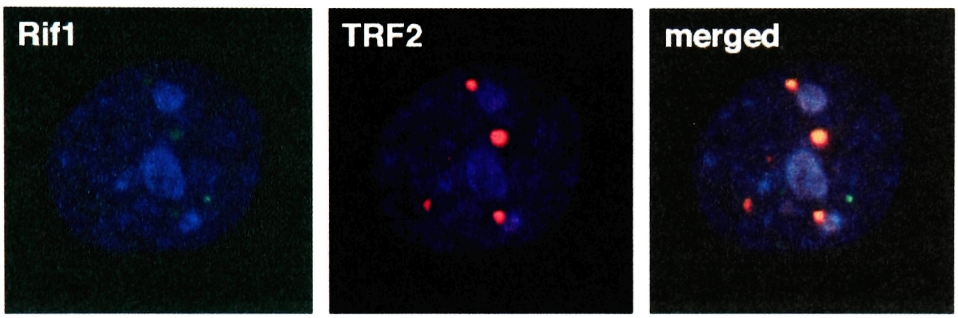

Figure 1-13. Rif1 is found at APBs in ALT cells.

IF of Rif1 (1060) with TRF2 (monoclonal anti-TRF2) on APBs in the ALT cell line GM847.

Discusssion

This chapter discusses the identification and initial characterization of human Rif1, an ortholog of Rif1 in yeast. Orthologs are genes that have primary sequence similarity between two organisms, whereas homologs have primary sequence similarity and the same function. We classify human Rif1 as an ortholog rather than a homolog because Rif1 plays a role in telomere biology in yeast and a role in the DNA damage response in human cells. Further work may establish that yeast and human Rif1 are homologs. Antibodies were raised against this large molecular weight protein in order to address whether or not human Rif1 is found at human telomeres. IF studies, co-immunoprecipitation experiments, and ChIP failed to detect an accumulation of Rif1 at telomeres, an interaction with telomeric proteins, or an association with telomeric chromatin, respectively. The failure to detect Rif1 at human telomeres under the conditions tested does not conclusively rule out a possible role for Rif1 at human telomeres. Rif1 can be found at APBs, although this is no guarantee that hRif1 localizes to human telomeres because APBs may contain other factors not normally found at telomeres such as Rad52 (Yeager et al. 1999).

There are both possible technical reasons and biological reasons that these experiments may represent a false negative result for Rif1 at telomeres. Technical limitations involve the ability of antibodies to recognize a potentially small amount of telomeric Rif1 and possibly weak or transient interactions between Rif1 and telomeric protein complexes. A number of biological factors may contribute to an inability to localize Rif1 to the telomere in human cells. First, Rif1 may not be constuitively at

telomeres and may require a signal or some other condition to localize to telomeres. There is a precedent for the inability to detect Rif1 at telomeres even when it is clearly telomeric. The primary IF data in *S. pombe* reveals that spRif1 only co-localizes with Taz1 in strains lacking spRap1; wild type strains display a diffuse nucleoplasmic staining for tagged spRif1 (Kanoh and Ishikawa 2001). However, spRif1 accumulates at telomeric chromatin (Kanoh and Ishikawa 2001). Thus, further work is needed to address the issue of whether Rif1 is at telomeres. A complete data set would include an analysis of telomere length when levels of human Rif1 are perturbed and studying cells expressing altered alleles of human Rif1. The human situation may also resemble the situation in *S. pombe* where a component of the telomeric complex, such as Rap1, must be deleted or altered before Rif1 is detected at telomeres.

Rif1 was also found at a variety of other sites in the cell and the exact role of Rif1 at these sites remains unclear. The cell-cycle nuclear dot pattern is a complete mystery. The localization of Rif1 at the Golgi apparatus is likely to be an artifact as it is only detected with the 1025 antibody and no others. The finding of Rif1 at the mid-body is more robust, seen with multiple antibodies, and may well represent a physiologic role for Rif1 in the execution of mitosis. It is possible that mice lacking Rif1 will demonstrate phenotypes related to these other cellular localizations for Rif1.

Chapter 2 – The role of human Rif1 in the DNA damage response

Introduction

Evidence in yeast telomere biology suggests that Rif1 is in a common pathway with TEL1 and MEC1, orthologs of mammalian ATM and ATR. Rif1, Tel1 and Mec1 play important roles in telomere length regulation in both *S. cerevisiae* and *S. pombe*. As mentioned previously, yeast strains deficient in Rif1 have elongated telomeres (Hardy et al. 1992). Rif1 is in the telomerase epistasis group in terms of telomere length regulation with the other two groups being the Ku/Mre11/Xrs2/Rad50 group and the Cdc13 group (Nugent et al. 1998). Mutations in *S. cerevisiae* TEL1, the ATM ortholog, result in telomere shortening (Greenwell et al. 1995). Deletion of *S. cerevisiae* MEC1 and its ortholog *S. pombe* Rad3 leads to telomere shortening as well (Dahlen et al. 1998; Naito et al. 1998; Ritchie et al. 1999). Tel1 and Mre11, Xrs2, and Rad50 are in the same telomere length epistasis group (Ritchie and Petes 2000). Like ATM and ATR, Tel1 and Mec1 possess kinase activity and mutations in Tel1 and Mec1 that abolish kinase activity result in phenotypes identical to TEL1 and MEC1 deletion (Mallory and Petes 2000).

The combination of loss of TEL1 and MEC1 in *S. cerevisiae* or $tel1^+$ and $rad3^+$ in *S. pombe* results in disastrous consequences for yeast cells (Naito et al. 1998; Ritchie and Petes 2000). tel1-Δ mec1-Δ cells undergo telomere loss and senescence. Deletion of both tel1 and rad3 in *S. pombe* leads to the loss of all telomeric DNA and $tel1^-$ $rad3^-$ cells survive by circularizing their chromosomes (Naito et al. 1998). *S. cerevisiae* tel1 mec1 cells can not circularize their chromosomes and undergo a senescence phenotype similar to the loss of telomerase (Ritchie et al. 1999). Thus, *S. pombe* cells survive only because they are able to circularize their chromosomes after the loss of telomeric DNA. Strains

lacking TEL1 and MEC1 senesce later than tel1 mec1 tlc1 strains and strains deleted for tel1 and mec1 still have telomerase activity in vitro, suggesting that Tel1 and Mec1 do not act by changing telomerase activity (Chan et al. 2001).

Studies of telomeres with X subtelomeric repeats and Y' subtelomeric repeats initially demonstrated that the telomere length regulation of Rif1 is affected by Tel1 (Craven and Petes 1999). Rif1 deletion is able to bypass the senescence phenotype of tel1 mec1 cells because tel1 mec1 cells undergo senescence, yet tel1 mec1 rif1 yeast are able to survive (Chan et al. 2001). Thus, the deletion of Rif1 enables tel1 mec1 cells to bypass senescence, which suggests that Rif1 may function in the same pathway as Tel1 and Mec1. Additionally, rif1 rif2 cells have long, heterogeneous telomeres, whereas tel1 mec1 sml1 rif1 rif2 (the SML1 deletion is necessary to maintain viable cells in a MEC1 delete strain) do not have heterogeneous telomeres (Chan et al. 2001). The epistatic relationship and underlying mechanism between TEL1 and RIF1 is unclear. Because of this link in yeast, we examined the possible relationship between Rif1 and ATM and ATR in human cells.

This chapter documents the unexpected discovery that human Rif1 is involved in the DNA damage response. The characteristics of Rif1 ionizing radiation induced foci (IRIF), such as the rapid kinetics of formation and dose response are discussed. Rif1 IRIF co-localize with a number of other previously identified DNA damage response proteins, specifically ATM, BRCA1, Chk1, γ-H2AX, 53BP1 and the Mre11 complex. Furthermore, Rif1 localized to uncapped telomeres, as do other DNA damage response factors. Whereas inhibition of ATR signaling did not inhibit the Rif1 response, ATM deficient cells treated with IR or UV lacked Rif1 foci even after prolonged incubation or

high radiation dose. The Rif1 response also depended on the presence of 53BP1 but was not affected by reduced function of BRCA1, Chk2, Nbs1, and Mre11. RNAi-mediated Rif1 inhibition resulted in increased radiosensitivity, indicating that Rif1 function contributes to the ATM-mediated protection against exposure to ionizing radiation.

Results

In cells treated with IR, the Rif1 IF signal became redistributed into discrete foci that were detectable with all Rif1 antibodies (Figure 2-1). This response was rapid, occurring within 5 min, and persisted for many hours (Fig. 2-1C). All cells of an asynchronous population showed the same or a similar response indicating that Rif1 can relocalize in G1, S, and G2 cells. Rif1 foci were observed after an IR dose as low as 0.5 Gy and the number of foci increased with higher doses, reaching a plateau between 10 and 20 Gy (Fig. 2-1A). Rif1 ionizing-radiation-induced foci (IRIF) exhibit similar behavior, such as a distribution in number of IRIF per cell, a dose-response relationship in average number of foci, and changes in foci number and size over time, to previously described DNA damage response factors such as Mre11 and 53BP1 (Schultz et al. 2000; Mirzoeva and Petrini 2001). IRIF were observed in BJ cells using the four antibodies 1025, 1060, 1066, and 1067 that recognize human Rif1 (Figure 2-2).

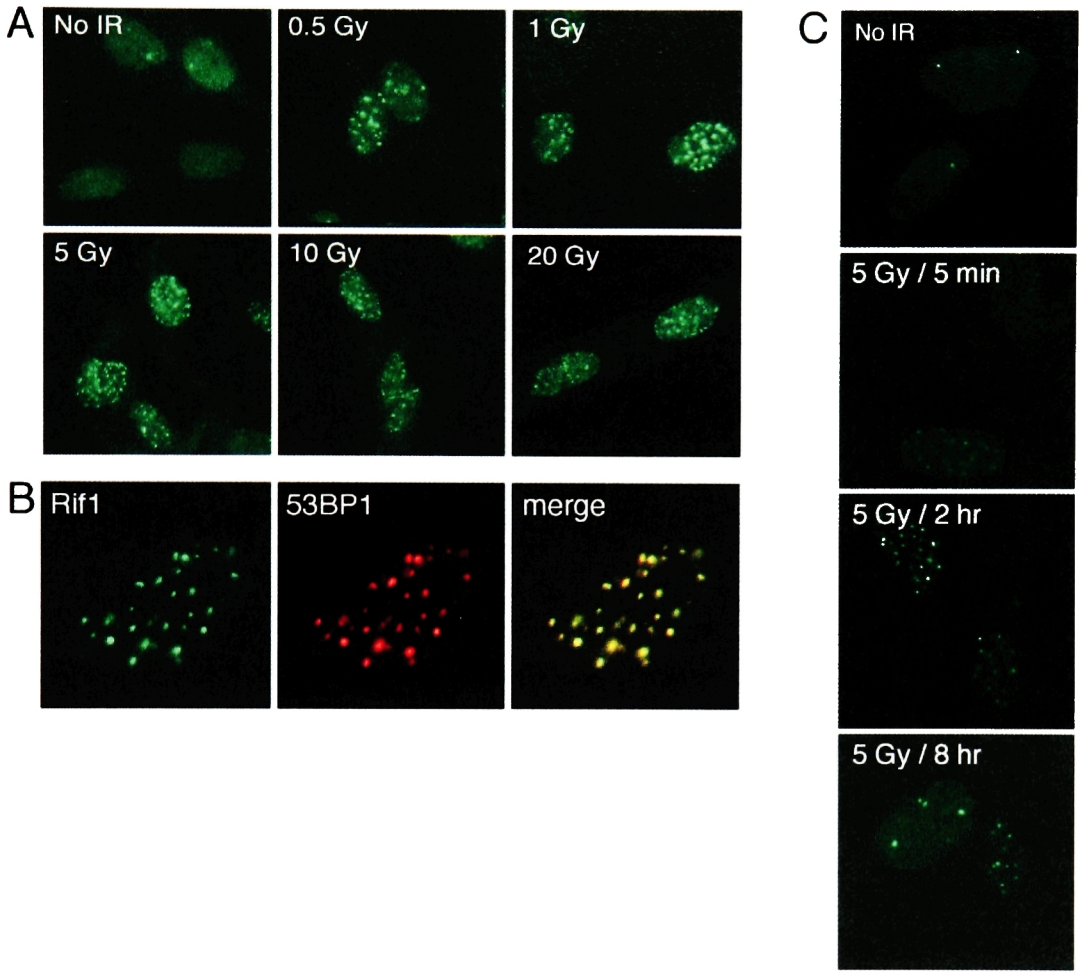

Figure 2-1. Human Rif1 forms foci in cells exposed to ionizing radiation.

A. Rif1 foci after IR treatment. Rif1 IF (Ab 1060) of IMR90 primary fibroblasts (p17), exposed to the indicated levels of IR and fixed after 30 min.

B. Co-localization of Rif1 with 53BP1. IF of IMR90 (p15) cells, exposed to 5 Gy IR and fixed 2 hr post-IR. Cells were then stained with Rif1 (green) and 53BP1 (red) antibodies for IF.

C. Time course of the Rif1 response. IF as in A. but after 5 Gy IR and with fixation at the indicated time points.

IR-induced foci were observed in a wide range of cell lines examined, including IMR90, BJ, HeLa, and U2OS cells (Figure 2-1, 2-2, 2-10B and 2-12B). The IR-induced Rif1 foci showed a complete co-localization with the DNA damage response factor 53BP1 (Anderson et al. 2001; DiTullio et al. 2002; Wang et al. 2002) (Fig. 2-1B and see below), consistent with the idea that Rif1 re-localizes to sites of DNA damage. Rif1 does not form these foci or co-localize with 53BP1 in cells not exposed to radiation (Figure 2-2, 2-3, 2-4 and 2-7A). IR-induced foci did not co-localize with the known telomeric proteins TRF1, TRF2, and Rap1 (Figure 2-3).

Rif1 also formed foci after treatment of cells with MMS or etoposide and the Rif1 foci in these cells co-localized with 53BP1 foci (Figure 2-4A). UV treatment resulted in the formation of Rif1 foci which co-localized with 53BP1 foci (Figure 2-4B). UV treatment induced a Rif1 response in a subset of the cells (~20-30%) whereas IR-induced Rif1 foci occurred in all interphase cells (Figure 2-1 and 2-4C). Furthermore, the UV-induced Rif1 foci were slow to develop compared with IR-induced Rif1 foci. The UV-induced foci first appear 1 hr after UV exposure (Figure 2-4B). This time frame is markedly different from the rapid response after IR. A possible explanation for the occurrence of foci in only a subset of cells treated with UV as well as the delay in Rif1 response to UV is that the primary UV-induced lesions are converted into double-stranded breaks (DSBs) during S phase and that Rif1 actually responds to these DSBs.

In addition to 53BP1, the Rif1 foci contained several other DNA damage response factors, including γ-H2AX, Chk1 phosphorylated on S317, ATM phosphorylated on S1981, Rad17 phosphorylated on S645, Mre11, and BRCA1 (Figure

Figure 2-2. Multiple Rif1 antibodies recognize Rif1 IRIF.

BJ primary fibroblasts were fixed 2 hr after exposure to 5 Gy IR. Cells were stained with Rif1 (antibody 1025 in A., antibody 1060 in B., antibody 1066 in C., and antibody 1067 in D.). In A. and B., cells were also stained with 53BP1 antibodies (red). In C. and D., cells were also treated with DAPI (blue).

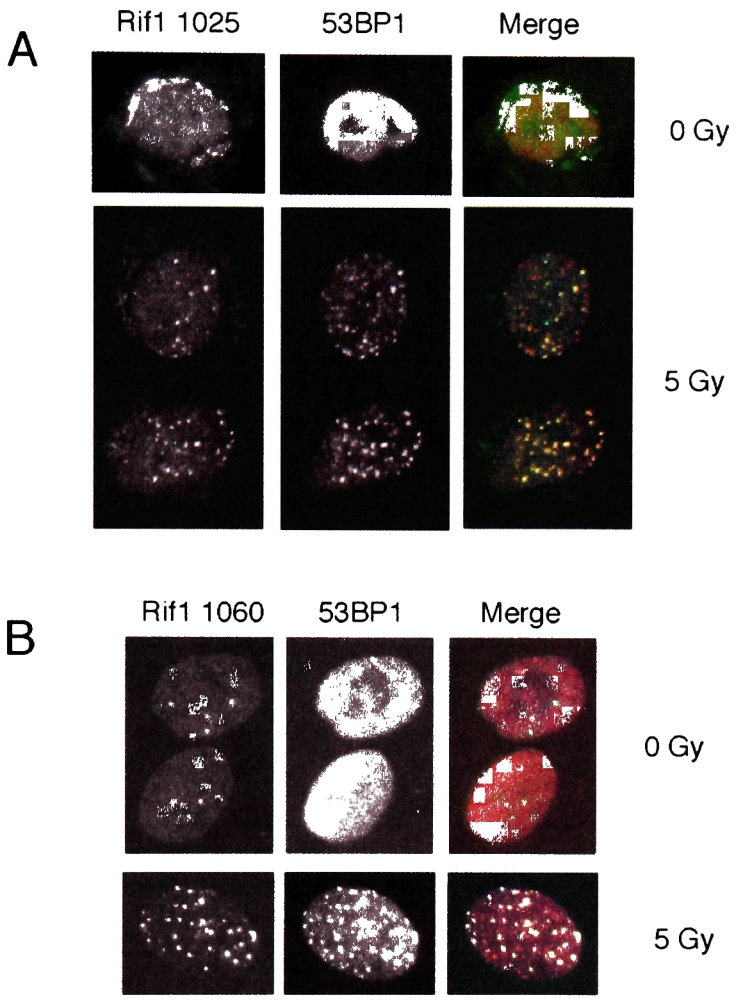
A
Rif1 1025
53BP1
Merge
0 Gy
5 Gy
B
Rif1 1060
53BP1
Merge
0 Gy
5 Gy
C
Rif1
1066
Merge
0 Gy
5 Gy
D
Rif1
1067
Merge
0 Gy
5 Gy

Figure 2-3. Rif1 IRIF do not co-localize with human telomeres.

A. HeLa1.2.11 cells were either untreated or exposed to 5 Gy IR and fixed 30 minutes post-IR. Cells were then stained with Rif1 (green), TRF1 (red) and DAPI (blue).

B. HeLa1.2.11 cells were either untreated or exposed to 5 Gy IR and fixed 30 minutes post-IR. Cells were then stained with Rif1 (green), TRF2 (red) and DAPI (blue).

C. HeLa1.2.11 cells were either untreated or exposed to 5 Gy IR and fixed 30 minutes post-IR. Cells were then stained with Rif1 (green), Rap1 (red) and DAPI (blue).

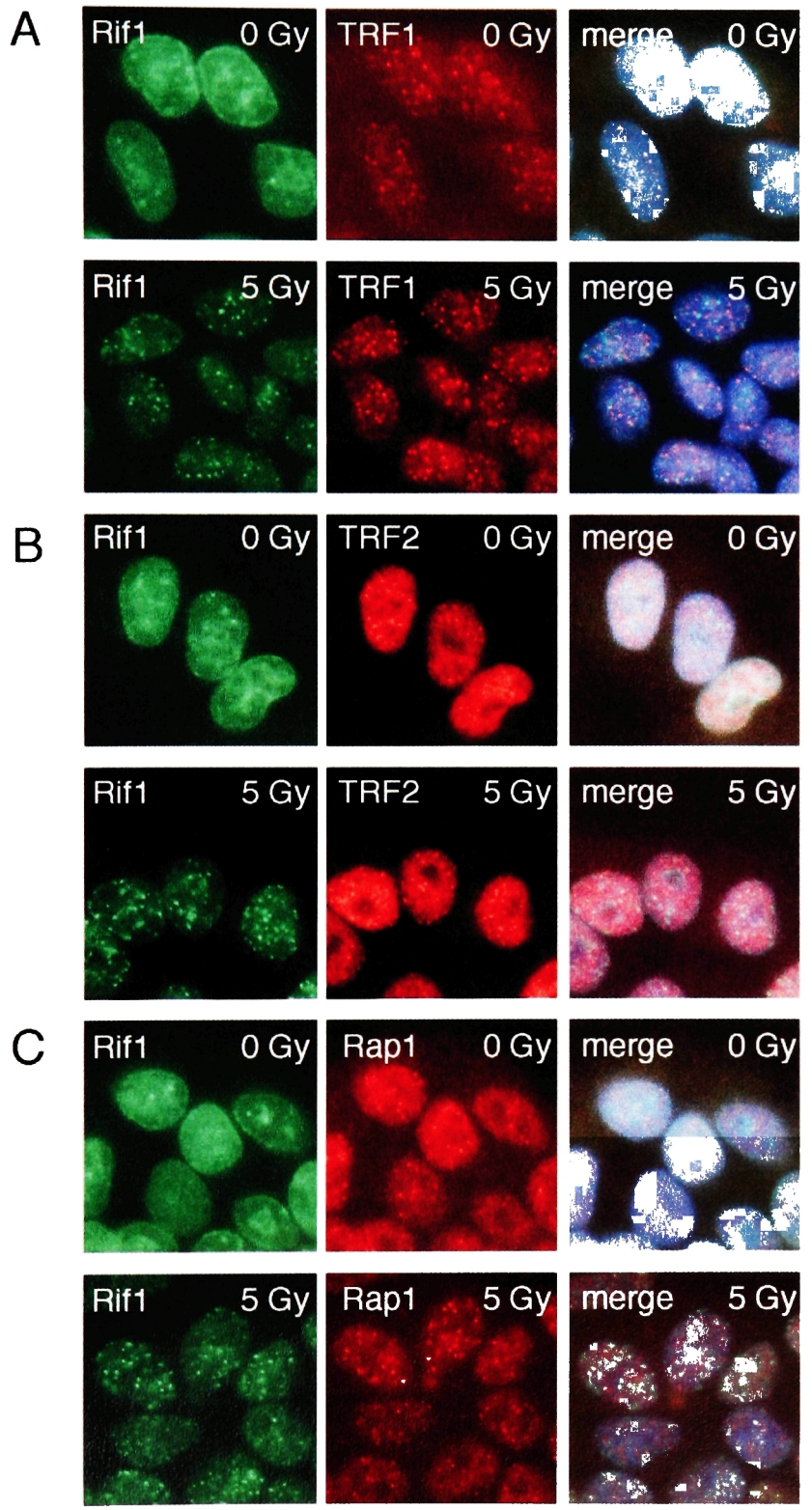
A
Rif1 0 Gy
TRF1 0 Gy
merge 0 Gy
Rif1 5 Gy
TRF1 5 Gy
merge 5 Gy
B
Rif1 0 Gy
TRF2 0 Gy
merge 0 Gy
Rif1 5 Gy
TRF2 5 Gy
merge 5 Gy
C
Rif1 0 Gy
Rap1 0 Gy
merge 0 Gy
Rif1 5 Gy
Rap1 5 Gy
merge 5 Gy

Figure 2-4. Rif1 forms foci following exposure to clastogenic drugs and UV treatment.

A. Rif1 foci in response to MMS, etoposide and hydroxyurea treatment. IMR90 (P15) cells were treated for 1 hr with 0.01% MMS, 50 mg/ml etoposide, or no drug prior to fixation. For HU treatment, IMR90 (p26) cells were incubated for 18 hr with 2 mM hydroxyurea prior to fixation. Rif1 and 53BP1 were detected as in Figure 1B.

B. Response of Rif1 to UV irradiation. IMR90 (P14) cells were exposed to UV light (25 J/m2), fixed at the indicated time points, and processed for Rif1 and 53BP1 IF as in A.

C. A subset of cells responds to UV irradiation. IMR90 (P14) cells were exposed to UV light (25 J/m2), fixed 1 hr post-UV, and stained with Rif1 antibody (green), 53BP1 antibody (red) and DAPI (blue).

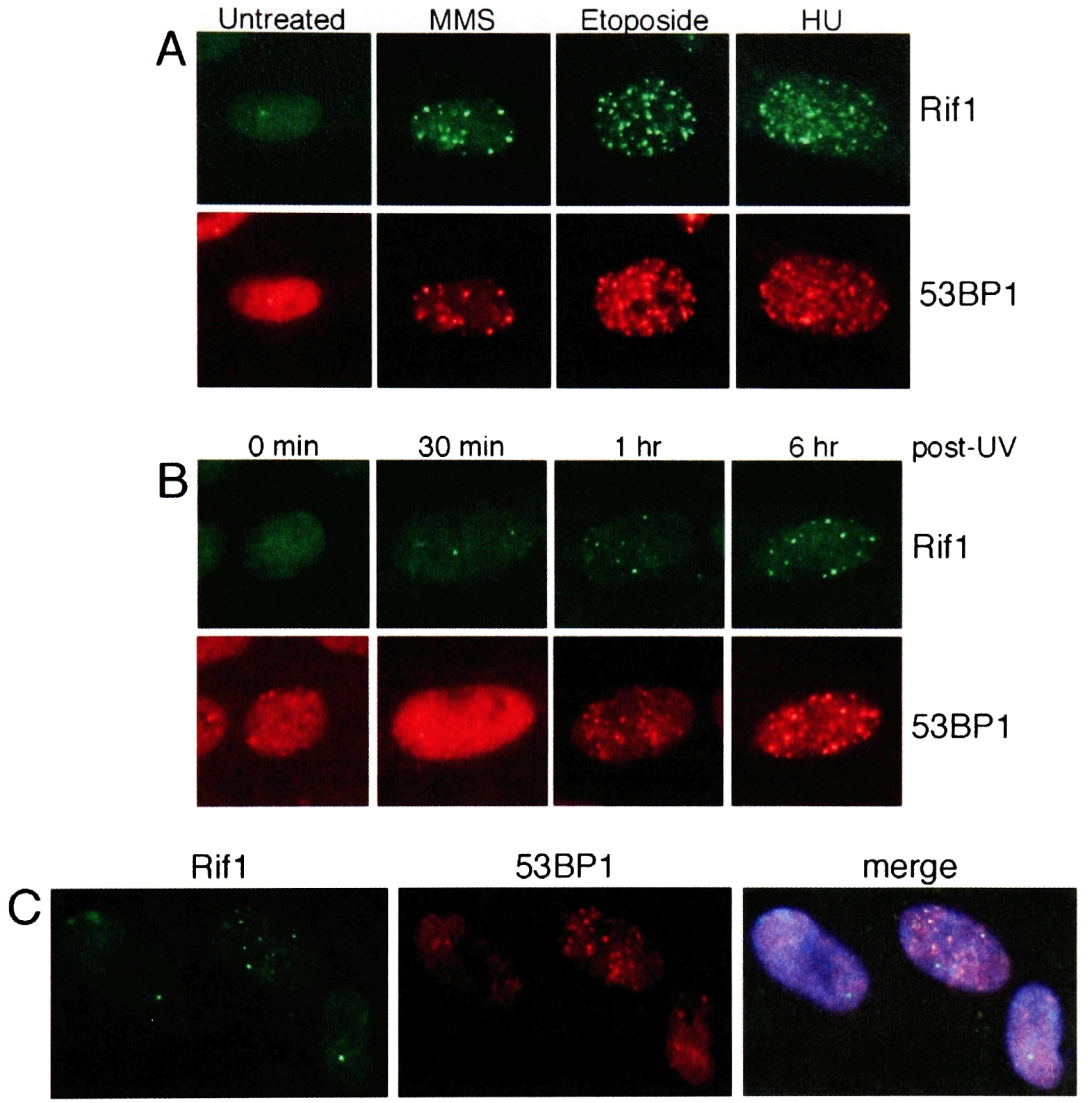
A
Untreated
MMS
Etoposide
HU
Rif1
53BP1
B
0 min
30 min
1 hr
6 hr
post-UV
Rif1
53BP1
C
Rif1
53BP1
merge

2-5). As a control, Rif1 IR-induced foci do not co-localize with the telomere proteins TRF1, TRF2, and Rap1 (Figure 2-3A-C). It has previously been shown that γ-H2AX, ATM phosphorylated on S1981, 53BP1, Rad17 phosphorylated on S645 and the Mre11 complex do not co-localize with telomeric proteins (Zhu et al. 2000; Takai et al. 2003). Rif1 behaves similarly to previously described factors that respond to the formation of double strand DNA breaks.

Work in the de Lange lab has previously shown that dysfunctional telomeres are recognized as sites of DNA damage (Takai et al. 2003). Cells have the ability to distinguish functional telomeres from DNA breaks and this distinction is made based on the presence of a specific telomeric protein complex (de Lange 2002). The main protective protein at telomeres is TRF2. Inhibition of TRF2 with a dominant negative allele or siRNA results in telomere uncapping. Such uncapped telomeres induce a cell cycle arrest and are processed by DNA damage repair pathways, including the NHEJ pathway which generates chromosome end fusions. Furthermore, uncapped telomeres activate the ATM-dependent DNA damage response (Takai et al. 2003). As a consequence, telomeres become associated with DNA damage response factors, such as Nbs1, 53BP1, ATM, Rad17, and γ-H2AX (Takai et al. 2003). The foci formed at uncapped telomeres resemble DNA damage response foci and are referred to as Telomere Dysfunction Induced Foci (TIFs). To test whether Rif1 is a component of the TIFs formed at uncapped, dysfunctional telomeres, IF was done in BJ/hTERT cells that were infected with an adenovirus expressing the dominant negative allele of TRF2 (Ad-TRF2$^{\Delta B\Delta M}$; (Karlseder et al. 1999)). Co-staining with an antibody to TRF1 was used to determine whether Rif1 binds to the telomeric sites.

Figure 2-5. Rif1 IRIF co-localize with other known DNA damage response proteins. IMR90 cells were treated with 5 Gy IR and fixed with paraformaldehyde 1 hr later. Cells were then co-stained for Rif1 (rabbit 1060, green) and BRCA1 (red) or Rif1 (mouse 1060, green) and ATM-S1981-P, Chk1-S317-P, g-H2AX, Rad17-S645-P and Nbs1 (red) as indicated. The merged images include DAPI stain (blue). For co-staining of Rif1 and Nbs1, cells were treated with cytoskeleton extraction buffer and fixed as in (Mirzoeva and Petrini 2001).

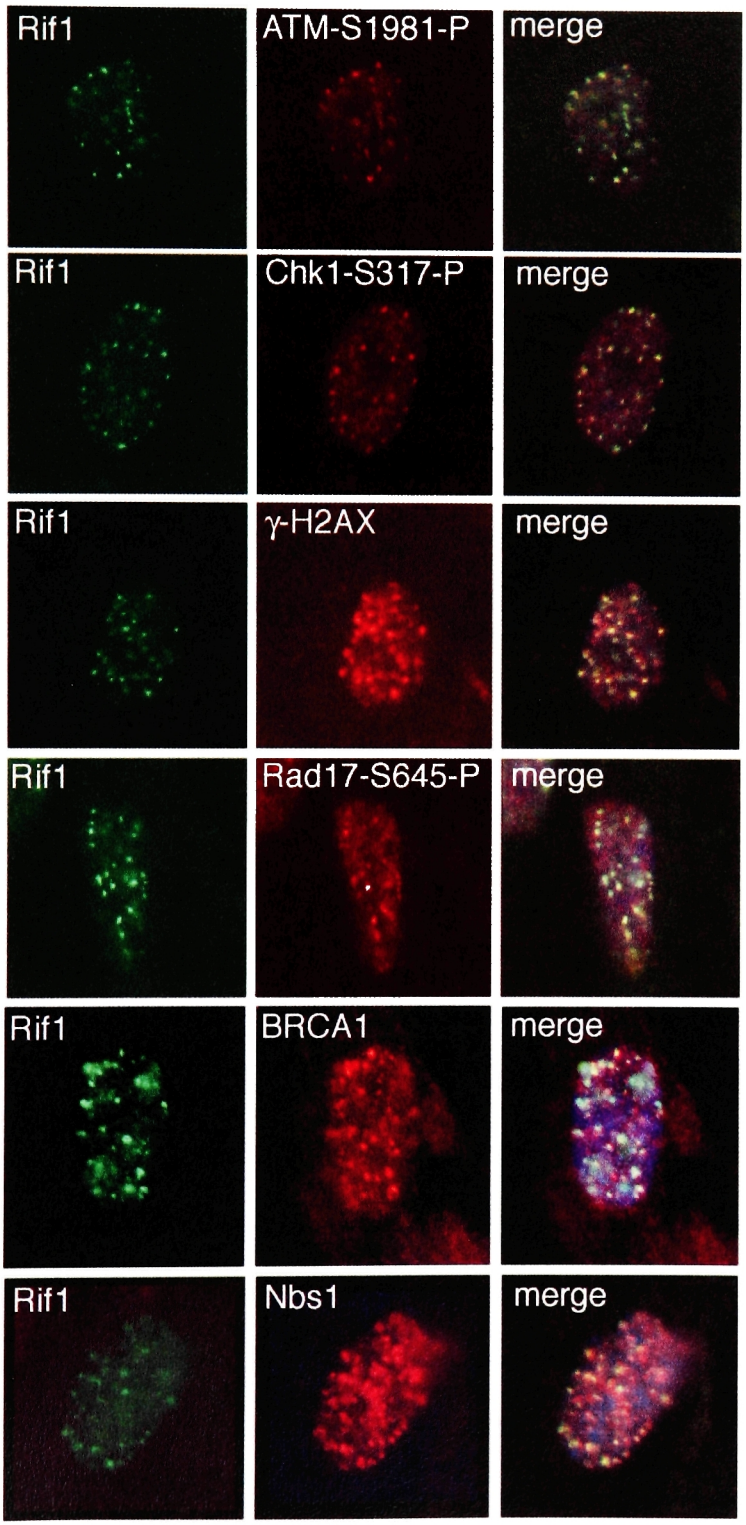
Rif1
ATM-S1981-P
merge
Rif1
Chk1-S317-P
merge
Rif1
γ-H2AX
merge
Rif1
Rad17-S645-P
merge
Rif1
BRCA1
merge
Rif1
Nbs1
merge

Comparison of cells infected with a control adenovirus and cells in which TRF2 was inhibited using Ad-TRF2$^{\Delta B \Delta M}$ showed that Rif1 formed foci on uncapped telomeres (Figure 2-6; experiment performed by Hiroyuki Takai). Thus, also in this regard, Rif1 behaves as other DNA damage response factors, many of which have no known role in normal telomere function.

The induction of Rif1 foci was severely reduced when cells were treated with inhibitors of the PI3 kinase-related family of kinases (PIKKs), which includes ATM and ATR. The central role of the ATM and ATR in the DNA damage response makes the dependence of Rif1 IRIF on ATM and ATR signaling an important question. The drugs caffeine and wortmannin were used in order to initially address whether Rif1 is dependent on PIKK family members in terms of foci formation. Treatment with caffeine and wortmannin almost completely abolished the Rif1 response to IR (Figure 2-7A and 2-7B). The effect of caffeine on Rif1 was more pronounced than its effect on 53BP1 (Figure 2-7A), suggesting that Rif1 is exquisitely sensitive to signaling by one or more PIKKs.

In order to test the dependence of Rif1 on the ATM kinase, we examined the response of Rif1 to IR and UV in cells derived from A-T patients. Two unrelated A-T fibroblast strains, AG02496 and AG04405, lacked the ATM kinase as verified by immunoblotting (Takai et al. 2003). These A-T cells failed to show Rif1 foci when examined 2 hr after 5 Gy (Figure 2-8A). Rif1 foci were also not observed after treatment with 20 Gy and at later time-points (up to 8 hr) (Figure 2-8A). By contrast, the A-T cells formed 53BP1 foci after IR (Figure 2-8A), albeit at diminished levels as previously noted

(Rappold et al. 2001). The A-T cells contained normal amounts of Rif1 proteins as detected by immunoblotting (Figure 2-8B). Although the figure depicts elevated Rif1 in cells exposed to 20 Gy, this is not reproducible.

Human Rif1 contains 11 ST and 13 QT sites that could potentially be a direct target of the ATM kinase, but direct evidence for the phosphorylation of Rif1 by ATM is not available at this stage. A number of DNA damage response proteins, including the large molecular weight proteins BRCA1, MDC1 and 53BP1, shift upward in immunoblots after being phosphorylated by ATM or ATR (Cortez et al. 1999; Goldberg et al. 2003; Lou et al. 2003a; Stewart et al. 2003). Rif1 does not have a detectable shift in immunoblots 4 hours after cells are exposed to 20 Gy IR (Figure 2-9). The blot shown contains varying amounts of Rif1 in the lanes, making interpretation difficult. In other experiments, the amount of Rif1 is equal between untreated and irradiated cells and no shift is detected. It is important to note that a lack of Rif1 shift in immunoblot following radiation exposure is not conclusive evidence that Rif1 is not phosphorylated by ATM. In vitro phosphorylation assays are underway to determine if Rif1 is directly phosphorylated by ATM.

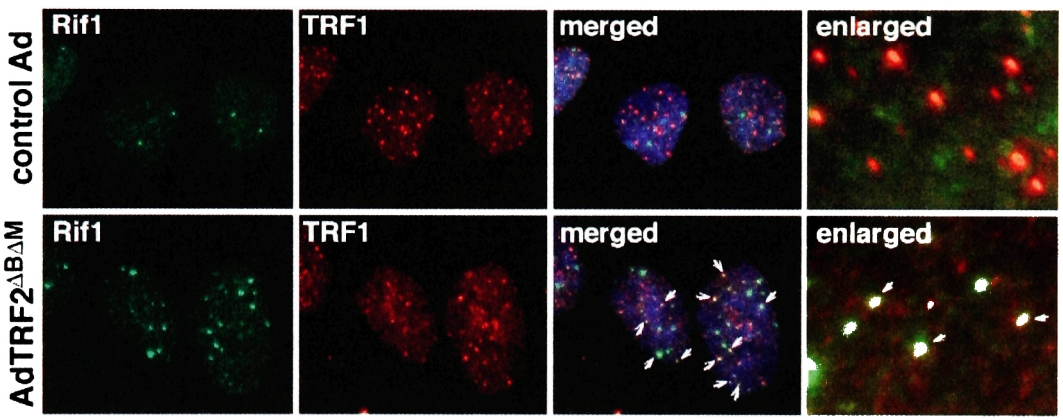

Figure 2-6. Rif1 localizes to dysfunctional telomeres.

hTERT-BJ cells were infected with the indicated adenoviruses (control: b-galactosidase virus) fixed 48-52 hr post-infection and processed for Rif1 (mouse anti-1060, green) and TRF1 (Ab 371; red) IF as described in (Takai et al. 2003). DNA was stained (DAPI, blue) in the merged images. White arrows highlight a subset of the Rif1 foci at telomeres. The enlarged images are derived from the same experiment. This experiment was conducted by Hiroyuki Takai.

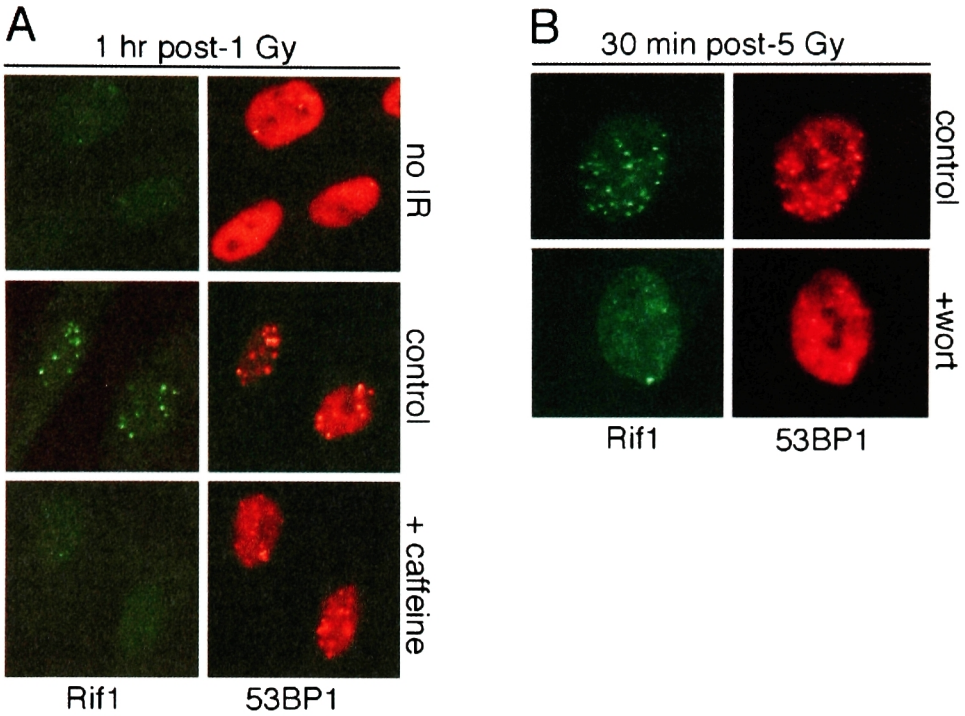

Figure 2-7. The PIKK inhibitors caffeine and wortmannin inhibit Rif1 IRIF formation.

A. Effect of caffeine on Rif1 foci. IMR90 (P14) cells were treated with 20 mM caffeine 2 hr prior to 1 Gy IR and fixed 30 min post-IR. IF for Rif1 and 53BP1 as in Figure 1B.

B. Effect of wortmannin on Rif1 foci. IMR90 (P29) cells were treated with 100 mM wortmannin 1 hr prior to 5 Gy IR, fixed 30 min post-IR, and processed for IF as in A.

Figure 2-8. Absence of Rif1 foci in A-T cells.

A. A-T fibroblasts (AG02496 and AG04405) which lack the ATM kinase were exposed to either 5 Gy IR or 25 J/m2 UV. Cells were fixed 2 hr or 8 hr after IR and 6 hr after UV and processed for IF as in Figure 1B.

B. A-T fibroblasts (AG04405) were exposed to IR as indicated and whole cell lysates were prepared 1 hr post-IR. Immunoblotting was performed using Rif1 and tubulin antibodies.

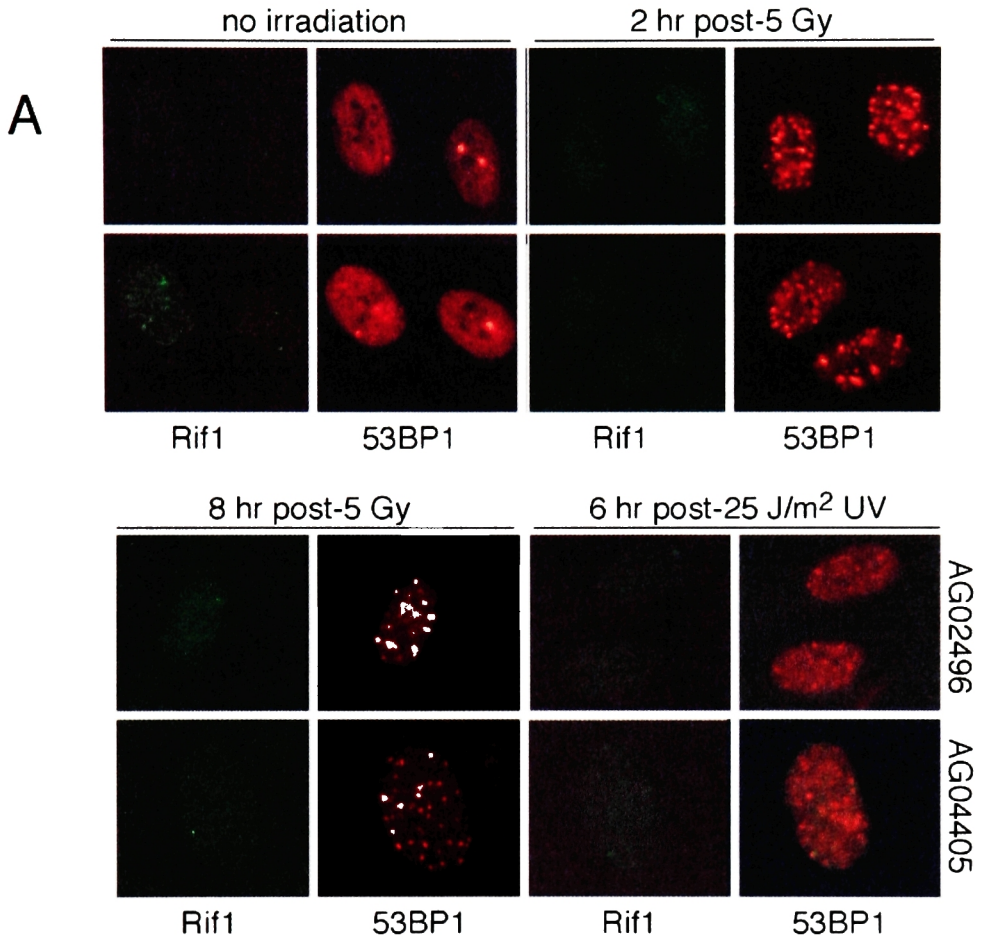
A
no irradiation
2 hr post-5 Gy
Rif1
53BP1
Rif1
53BP1
8 hr post-5 Gy
6 hr post-25 J/m2 UV
AG02496
AG04405
Rif1
53BP1
Rif1
53BP1

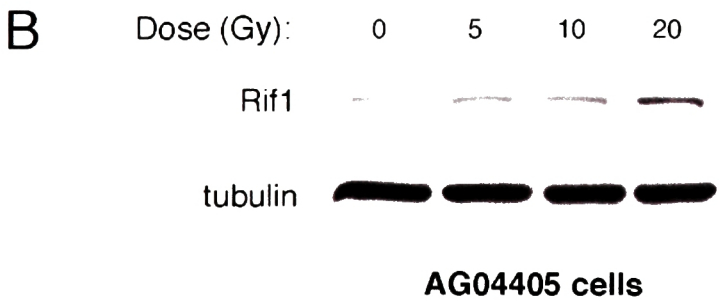
B
Dose (Gy):
0
5
10
20
Rif1
tubulin
AG04405 cells

Since Rif1 forms foci after treatment with UV, which is thought to activate the ATR kinase, we tested whether Rif1 depends on both ATR and ATM, as is the case for numerous other DNA damage response factors. ATR signaling can be inhibited using siRNAs against ATRIP, an essential partner for ATR (Cortez et al. 2001). As previously shown, two different ATRIP siRNAs resulted in strong reduction of the ATRIP protein (Figure 2-10A). These siRNAs did not affect Rif1 protein levels (Figure 2-10A). Despite the reduction in ATRIP protein levels, UV treatment continued to induce Rif1 foci in these cells (Figure 2-10B). Therefore, we tested whether the Rif1 foci formed after UV treatment were dependent of ATM signaling. No Rif1 foci were formed upon UV treatment of A-T cells (Figure 2-8A), even though the cells formed 53BP1 foci. Thus, Rif1 appears to depend exclusively on ATM rather than ATR for its response to DNA damage, even when the damage is a consequence of UV treatment.

Several components of the ATM signaling pathway were tested for their role in Rif1 regulation. Although Chk2 is a downstream target of ATM (Matsuoka et al. 1998), its activity was not required for Rif1 regulation; Chk2-deficient HCT15 cells still displayed Rif1 foci after IR (Figure 2-11A). Furthermore, we tested the role of the Mre11 complex, which has been shown to contribute to the ATM pathway both upstream and downstream of ATM ((Carney et al. 1998; Lim et al. 2000); reviewed in (Petrini and Stracker 2003)). LB1 cells derived from a Nijmegen breakage syndrome patient with a hypomorphic mutation in the Nbs1 component of the Mre11 complex, specifically a 657del5 mutations in NBS1, did not display an obvious defect in Rif1 focus formation (Zdzienicka 1999) (Figure 2-11B). Similarly, two Mre11 mutant cell lines (ATLD3 and 4; (Stewart et al. 1999)) formed Rif1 foci after IR (Figure 2-11C). ATLD3 and ATLD4

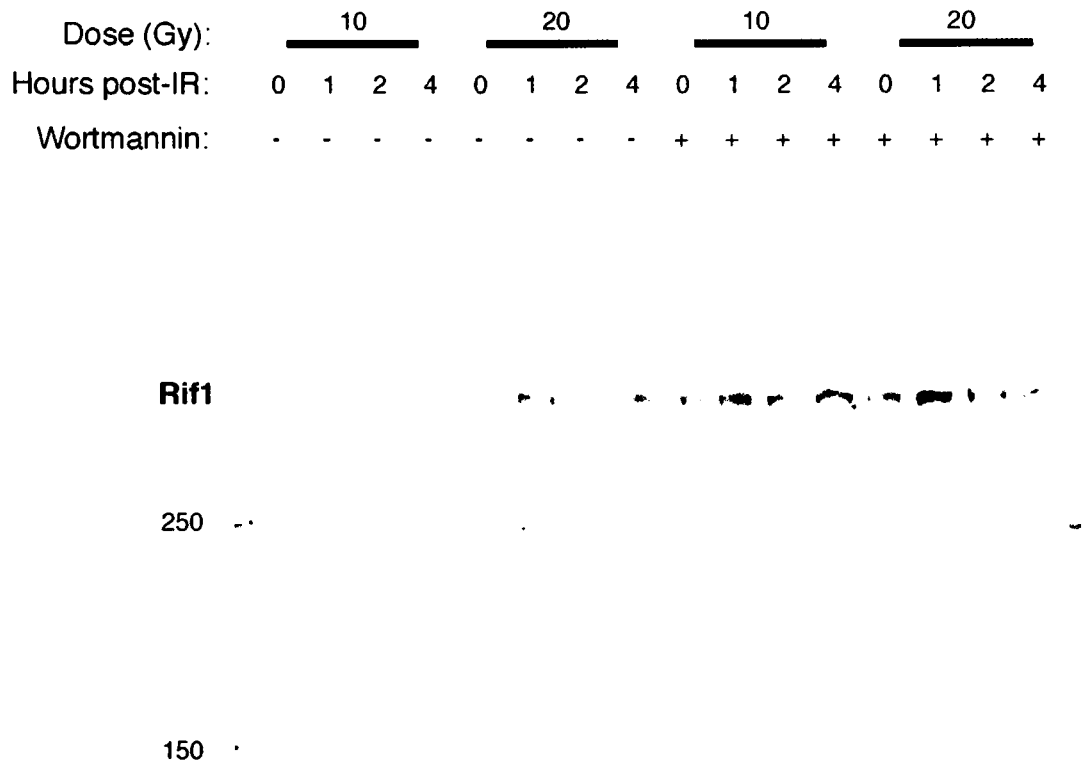

Figure 2-9. Rif1 immunoblot following ionizing radiation.

U2OS cells were pretreated with 100 mm wortmannin as indicated 1 hr prior to IR exposure of 0, 10, or 20 Gy IR as indicated. Whole cell lysates were prepared at indicated times following IR and cells were immunoblotted using an anti-hRif1 antibody.

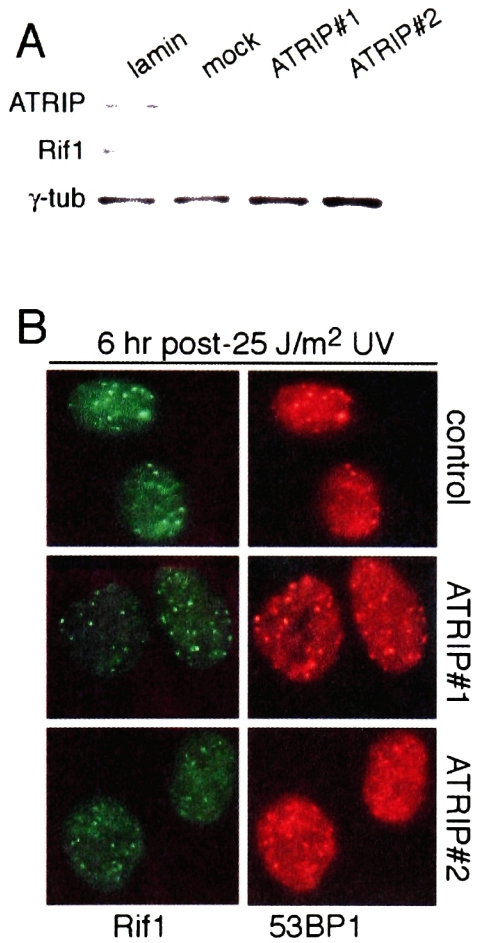

Figure 2-10. ATRIP siRNA treatment does not inhibit UV-induced Rif1 foci.

A. Immunoblotting analysis of the effect of ATRIP siRNAs. HeLa1.2.11 cells were transfected twice with the indicated siRNAs and analyzed by immunoblotting 72 hr after the first transfection for expression of the indicated proteins. Rif1 was detected with mouse serum 1060.

B. UV-induced Rif1 foci in cells treated with ATRIP siRNA. HeLa1.2.11 cells were exposed to 25 J/m2 UV 72 hr after siRNA transfection. Cells were fixed after 6 hr and processed for IF as in Figure 1B.

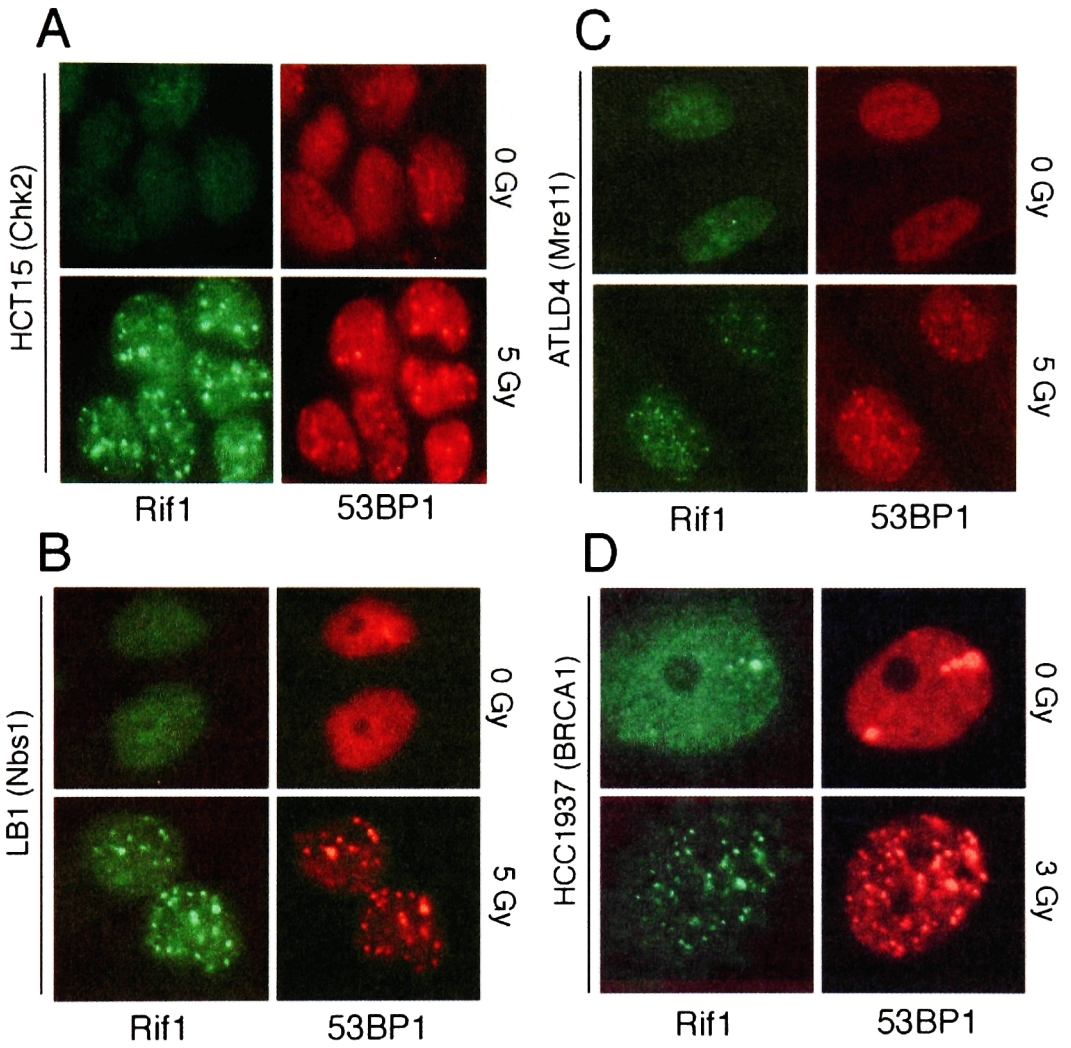

Figure 2-11. Deficiency of Chk2, Nbs1, Mre11 or Nbs1 does not affect Rif1 IRIF.

A. Effect of Chk2 deficiency on response of Rif1 to IR. Chk2 deficient HCT15 cells. For panels A-D, cells were treated with 5 Gy and processed for Rif1 and 53BP1 IF after 1 hr as in Figure 1B.

B. Effect of Nbs1 deficiency on response of Rif1 to IR. SV40-transformed NBS1-LB1 cells.

C. Effect of Mre11 deficiency on response of Rif1 to IR. Mre11 mutated ATLD4 cells.

D. Effect of BRCA1 deficiency on response of Rif1 to IR. BRCA1 deficient HCC1937 cells.

Figure 2-12. Rif1 IR-induced foci are dependent on 53BP1.

A. Immunoblotting analysis of the effect of 53BP1 siRNAs. HeLa cells were transfected twice with the indicated siRNAs and analyzed by immunoblotting 72 hr after the first transfection for expression of the indicated proteins. Rif1 was detected with mouse 1060.

B. Rif1 foci formation upon IR in cells treated with 53BP1 siRNA. Cells were exposed to 5 Gy IR 72 hr after mock transfection or transfection with either control (GFP) or 53BP1 siRNA olgionucleotides. Cells were fixed 1 hr after exposure and processed for IF as in Figure 1B.

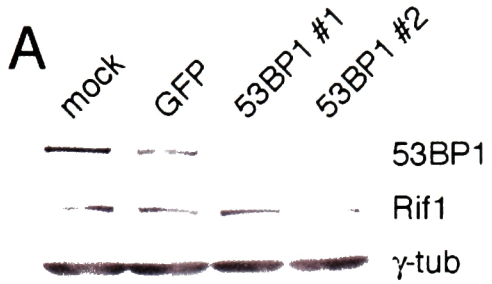
A
mock
GFP
53BP1 #1
53BP1 #2
53BP1
Rif1
γ-tub

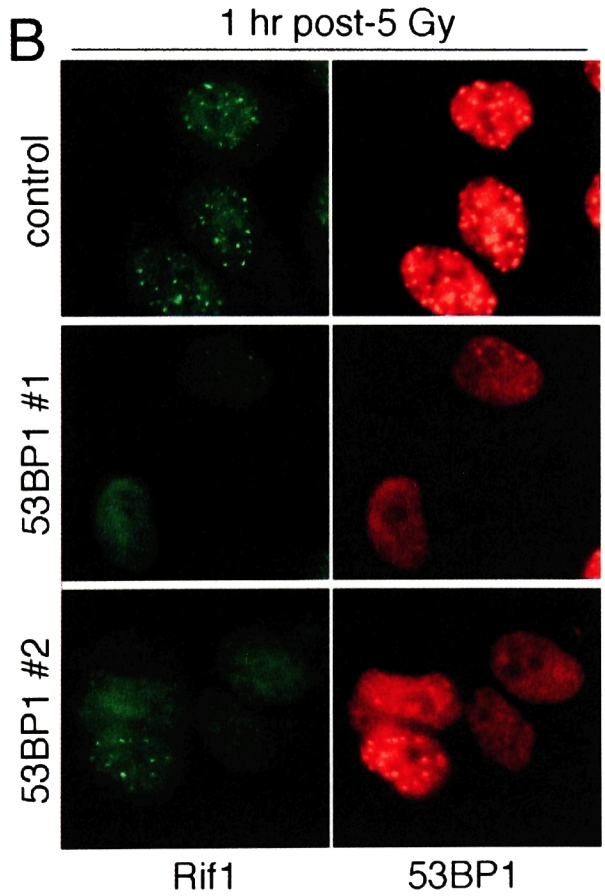
B
1 hr post-5 Gy
control
53BP1 #1
53BP1 #2
Rif1
53BP1

cell lines are primary fibroblasts derived from siblings that carry an A to G missense mutation at nt 350 that results in an N → S amino acid change (Stewart et al. 1999). Finally, HCC1937 cells deficient for the ATM target BRCA1 retained the ability to form Rif1 foci (Tomlinson et al. 1998) (Figure 2-11D). HCC1937 cells produce a truncated disease-producing mutant allele (5382insertC) and no wild type protein (Chen et al. 1998; Tomlinson et al. 1998).

In contrast, inhibition of 53BP1 completely abolished the Rif1 DNA damage response. Reduction in 53BP1 expression was achieved with two different siRNAs as demonstrated by Western analysis ((Wang et al. 2002); Figure 2-12A). Rif1 protein expression was not affected by these siRNAs (Figure 2-12A). As expected, the induction of 53BP1 foci by IR was strongly reduced in cells treated with the 53BP1 siRNAs (Figure 2-12B). Cells without 53BP1 foci also lacked Rif1 foci indicating a Rif1 depends on 53BP1 for its localization to damage foci. Normal Rif1 foci occurred in the few cells that had escaped the effects of the 53BP1 siRNAs, providing an internal control in the experiments (Figure 2-12B). The repression of Rif1 foci with two independent 53BP1 siRNAs argues against off-target siRNA effects, namely the suppression of mRNA and protein levels of other genes by a given siRNA sequence. Off target effects are minimized by obtaining similar results with multiple siRNAs and by checking that siRNA target sequences are unique within the genome. Furthermore, the Rif1 response was not affected by several other siRNAs (GFP, BRCA1, ATRIP, and luciferase; Figures 2-10A and 2-12A), demonstrating the specificity of the 53BP1 siRNA effect. Thus, Rif1 appears to be regulated by two components of the ATM pathway, 53BP1 and ATM itself. Since 53BP1 forms foci in A- T cells but Rif1 does not (Figure 2-8A), it appears that Rif1

requires an ATM regulated event in addition to 53BP1 foci formation. This implies that at least two independent molecular events, one ATM-dependent and the other 53BP1-dependent are required for the recruitment of Rif1 to sites of DNA damage. It is currently unclear whether or not ATM acts to directly phosphorylate Rif1. As mentioned previously, Rif1 does not shift in immunoblots after radiation (Figure 2-9). As mentioned previously, in vitro kinase assays to address whether ATM directly phosphorylates Rif1 are being performed.

RNAi was used to study the consequences of diminished Rif1 functions. We created 8 independent sets of siRNA oligonucleotides to Rif1 (Chapter 1). The siRNA nucleotides were designed through inspection of the Rif1 sequence (using the guidelines set forth in (Elbashir et al. 2001)). Additionally, a goal was to design siRNA oligonucleotides that were distributed throughout the predicted Rif1 open reading frame. Six of these eight siRNAs strongly reduced Rif1 protein levels and the other two siRNAs led to a 50% decrease in Rif1 protein levels (Figure 2-13A). The siRNAs also interfered with the formation of Rif1 foci after ionizing radiation (Figure 2-13B). siRNA transient transfection affects approximately 90% of cells. The untranfected cells shown in the bottom right panel of Figure 2-13B) still display foci formation after radiation and act as an internal positive control. As mentioned above, control siRNAs do not have this effect, demonstrating the specificity of the Rif1 siRNAs. Temporary knock-down of Rif1 expression with siRNA did not affect cell viability or long term growth. This is demonstrated by the ability of Rif1 siRNA treated cells to form similar numbers of colonies as control cells in a colony formation assay without radiation (Figure 2-16B). Furthermore, in keeping with the lack of obvious association of Rif1 with telomeres, Rif1

siRNA treatment did not have an acute effect on telomere function. For instance, the telomeric DNA remained intact and telomere fusions, which are indicative of telomere uncapping, were not induced (Figure 2-14). In fact, metaphase spreads in Rif1 siRNA treated cells did not appear to be abnormal or different from control treated metaphase spreads (Figure 2-14).

As Rif1 is a component of the ATM pathway, we examined the effect of Rif1 siRNAs on several aspects of ATM signaling. The activating auto-phosphorylation of ATM at serine 1981 was not affected by Rif1 siRNA treatment and the phosphorylation of Nbs1, Chk1, BRCA1, and p53 on ATM target sites occurred normally in irradiated cells with reduced Rif1 (Figure 2-15A). This demonstrates that Rif1 siRNA treatment does not affect the ability of ATM to phosphorylate these targets. Furthermore, Rif1 inhibition did not affect IR-induced focus formation by 53BP1 (Figure 2-13C), showing that Rif1 is downstream of 53BP1 in terms of focus formation.

Exposure of cells to IR leads to the accumulation of p53, transcriptional activation of p21, and subsequently the induction of a G1/S cell cycle arrest. U2OS cells treated with Rif1 siRNAs had a comparable level of p21 induction to Mock, GFP and 53BP1 treated cells (Figure 2-15B).

Although ATM signaling was not strongly affected, treatment of HeLa cells with two different Rif1 siRNAs resulted in decreased clonogenic survival after ionizing radiation (Figure 2-16A). Control cultures were either mock treated or treated with an

Figure 2-13. Rif1 siRNA.

A. Immunoblotting analysis of Rif1 siRNAs. HeLa cells were transfected twice with the indicated siRNAs and analyzed by immunoblotting 72 hr after the first transfection for expression of the indicated proteins. Rif1 was detected with Ab 1060.

B. Rif1 siRNA abrogates Rif1 ionizing radiation-induced foci. Rif1 siRNA treatment as in (A). Cells were fixed 1 hr after IR. IF for Rif1 (green) was performed using antibody 1060.

C. IR-induced 53BP1 foci in cells treated with Rif1 siRNA. U2OS cells were exposed to 5 Gy IR 72 hr after mock transfection or transfection with Rif1 siRNA #2. Cells were fixed 1 hr post-IR and processed for 53 BP1 IF. DNA is stained with DAPI.

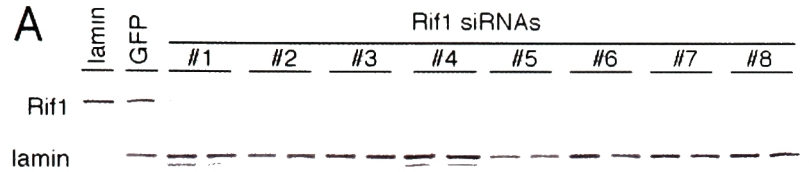
A
lamin
GFP
Rif1 siRNAs
#1
#2
#3
#4
#5
#6
#7
#8
Rif1
lamin

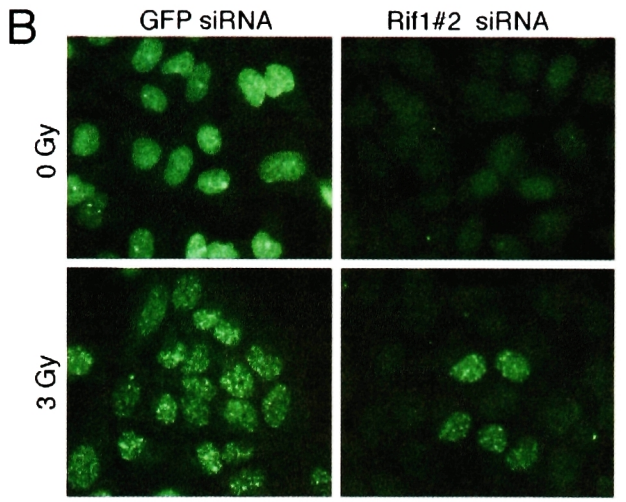
B
GFP siRNA
Rif1#2 siRNA
0 Gy
3 Gy

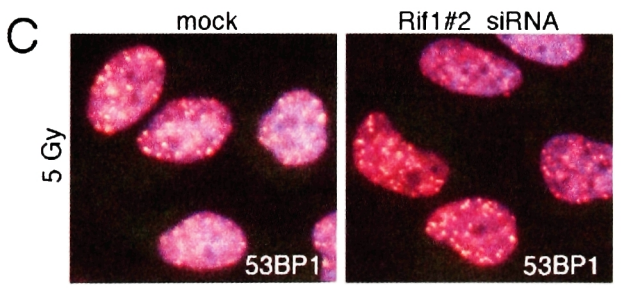
C
mock
Rif1#2 siRNA
5 Gy
53BP1
53BP1

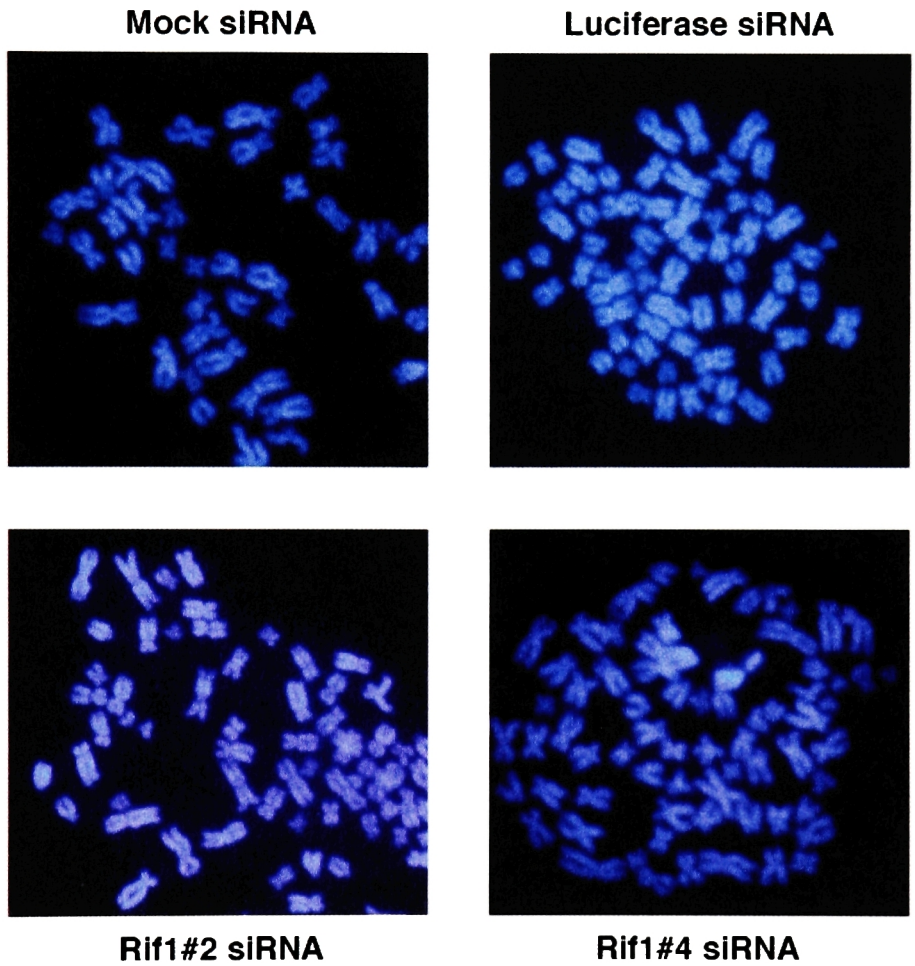

Figure 2-14. Metaphase spreads of cells treated with Rif1 siRNA.
HeLa1.2.11 cells were transfected twice with the indicated siRNAs and metaphase spreads were prepared 72 hr after the first transfection. Metaphase spreads were stained with DAPI (blue).

Figure 2-15. ATM-dependent phosphorylation of targets and p53 IR response in cells treated with Rif1 siRNAs.

A. U2OS cells were transfected twice with the indicated siRNAs and treated with either 0 Gy or 10 Gy IR 72 hr after the first transfection. Whole cells lysates were then prepared 1 hr after IR exposure. Immunoblotting of these lysates was performed using mouse 1060 antisera and antibodies recognizing ATM-S1981-P, BRCA1-S1524-P, Chk1-S317-P, p53-Ser15-P and Nbs1-S343-P. Anti-tubulin blotting was used as a loading control.

B. U2OS cells were transfected twice with the indicated siRNAs and treated with either 0 Gy or 10 Gy IR 72 hr after the first transfection. Whole cells lysates were then prepared at 0, 1, 2, or 4 hr after IR exposure as indicated. Immunoblotting of these lysates was performed using mouse 1060 antisera and antibodies recognizing p53 and p21. Anti-tubulin blotting was used as a loading control.

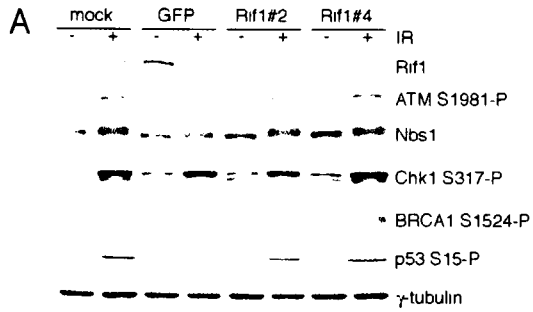
A
mock
GFP
Rif1#2
Rif1#4
- + - + - + - +
IR
Rif1
ATM S1981-P
Nbs1
Chk1 S317-P
BRCA1 S1524-P
p53 S15-P
γ-tubulin

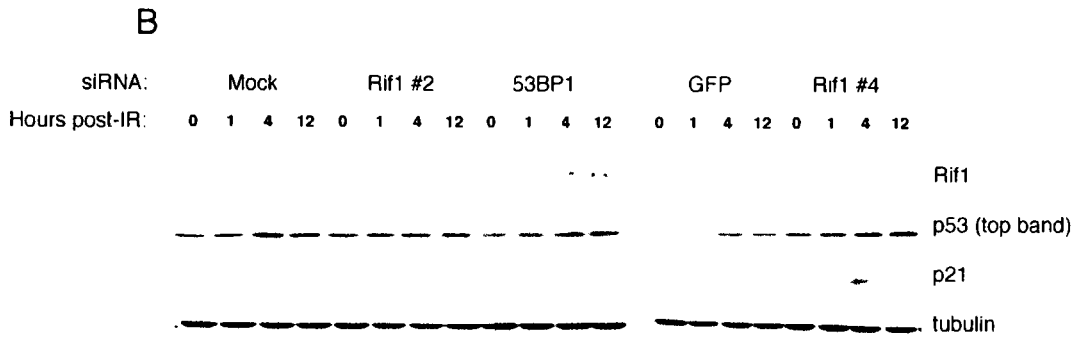
B
siRNA:
Mock
Rif1 #2
53BP1
GFP
Rif1 #4
Hours post-IR:
0 1 4 12 0 1 4 12 0 1 4 12 0 1 4 12 0 1 4 12
Rif1
p53 (top band)
p21
tubulin

Figure 2-16. Cells deficient in Rif1 are radiosensitive.

A. Effect on Rif1 siRNA on clonogenic survival after IR. Cells treated with siRNA as indicated were brought to the same concentration and irradiated with the indicated dose of IR 72 hr after transfection and plated in triplicate at multiple concentrations. Commassie stained colonies were counted after 14 days using dilutions resulting in similar colony numbers for the various treatments. Error bars indicate standard deviation within triplicate plating for each experiment. Dashed lines indicate the least squared linear regression through either mock and Scrambled I (black) or two independent Rif1 siRNAs (#2 and #4) (red) data points.

B. Clonogenic survival assay. Cells treated, plated and stained as in A. Photograph of coomassie stained sample plates (10^4 cells plated per 6 cm^2 dish) from mock and Rif1 set #2 siRNA treated cells.

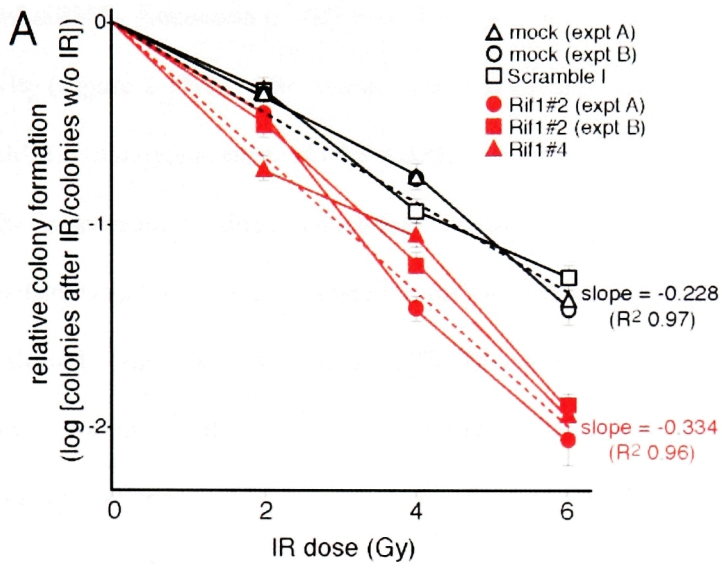
A
relative colony formation
(log [colonies after IR/colonies w/o IR])
0
-1
-2
0
2
4
6
IR dose (Gy)
mock (expt A)
mock (expt B)
Scramble I
Rif1#2 (expt A)
Rif1#2 (expt B)
Rif1#4
slope = -0.228
(R2 0.97)
slope = -0.334
(R2 0.96)

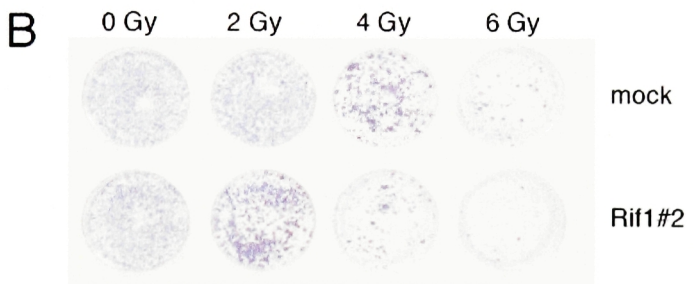
B
0 Gy
2 Gy
4 Gy
6 Gy
mock
Rif1#2

irrelevant control siRNA. Reduction in Rif1 reproducibly resulted in a 50% increase in the radiosensitivity (Figure 2-16A). After radiation with 6 Gy, Rif1 knockdown cells showed a 4.3-fold less clonogenic survival ($P < 0.0001$, students t test). This effect is comparable to the radiosensitivity due to knockdown of BRCA1 with siRNA (Ganesan et al. 2002) (data not shown), but modest compared to the radiosensitivity of A-T cells which typically show 10-fold lower survival rates. The RNAi experiments may underestimate the importance of Rif1 for survival after DNA damage as siRNA effects are incomplete and short-lived.

Discussion

Rif1 is a bona fide member of the DNA damage response in human cells. Rif1 forms IRIF and co-localizes with other DNA damage components. Rif1 critically depends on both ATM and 53BP1 for its localization to sites of damage after IR. The radiosensitivity of cells deficient in Rif1 confirms that Rif1 plays a biologically significant role in the cellular response to IR. These results were quite surprising given the role of Rif1 in yeast telomere biology. The observation that rif1-Δ yeast strains display significantly elevated rates of chromosome loss suggests that Rif1 may play a role in the maintenance of genomic stability and DNA damage response in yeast (Wotton and Shore 1997). However, rif1-Δ yeast do not have a GCR phenotype (Myung et al. 2001). As mentioned, RIF1 deletion also allows tel1 mec1 strains to bypass senescence, which suggests that ATM and Rif1 are in a common pathway in telomere maintenance. It appears that this pathway extends to the DNA damage response in mammalian cells.

The elucidation of more details about the role of Rif1 in the DNA damage response could provide light as to the exact function of Rif1 in the DNA damage response. One of the basic issues that remains is the determination of whether or not Rif1 is phosphorylated directly by ATM (and/or other kinases) in response to IR and the location(s) of these phosphorylation sites. This would allow one to test the consequences of re-introducing Rif1 with mutated phosphorylation sites back into cells. Another important piece of work that would aid in the understanding of Rif1 is the cloning of the full-length Rif1 cDNA to determine which domains are responsible for recruitment to sites of damage and hypersensitivity phenotype. Finally, the limitations of the transient

nature of the siRNA transfections used to study Rif1 could be overcome through either the use of retroviruses that express shRNA hairpin oligonucleotides which allow for a longer-term knockdown of Rif1. Questions such as a possible role of Rif1 in telomere length regulation and the issue of whether or not Rif1 deficiency results in genomic instability could be addressed this way.

A critical issue involves the molecular mechanism underlying the radiosensitivity of Rif1. The possible mechanisms of hypersensitivity involve roles in ATM signaling, one or more cell-cycle checkpoints, apoptosis and repair. The ability of ATM to phosphorylate many of its targets remains intact in cells treated with Rif1 siRNAs. This suggests that ATM signaling remains intact in Rif1-deficient cells, although there may still be an as-of-yet unidentified target of ATM. It is still possible that Rif1 could play a role in either the G1/S or intra-S-phase checkpoint. Radioresistance DNA synthesis (RDS) assays should be performed on cells deficient in Rif1 to assay the intra-S-phase checkpoint. Rif1 does not seem to affect IR-induced apoptosis as assayed by TUNEL. Finally, a role for Rif1 in DNA repair may explain the radiosensitivity of Rif1-deficient cells.

Chapter 3 –
Identification of novel Rap1-interacting factors using yeast two-hybrid screening

Introduction

The identification and characterization hRap1-interacting factors could potentially answer a number of important questions in the field of telomere biology. First, it could provide insight into the differences between mammalian and yeast telomeric complexes in terms of both evolutionary considerations and mechanisms of telomere length regulation. As mentioned in the introduction, Rap1 binds directly to telomeric DNA directly in *S. cerevisiae*, while it is recruited to telomeres through its interaction with TRF2 in human cells and the TRF-like Taz1p in *S. pombe*. The identification of additional protein components at telomeres could help shed light on the evolution of the Rap1 complex and explain the differences between these complexes in *S. cerevisiae*, *S. pombe* and mammalian cells. The elucidation of Rap1-interacting factors would also extend current knowledge regarding telomere length regulation in telomerase-positive mammalian cells. Presumably, other factors besides telomerase, TRF1, and TRF2 function to regulate telomere length either via influencing the properties of t-loops or via some other mechanism.

An understanding of the domain structure of hRap1 is necessary in order to select baits for yeast two-hybrid screens. The most obvious candidate for a protein interaction domain is the C-terminal domain of Rap1, termed the RCT (Li et al. 2000). In *S. cerevisiae*, this domain recruits Sir3, Sir4, Rif1 and Rif2 (Hardy et al. 1992; Moretti et al. 1994; Cockell et al. 1995; Liu and Lustig 1996; Wotton and Shore 1997). Additionally, Rap1 in *S. cerevisiae* contains an N-terminal BRCA1 C-terminal (BRCT) domain, which is a domain known to be involved in protein-protein interactions (Bork et al. 1997;

Callebaut and Mornon 1997). Both the RCT and BRCT domains are conserved in human Rap1 (Li et al. 2000). *S. cerevisiae* Rap1 contains two Myb-type helix-turn-helix motifs, which recognize two tandem GGTGT sites spaced 8 bp apart (Konig et al. 1996). This domain has been crystallized bound to DNA and folds like two copies of the Myb proto-oncogene DNA binding domain (Konig et al. 1996). Human Rap1 contains a single Myb domain and is unable to directly bind to telomeric DNA (Li et al. 2000). TRF1 and TRF2 each contain a single Myb domain, but both TRF1 and TRF2 homodimerize in order to be able to bind to telomeric DNA (Bianchi et al. 1997; Broccoli et al. 1997a; Bianchi et al. 1999). Rap1 has a transcriptional activation domain in *S. cerevisiae*, but this is not conserved in human Rap1 (Li et al. 2000). Finally, hRap1 contains a coiled-coil region which may be involved in protein-protein interactions. Thus, both the N-terminal BRCT domain and the C-terminal RCT are reasonable candidates for regions of hRap1 that might interact with proteins. As described in this chapter, a bait consisting of the hRap1 C-terminus was used to perform a yeast two-hybrid screen. Recent data based on both the localization of various Rap1 alleles to telomeres and the telomere length phenotypes of these alleles suggests that both the BRCT domain and the Myb domain of hRap1 recruit an as-of-yet unidentified factor that inhibits telomere elongation (Li and De Lange 2003).

This chapter describes the execution of a series of yeast two-hybrid screens in order to screen for proteins that interact with hRap1. The positive clones in a screen using the C-terminus of hRap1 as a bait correspond to two genes, a novel zinc finger protein referred to as C144, and a previously identified factor called FLASH which is known to play a role in apoptosis. The full-length C144 was cloned and experiments

were conducted to determine whether or not C144 has a role in human telomere biology. Co-immunoprecipitation and studies fail to show that C144 interacts with known telomere proteins or that C144 localizes to telomeres. A yeast ortholog of C144 was identified and yeast strains lacking this C144 ortholog do not experience changes in telomere length over the course of 100 generations.

Results and discussion

A standard yeast two-hybrid screen was used in order to search for factors that interact with hRap1. An initial screen was carried out using an N-terminal LexA fused to a full-length hRap1 as bait to screen a human fetal liver cDNA library. The full-length hRap1-LexA fusion bait was slightly toxic to cells as indicated by slow cell growth in liquid culture and a delay in colony formation. This bait behaved as expected in terms of yeast two-hybrid interaction, interacting with TRF2 but not TRF1 (Li et al. 2000). Analysis of several hundred colonies that grew on histidine-deficient plates out of the initial 4 million transformants resulted in no true positive results for this initial screen. Several criteria were used in order to verify that a colony growing on histidine dropout plates is a true positive in the screen. First, colonies were restreaked on histidine dropout plates to verify phenotype. Secondly, a filter lift assay was used to verify that the bait-prey combination could turn on the β-galactosidase gene as well. Finally, the prey plasmid DNA was then isolated, re-transformed into yeast and both nutritional and β-galactosidase phenotypes are tested to verify that the phenotype is plasmid-linked.

A second screen was undertaken using the C-terminus of hRap1 as a bait. The C-terminal bait consisted of LexA fused to amino aids 128-399 of hRap1. This bait contains the myb domains, coiled-coil domain and RCT of hRap1 and interacts with hTRF2 in a yeast two-hybrid setting (Li et al. 2000). The C-terminus of scRap1 was chosen because it is the portion of the protein that interacts with Rif1p, Rif2p, Sir3p, and Sir4p. The background of this screen was high due to the ability of the C-terminal Rap1 bait to activate transcription. An inhibitor of His, 3-AT, was used in the third screen.

A third screen was executed using 3-AT and approximately 300 colonies grew on selective plates out of approximately four million transformants. Further analysis revealed approximately 120 positives in the screen that fell into 5 groups. These groups were based on similar restriction digestion patterns after the prey plasmid DNA was isolated. These clones met the re-screening criteria mentioned above. A quantitative β-galactosidase assay was performed after verification that growth on histidine-deficient plates and β-galactosidase activation were plasmid-linked (Figure 3-1).

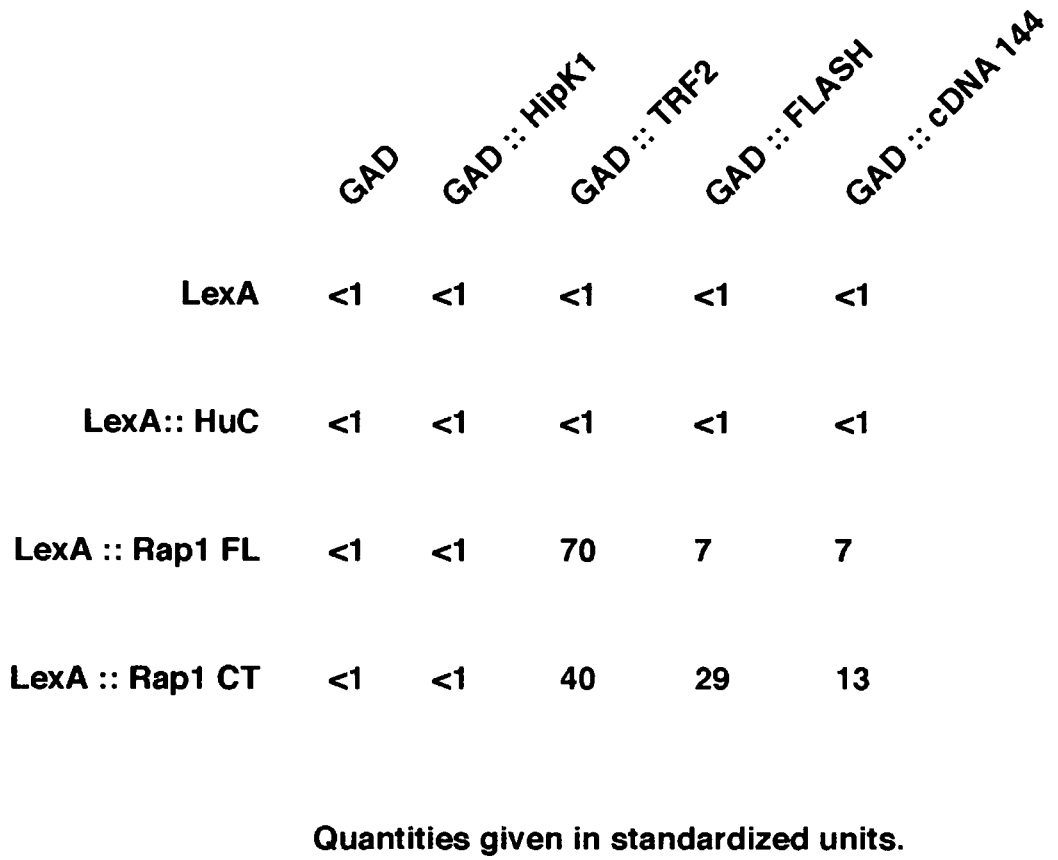

Figure 3-1. Quantitative β-galactosidase results for yeast two-hybrid screen.

A quantitative β-galactosidase liquid culture assay was performed on the indicated strains of yeast. Results are given in standardize units. The formula for b-galactosidase units = (1000 x OD420) / (t x V x OD600) where t = elapsed time in minutes of incubation and V = 0.1 ml x concentration factor.

The positive clones in the screen were sequenced and the resulting sequences were entered as queries against the Genbank database using a standard BLAST algorithm. The sequences corresponded to two genes. The first is a human gene with no homology to known genes in the human genome. This gene, designated C144 because it corresponds to clone 144 of the 300 initial colonies picked in the screen, is a novel human gene containing a CCHC-type zinc finger domain. The second clone identified was the previously identified human gene FLASH (Flice - Associated Huge) (Imai et al. 1999). This gene has no known role in human telomere biology. A number of proteins that might be expected to appear in the screen did not appear amongst the clones. Neither TRF2 nor hRap1 (Rap1 is capable of forming homodimers) were identified. This suggested that the screen was not performed under saturating conditions or that TRF2 or Rap1 were somehow under-represented in the cDNA library used. Also, no obvious homologs of Rif1, Rif2, Sir3, or Sir4 proteins were identified.

The yeast two-hybrid prey contained only a portion of the full-length C144. The 1.2 kb fragment of C144 in the prey plasmid was excised and used as a probe to screen a human kidney cDNA library in order to determine the full-length sequence of C144. A full-length clone containing a 1.6 kb predicted open reading frame (ORF) was isolated and sequenced using standard cloning methods. The C144 ORF contains a 543 amino acid protein with a predicted molecular weight of 65 kilodaltons (Figure 3-2). The predicted starting ATG has an upstream sequence of CAAATCTTG which represents a weak Kozak sequence. However, there is also an in-frame stop codon located 60 base pairs upstream of the ATG in the full-length clone, which points to the predicted ATG as

A

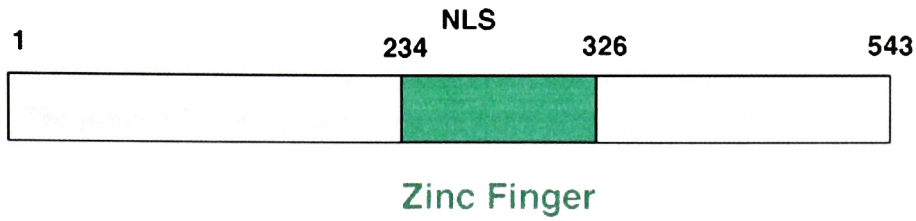

B

MMFGGYETIEAYEDDLYRDESSSELSVDSEVEFQLYSQIHYAQDLDDVIREEEH
EEKNSGNSESSSSKPNQKKLIVLSDSEVIQLSDGSEVITLSDEDSIYRCKGKNVR
VQAQENAHGLSSSLQSNELVDKKCKSDIEKPKSEERSGVIREVMIIEVSSSEEEE
STISEGDNVESWMLLGCEVDDKDDDILLNLVGCENSVTEGEDGINWSISDKDIE
AQIANNRTPGRWTQXYYSANKNIICRNCDKRGHLSKNCPLPRKVRRCFLCSRR
GHLLYSCPAPLCEYCPVPKMLDHSCLFRHSWDKQCDRCHMLGHYTDACTEIW
RQYHLTTKPGPPKKPKTPSRPSALAYCYHCAQKGHYGHECPEREVYDPSPVS
PFIXYYDDKYEIQEREKRLKQKIKVLKKNGVIPEPSKLPYIKAANENPHHDIRKGR
ASWKSNRWPQENKETQKEMKNKNRNWEKHRKADRHREVDEDFPRGPKTY

Figure 3-2. C144, a novel CCHC-type zinc finger protein.

A. A schematic diagram of C144. The CCHC zinc finger domain is shown in green.

B. The protein sequence of the full-length C144 gene.

the correct one. The 1.2 kb yeast two-hybrid fragment contains the N-terminal portion of C144 extending from amino acid 1 through amino acid 370.

The predicted C144 protein contains four CCHC-type zinc finger domains in the central portion of the open reading frame (Figure 3-1 and 3-2). CCHC-type zinc finger domains are a family of widely conserved domains that are able to bind a variety of nucleic acid structures, including both ssDNA and dsDNA (Summers 1991). CCHC-type zinc finger domains are also found in retroviral gag proteins and are thought to play a role in the binding of retroviral RNA genomes to the viral particle (Ramboarina et al. 1999). Figure 3-2 depicts the alignment of the C144 CCHC-type zinc finger domains with CCHC-type zinc finger domains in a variety of other organisms (Figure 3-3).

In order to study the possible role of C144 at telomeres and determine whether or not C144 is a bona fide hRap1-interacting factor, the full-length cDNA was subcloned into pcDNA3-Nmyc and pLPC-Nmyc. In both cases, an amino-terminal myc epitope tag was present in the vector and the fusion site began at amino acid number three of the predicted protein.

The presence of a T7 promoter in the pcDNA-Nmyc-C144 construct allowed for the expression of C144 in vitro using a rabbit reticulocyte lysate system to perform in vitro transcription and translation (IVTT) of C144 (Promega TNT coupled reticulocyte system). This construct was also transiently transfected into 293T cells to express myc-tagged C144 in mammalian cells. Western analysis of both the IVTT and ectopically expressed products using SDS-PAGE revealed that C144 indeed encodes an expressed

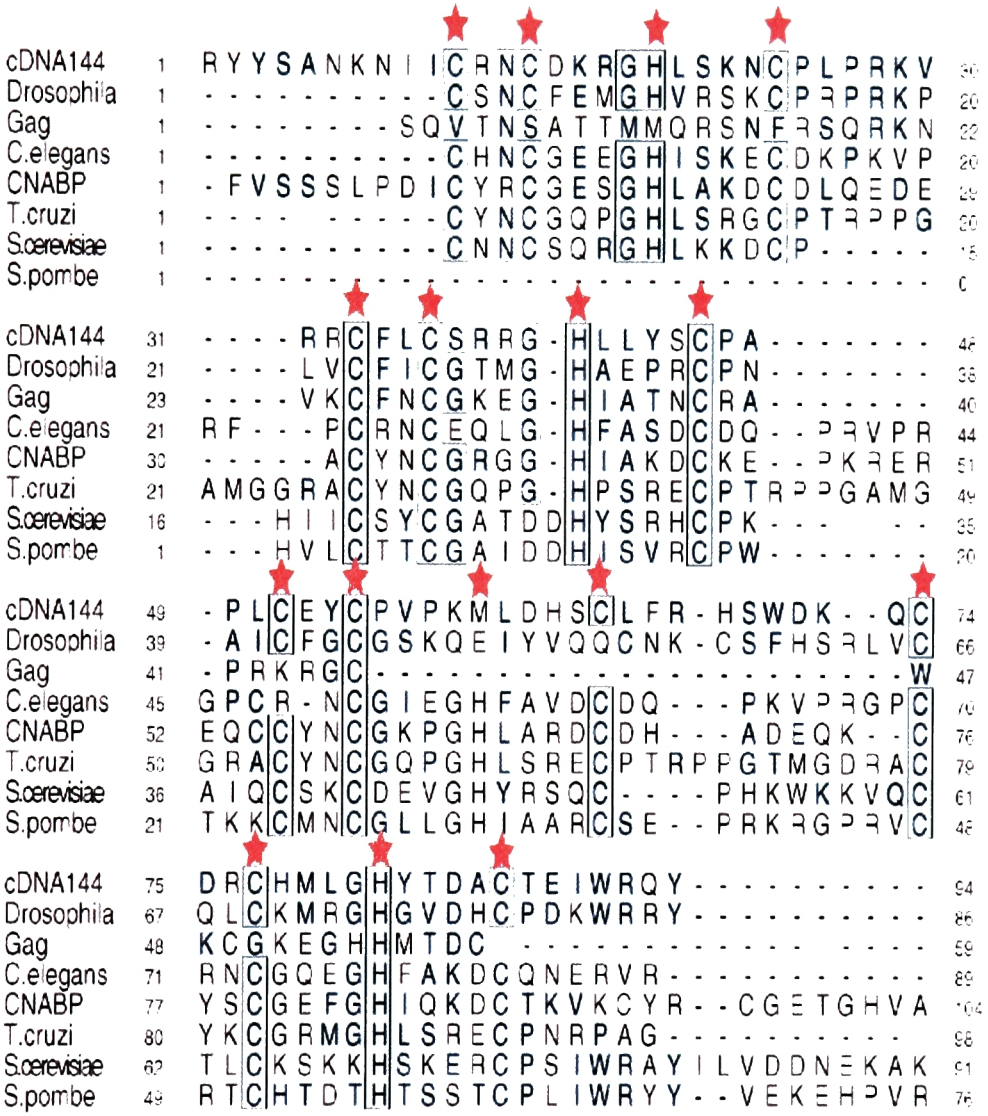

Figure 3-3. The conservation of the CCHC zinc fingers of C144.

The CCHC zinc finger of C144 is aligned with a number of other CCHC domain containing proteins from a variety of organisms. Similar amino acids as determined by Kyte-Doolittle criteria are shaded in blue and identical amino acids are boxed. Red stars indicated the conserved canonical CCHC residues that define the CCHC domain.

protein with an apparent molecular weight of 85 kilodaltons (Figure 3-4). It is interesting to note that the IVTT C144 product runs as a single band, whereas ectopically expressed C144 in mammalian cells runs as a doublet. This protein runs as a doublet in both 293T and HT1080 cells, suggesting that it is not a cell-type specific event. The C144 doublet suggests that a post-translational modification occurs under physiologic conditions. The nature of this modification is currently unclear.

Co-immunprecipitation was used to determine if C144 interacts with hRap1 and other known telomere-bound factors. Tagged versions of C144 and other telomere proteins were transfected into 293T cells and co-IP was performed. These experiments failed to reveal an interaction between C144 and TRF1, TRF2, or Rap1 (Figure 3-5). The interaction between TRF2 and hRap1 serves as a positive control and ability of these proteins to interact confirmed that the technique worked. Co-immunoprecipitation experiments using endogenous levels of telomeric proteins rather than this over-expression system were not carried out because attempts to generate antibodies against C144 were unsuccessful. The two peptides used to generate antibodies were K Y G K G E P K Y E S K S S K F K S N S D S D Y K C and PHKKQRKETDLTNKEKTKKPTQDSC. Co-immunoprecipitation using endogenous protein would be more reflective of physiologic conditions and complex formation of C144 may require more than one binding partner, which would not be detected in an experiment in which only pairs of proteins are over-expressed.

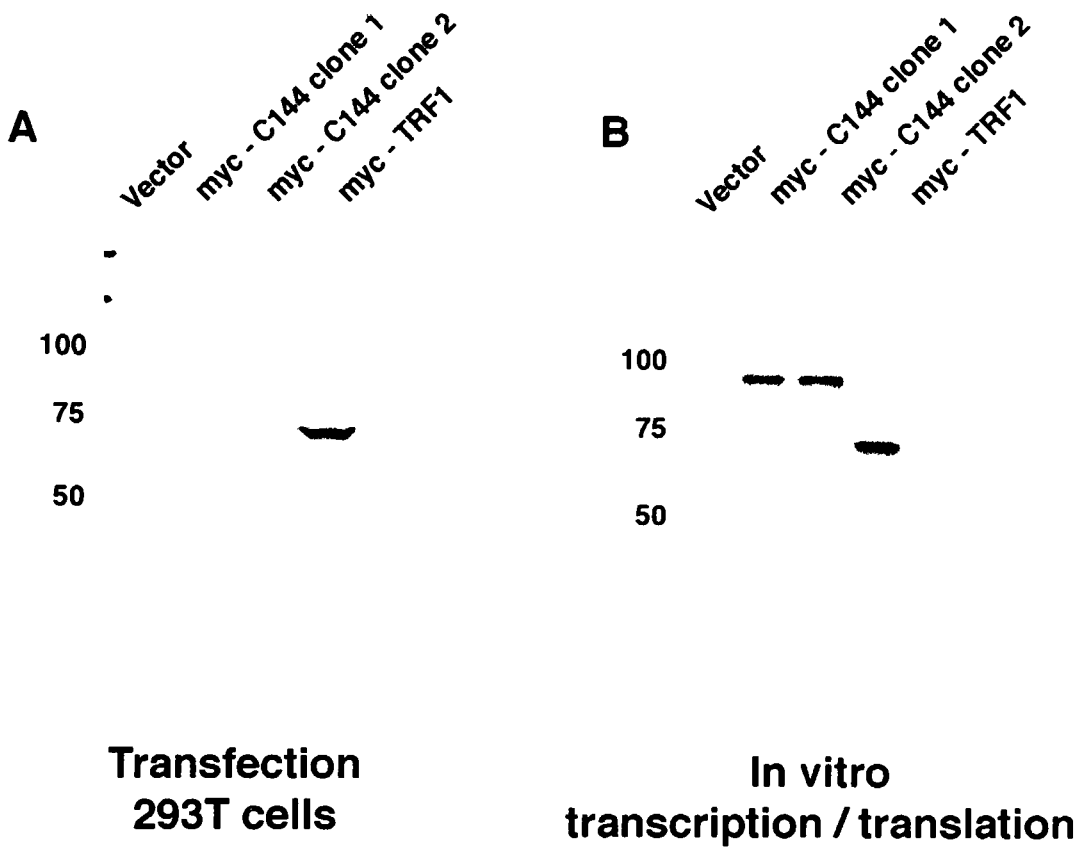

Figure 3-4. Protein expression of C144.

A. Calcium phosphate transfection of 293T cells was performed using empty vector and pcDNA3 with myc-tagged C144 or TRF1. Whole cells lysates were prepared 48 hr post-transfection and used for immunoblots using an anti-myc antibody.

B. In vitro transcription / translation (IVTT) was performed using the Promega TNT reticulocyte lysate system with the same plasmids used in A. S^{35}-methionine was added to the IVTT reaction. The reactions were subjected to SDS-PAGE.

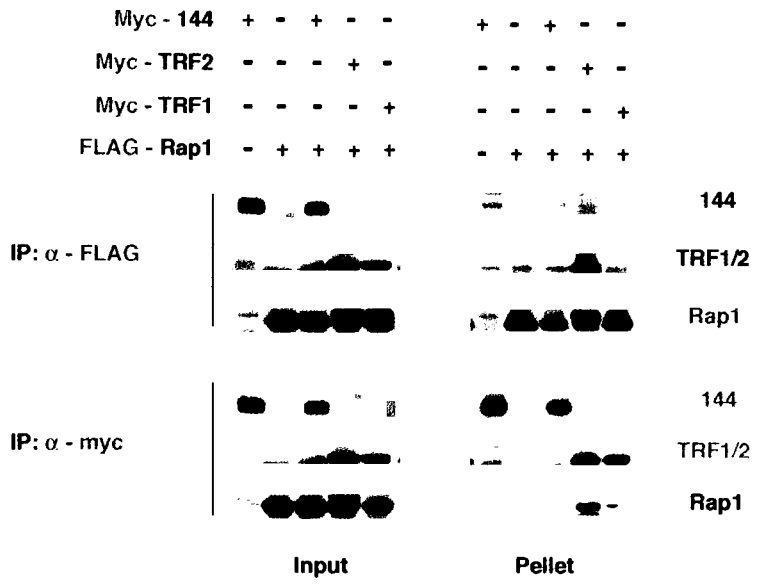

Figure 3-5. Co-immunoprecipitation of C144 and telomere proteins.

293T cells were trasfected with myc-tagged C144, TRF1 and TRF2 as well as FLAG-tagged Rap1 as indicated. Buffer C lysates were prepared and immunoprecipitations were performed using either anti-myc or anti-FLAG antibodies. Immunoblots of either the 1% of the input or the IP pellet were blotted with either anti-myc or anti-FLAG antibodies as indicated.

Figure 3-6. Alignment of C144 and yeast orthologs.

Alignment of C144 in human and its ortholog in *S. cerevisiae* and *S. pombe*. Similar amino acids as determined by Kyte-Doolittle criteria are shaded in blue and identical amino acids are boxed. The *S. cerevisiae* C144 ortholog is Genbank NP_010106; gi:6320026 and the *S. pombe* C144 ortholog is Genbank NP_595383; gi:19112175.

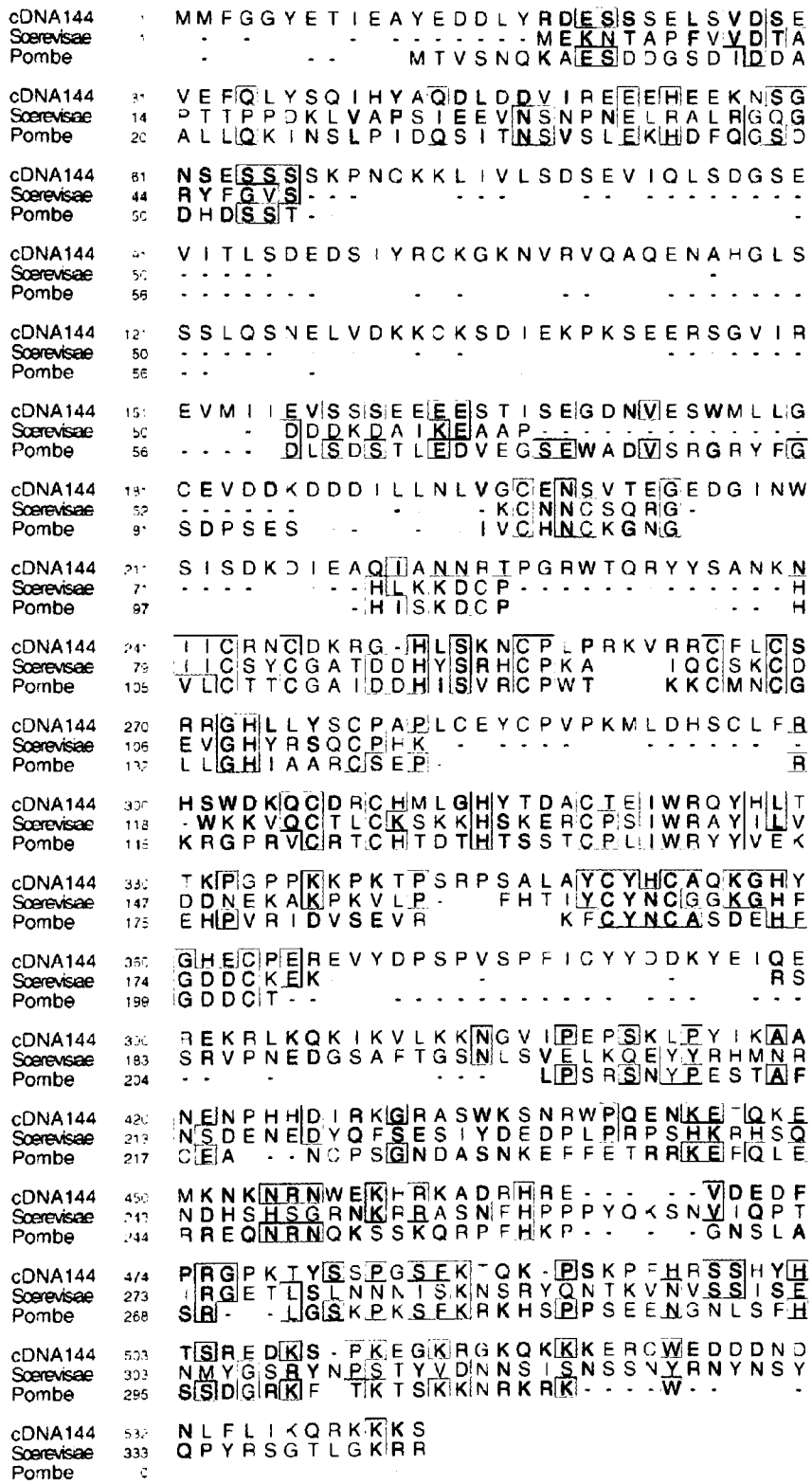

An ortholog of C144 was identified in *S. cerevisiae* in order to test the role of this gene at yeast telomeres (Figure 3-6). A yeast strain that lacked the *S. cerevisiae* C144 was obtained (gift of Harry Scherthan). In order to determine telomere length, genomic DNA was isolated from wild-type and yeast strains without the C144 ortholog. This DNA was cut with XhoI and a Southern blot of this genomic DNA was probed with radiolabeled telomeric probe. The resulting blot indicates that yeast deleted in the ortholog of C144 did not undergo observable telomere length change over the course of 100 generations (Figure 3-7). In additon, extensive screens for telomere mutants performed in the Lundblad laboratory failed to implicate this gene (personal communication).

The second gene identified in the yeast two-hybrid screen is the previously identified Flice-associated huge protein (FLASH). The yeast two-hybrid fragment in the prey plasmid contained sequence corresponding to amino acids 1253 through 1455 of the published FLASH sequence. FLASH (as its name indicates) is a large, 220 kilodalton protein which was initially pulled out of a two-hybrid screen using procaspase-8/FLICE as a bait (Imai et al. 1999). FLASH functions as an adapter molecule in the process of Fas-mediated apoptosis. FasL binds Fas on the cell surface and results in receptor trimerization, which, in turn, recruits a complex of other factor known as the DISC (death-induced signaling complex). The formation of the DISC ultimately results in the processing of procaspase-8 into caspase-8. Caspase-8 is a master caspase that activates downstream effector caspases and results in apoptosis. The Yonehara group demonstrated that FLASH co-immunoprecipitates with the DISC, with FADD and with

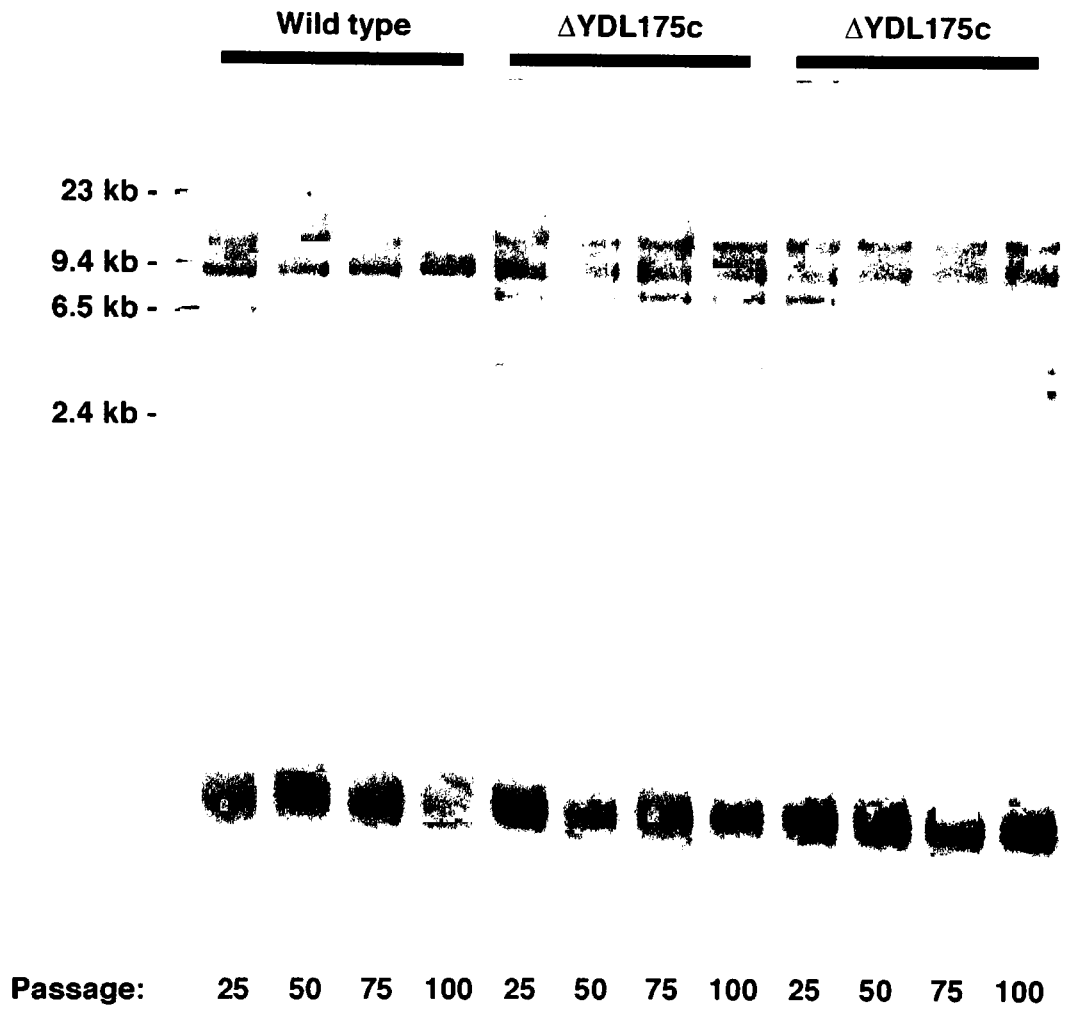

Figure 3-7. Telomere blot of *S. cerevisiae* C144 delete strain.

S. cerevisiae wild-type and YDL175c delete strains were streaked out for 4 successive rounds of colony formation (representing approximately 25, 50, 75 and 100 generations). Genomic DNA was isolated from these yeastand digested with *XhoI*. Southern blots were probed with a telomere-specfic radiolabeled probe.

procaspase-8 (Imai et al. 1999). Full-length FLASH potentiates Fas-mediated apoptosis and certain truncated alleles antagonize Fas-mediated apoptosis.

What, then, could be the role of FLASH at telomeres? It is known that overexpression of dominant-negative TRF2 alleles result in apoptosis and that deprotected telomeres recruit DNA damage proteins (Karlseder et al. 1999; Takai et al. 2003). One possibility is that FLASH acts as a sensor for telomere dysfunction and triggers apoptosis when a cell can not properly maintain its telomeres. A full-length expression construct containing the FLASH open-reading frame was obtained from Zhengcheng Zheng (Shanghai Institute of Biochemistry). It was difficult to detect over-expressed FLASH in 293T cells and the reason for this is unclear. It could be related to the relatively large size of FLASH or some aspect of FLASH biology. Anti-peptide antibodies were generated using the peptides YGKGEPKTESKSSKFKSNSDSDYKGC and HPHKKQRKETDLTNKEKTKKPTQDSC, but these were unable to recognize a large molecular weight band consistent with FLASH. IF performed using over-expressed myc-tagged FLASH demonstrates that FLASH is a nuclear protein and several (approximately 5 to 10) nuclear foci appear in FLASH-transfected cells. However, these foci do not colocalize with TRF1, a known telomere protein, in HeLa1.2.11 cells (Figure 3-8). The localization of FLASH to telomeres may well be stimulus-dependent or require the over-expression of Rap1 as well. Unfortunately, efforts to raise antibodies against endogenous FLASH were not successful. Further experiments need to be conducted in order to determine conclusively whether or not FLASH is at telomeres.

Figure 3-8. IF of FLASH and telomere proteins

HeLa1.2.11 cells were transfected by electroporation with myc-FLASH and cells were fixed 48 hr post-transfection. IF was performed with anti-myc (green) and anti-TRF1 (red) antibodies along with DAPI stain (blue). Top and bottom are two separate images using this staining.

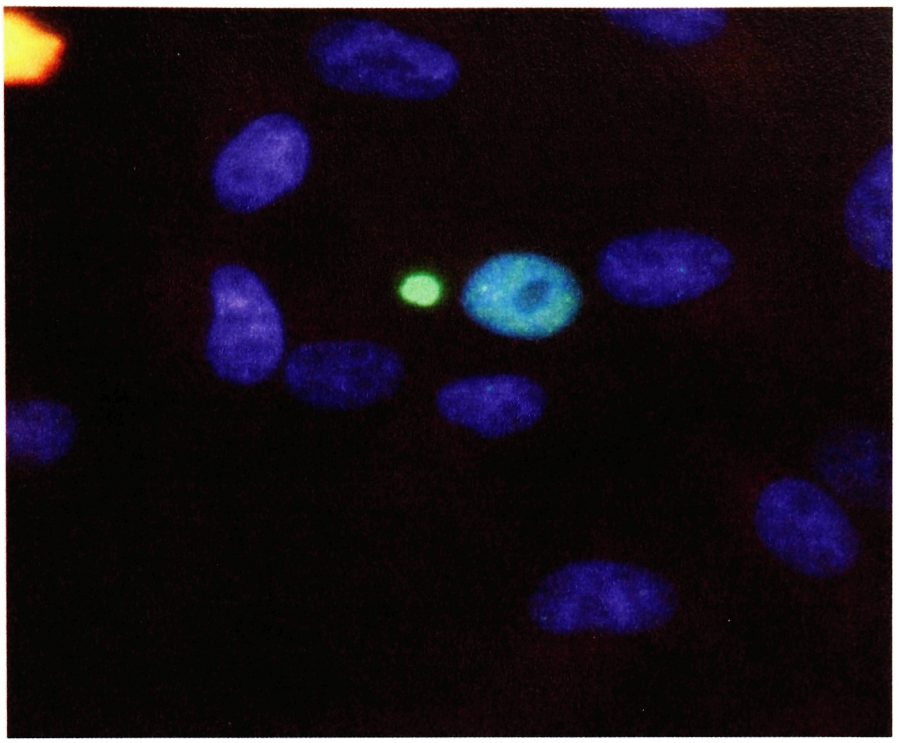

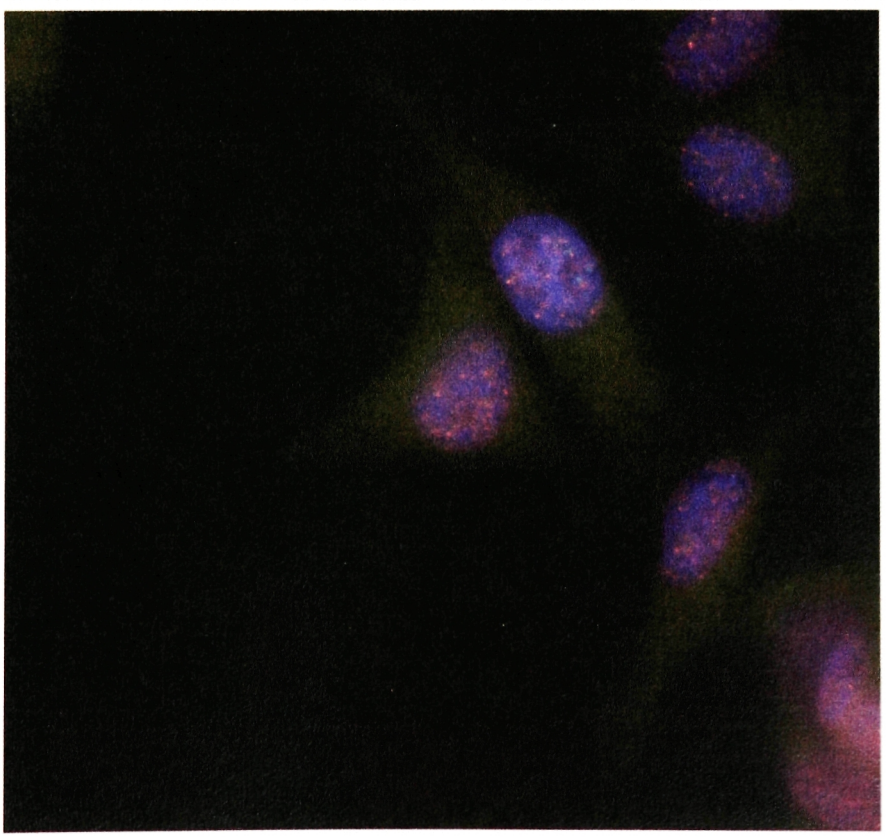

Conclusions

This thesis focuses primarily on the identification of human Rif1, an ortholog of yeast Rif1, and its role as a novel component of the ATM-dependent DNA damage response pathway. Rif1 localizes to sites of inferred DSBs shortly after the induction of DNA damage and this redistribution requires the function of both 53BP1 and ATM, but not ATR. RNAi-mediated depletion of Rif1 resulted in reduced cell survival after irradiation. The thesis also focuses on the identification of several putative Rap1-interacting factors. Neither C144, a novel zinc finger protein, nor FLASH, the two candidates obtained from the yeast two-hybrid screen using Rap1 as a bait, were confirmed to be bona fide telomere proteins. Finally, this thesis discusses attempts to analyze the interaction between the Mre11 complex and the TRF2 complex. The concluding remarks presented here will focus upon human Rif1 since it represents the most promising avenue of future research.

Rif1 as an ATM- and 53BP1- dependent DNA damage response factor

The experimental evidence from chapters 1 and 2 strongly support the role of Rif1 in the DNA damage response. Most importantly, human Rif1 localizes to inferred DSBs following ionizing radiation. Rif1 is able to form foci in response to several DNA damage stimuli, including IR, UV, MMS, HU and etoposide. The response to IR takes place within minutes of exposure. Rif1 displays similar kinetics to other known DNA damage response factors, such as BRCA1, 53BP1 and NBS1. Furthermore, Rif1 co-localizes with these factors following DNA damage.

A full description of the exact function(s) of human Rif1 in the DNA damage response was a goal of experiments carried out in this thesis as well as current and future experimental work. A systematic approach was taken to address which steps of the DNA damage response cascade require Rif1 function. The possible roles of human Rif1 at the outset included Rif1 as a primary sensor of DNA damage, Rif1 acting at the level of the PI3K-like transducers ATM and ATR, Rif1 as a direct target of ATM, and Rif1 as a player in one of the effector arms of the DNA damage response. The effector pathways of the DNA damage response include the establishment and maintenance of G1/S, intra-S phase, and G2/M cell cycle arrest, the HR and NHEJ repair pathways, damage-dependent apoptosis pathways, and recovery of cells from damage.

After identifying human Rif1 as a bona fide member of the DNA damage response, it became important to establish where in the DNA damage response pathway human Rif1 lies. The observation that 53BP1 and other DNA damage factors localize to sites of damage in cells treated with Rif1 siRNA indicates that it is unlikely that human Rif1 acts as the sole or dominant sensor of DNA damage. It is possible that Rif1 acts as a redundant sensor in certain situations, but there is no evidence to presently support this hypothesis. The use of the PI-3 kinase inhibitors caffeine and wortmannin as well as studies in A-T cells, which lack ATM, indicated that human Rif1 is completely dependent on ATM for its localization to sites of DNA damage. The inability of ATRIP siRNA to affect human Rif1 response to UV or IR supports the hypothesis that Rif1 is dependent on ATM, but not ATR. Further confirmation of this was accomplished by looking at Seckel cells, which have a splice defect in ATR (H. Takai, unpublished result). Rif1 doe not appear to act at the level of ATM because ATM targets are still

phosphorylated in Rif1 siRNA treated cells. Rif1 siRNA treatment also does not influence the level of ATM auto-phosphorylation in response to DNA damage. Together, these observations suggest that Rif1 acts strictly downstream of ATM.

The dependence of Rif1 function on ATM suggests that Rif1 might be directly phosphorylated by ATM. The primary sequence of Rif1 contains 14 SQ/TQ sites, the consensus site of the PI3K-like family members. Rif1 contains one site that represents a more specific consensus sequence (Kim, et al. 1999). Two experimental approaches were used to address whether ATM phosphorylated Rif1. First, co-immunoprecipitation experiments in extracts from untreated cells and irradiated cells failed to reveal an interaction between ATM and Rif1. It was also unclear whether Rif1 shifts in immunoblots in an IR- and ATM- dependent manner. Ongoing experiments using ATM kinase assays have yielded inconclusive results (S. Buonomo, unpublished observations). Experiments in which the putative ATM kinase site(s) are mutated have yet to be executed.

Rif1 also requires 53BP1 for its localization to sites of damage following DNA damage. Rif1 requires at least two independent molecular events in order to form DNA damage foci, since 53BP1 still forms foci, albeit to a lesser extent and with delayed kinetics, in A-T cells. It has not been formally demonstrated whether ATM-dependent phosphorylation of 53BP1 is required for Rif1 foci formation. The dependence of Rif1 on ATM and 53BP1 is specific. Rif1 still forms foci in cells deficient in Mre11, Nbs1, BRCA1, and Chk2.

The role of Rif1 in the DNA damage response effector pathways

The demonstration that cells deficient in Rif1 are radiosensitive indicates that Rif1 is necessary for cell survival in response to IR. Further experiments demonstrate that Rif1 siRNA treatment in other cell lines renders these cells radiosensitive, whereas Rif1 siRNA treated cells are not hypersensitive to MMS (H. Takai, unpublished results). Although these experiments demonstrate the importance of Rif1 in the DNA damage response, the specific mechanism of Rif1 in the DNA damage response was sought.

An analysis of the DNA damage response effector pathways was conducted. Cells are able to halt their progression through the cell cycle in response to DNA damage. These checkpoints occur at the G1/S, intra-S phase, and G2/M phases of the cell cycle and prevent the cell from both replicating damaged DNA and attempting to segregate damaged chromosomes. The G1/S transition is examined by assaying BrdU incorporation following IR, whereas the G2/M transition is observed by looking at the phosphorylation of hsitone H3 after damage. Experiments conducted by Hiro Takai in the de Lange lab have demonstrated that Rif1 plays a role in the intra-S phase checkpoint. In response to irradiation, cells halt replication presumably to prevent inappropriate copying of damaged DNA. Radioresistant DNA synthesis (RDS) occurs if the DNA damage response is not properly functioning. Two pathways have been described including one pathway in which Chk2 phosphorylates Cdc25A and results in Cdk2 inactivation and one pathway in which Nbs1 and Mre11 play a role (Falck et al. 2001; Falck et al. 2002). Cells treated with Rif1 siRNA display an RDS phenotype. Using cells deficient in Nbs1, a gene known to be involved in RDS, and complementation with wild type and mutant Nbs1

alleles, Hiro Takai demonstrated that the Rif1 RDS effect is distinct and in a separate pathway from Nbs1. It is still unclear as to whether Rif1 is in the Chk2 RDS pathway. Thus, Rif1 plays a role in S phase progression following IR that is a separate pathway from the previously described ATM-Chk2-Cdc25A checkpoint pathway.

The ability of Rif1 either to participate in or regulate the homologous recombination (HR) or non-homologous end-joining (NHEJ) pathways that repair the IR-induced DSBs was addressed. A number of repair assays were initiated in an attempt to determine whether cells deficient in Rif1 were competent in terms of DNA repair. These experiments were technically challenging because it is difficult to separate the damage-dependent cell cycle arrest from repair events. Initial experiments did not reveal any difference in repair events. These experiments involved observations of metaphase chromosomes after cells were exposed to radiation. Experiments were carried out in HeLa1.2.11 cells treated with caffeine and Rif1 siRNA. The interpretation of these experiments was difficult because it is technically difficult to have cells enter metaphase after irradiation-induced cell cycle arrest. The effects of cell cycle arrest, caffeine and repair events must all be considered. The ability of Rif1 to act as a direct participant in either HR or NHEJ is currently unresolved and should be addressed in the future.

Rif1 in yeast and human: a unifying view?

The difference between the role of Rif1 in yeast and human cells raises questions about the physiologic function and the evolutionary history of Rif1. Rif1 plays a role in telomere biology in yeast cells, whereas Rif1 plays a role in the DNA damage response in

human cells. There are several speculative possibilities that could explain this apparent discrepancy.

Rif1 could function in both the DNA damage response in both yeast and human cells. There is evidence to suggest that Rif1 plays a role in DNA damage in yeast. Rif1 deficiency results in a 10 fold increase in chromosome loss rates per generation; Rif2 deficiency results in a 4 fold increase in chromosome loss rate and loss of both Rif1 and Rif2 leads to a 40 fold increase in chromosome loss (Wotton and Shore 1997). It is not known whether this chromosome instability is associated with a DNA damage response role for Rif1 in yeast. However, rif1-Δ yeast do not have a GCR phenotype (Myung et al. 2001). As mentioned previously, Rif1 is in the Tel1 and Mec1 pathways in terms of telomere length. There is currently no evidence that Rif1 is involved in telomere biology in human cells. However, it is tempting to speculate that the telomere and DNA damage functions of Rif1 are related. S. cerevisiae could have co-opted the DNA damage factor Rif1 to protect its telomeres and Rif1 may actually not function in telomere biology in mammalian cells.

Human Rif1 and telomere biology

Although the experiments described in chapter 1 have failed to detect Rif1 at functional human telomeres, further studies need to be carried out in order to establish a possible role for Rif1 in human telomere biology. It is critical to determine whether nor not human Rif1 plays a role at functional telomeres. One avenue of research involves the use of an RNAi hairpin (shRNA) expressed from retroviruses in order to assess the role

of Rif1 in telomere length regulation. Since the RNAi strategy described in chapter 2 can not be used in long term experiments, shRNA might prove ideal for the study of telomere length, which requires successive passaging of cells. Additionally, the examination of the effects of over-expressed alleles of Rif1 may elucidate possible roles of this protein at telomeres.

So far, we have not been able to detect Rif1 at human telomeres. However, the fact that Rif1 has a telomeric function in *S. pombe* argues in favor of a role for Rif1 at human telomeres. The structure of fission yeast telomeres more closely resembles that of human telomeres than the budding yeast telomeric complex. As discussed above, further experiments will be required to determine whether Rif1 also plays a role at human telomeres. Although there have been several possibilities presented, it is still unclear why exactly Rif1 has apparently disparate roles in telomere biology in yeast and in the DNA damage response in human cells.

Rif1 in human disease and clinical therapy

Human Rif1, encoded by a gene on chromosome 2 (2q23.3), is a candidate tumor suppressor. This view is based on its involvement in the ATM pathway which contains other tumor suppressors, including ATM itself, Mre11, Nbs1, BRCA1, and Chk2. Similar to mutations in these genes, changes in human Rif1 may play a role in certain sporadic or familial human cancers. Treatment of cells with Rif1 siRNA did not reveal an acute cell lethal phenotype upon Rif1 inhibition. Mutations in Rif1 may therefore be tolerated in the germline. Such heterozygous individuals could be at risk for development of cancer if

loss of heterozygosity (LOH) at the Rif1 locus leads to cells with impaired ability to respond to DNA damage.

Recent data regarding the mouse ortholog of Rif1 suggests that Rif1 may have an entirely different role in development because mouse Rif1 was highly expressed in germ cells and embryo-derived pluripotent stem cells (Adams and McLaren 2004). It is possible that Rif1 still functions in the S-phase RDS pathway and that this pathway plays an important physiologic function in early cell division and development. Thus, it is possible that loss of function mutations may not be tolerated in human cells. The generation of mouse that lacks Rif1 is on-going (S. Buonomo, personal communication) and could address the issue of whether lack of Rif1 contributes to heritable, spontaneous, or induced tumorigenesis *in vivo*.

The strict dependence of Rif1 on ATM is unusual among the substrates of this kinase, which generally also respond to regulatory inputs from ATR. Because of this unique regulation, IR-induced Rif1 foci are an excellent indicator for ATM kinase activity. A cell-based assay for ATM activity based on Rif1 foci could rapidly identify individuals with alterations in this pathway and could reveal the ATM status of tumor samples, potentially improving cancer diagnosis and treatment. Furthermore, the Rif1 assay could be helpful in the identification of ATM inhibitors, which have potential application as radiosensitizing agents. Additionally, drugs targeting Rif1 directly may serve as radiosensitizing agents with applications in the clinic.

A final application of Rif1 in the clinic could be the use of genetic testing. If Rif1 turns out to be involved in human tumorigenesis (particularly intriguing given the role of several other DNA damage response factors in human cancer predisposition

syndromes), mutations of Rif1 could be characterized and screening paradigms can be designed to aid in patient care. Importantly, Rif1 status may serve as a prognostic marker for the responsiveness of individual tumors to radiotherapy. Since cells deficient in Rif1 are radiosensitive, one might reasonably predict that tumors lacking Rif1 and other DNA damage response factors would undergo a more dramatic response to radiation therapy.

Appendix – Investigating how the Mre11 complex interacts with the TRF2 complex

Introduction

The previous chapter discussed the use of a genetic method, the yeast two-hybrid screen, to search for novel Rap1-interacting factors. Work in the de Lange lab has led to the discovery of several Rap1-interacting factors in mammalian cells. In addition to TRF2, which interacts tightly with Rap1 and brings it to human telomeres, the Mre11 complex, including Mre11, Rad50 and Nbs1, has been shown to be present in a complex with TRF2 and hRap1 (Zhu et al. 2000). Most of the Mre11 complex is nucleoplasmic and only a small percentage of Mre11 complex components is localized to the telomere (Zhu et al. 2000). This is demonstrated by the observation that Triton X-100 pre-extraction of a large quantity of nucleoplasmic Mre11 complex is required in order to visualize the co-localization between the Mre11 complex and the telomeric protein TRF1 by IF (Zhu et al. 2000). Although the Mre11 complex is a component of IRIFs, the telomeric proteins TRF1 and TRF2 do not re-localize to IRIFs (Zhu et al. 2000). Furthermore, Nbs1 is phosphorylated in S phase and its localization at telomeres only occurs during S phase (Zhu et al. 2000). It is unclear what the role of the Mre11 complex is at human telomeres. As discussed in the introduction, the Mre11 complex contains several enzymatic activities that may have a role in t-loop processesing and the Mre11 complex is known to play a role in telomere length regulation in *S. cerevisiae.*

In order to further extend these observations, the specific binding interactions between the TRF2-hRap1-Mre11 complex must be defined and characterized. Although it is known that the Mre11 complex is found in a complex with TRF2, it is unclear whether this interaction is dependent upon hRap1. It is also unclear which component of the Mre11 complex binds to TRF2, hRap1, or a third protein that interacts with either

TRF2 or Rap1. Two approaches were taken to further study the protein-protein interactions between TRF2, Rap1 and the Mre11 complex. The first approach involves using a GST-hRap1 fusion to attempt to pull down baculovirus-derived Mre11 complex. The second approach involves using baculovirus-derived Mre11 complex to attempt to supershift TRF2-DNA or Rap1-TRF2-DNA complexes in electromobility shift assays (EMSAs).

Results and discussion

In order to study the interactions between the TRF2 complex and the Mre11 complex, the components of these complexes were produced in vitro through various methods. A baculovirus system was used to product TRF2, hRap1, and the Mre11 complex (Figure 4-1A). The TRF2 and hRAP1 baculoviruses were previously constructed in the de Lange lab (Broccoli et al. 1997a; Li et al. 2000), while the Mre11 complex baculoviruses were a generous gift of Tanya Paull and Martin Gellert (Paull and Gellert 1998; Paull and Gellert 1999). The baculoviruses for Mre11, Nbs1, and Rad50 must be used together to infect insect cells in order to obtain a stable Mre11 complex in vitro. Mre11 can be produced alone, but Nbs1 and Rad50 each require Mre11 for their stability. It is unclear whether the mechanism underlying the requirement of Mre11 for the stability of Nbs1 and Rad50 is co-translational or post-translational. The purity of the baculovirus-derived proteins was assessed through Coomassie-staining (Figure 4-1A). Mre11 protein itself could be isolated at high yield and purity (Figure 4-1A). The Mre11/Nbs1/Rad50 complex yielded less protein and relatively more contaminants (Figure 4-1A). Additionally, antibodies that recognize Mre11, Nbs1, and Rad50 reacted with bands of the appropriate size (Figure 4-1B).

Figure 4-1. Baculovirus-derived Mre11 and Mre11 complex.

A. Mre11 alone or Mre11, Nbs1 and Rad50 baculoviruses (gifts of Tanya Paull and Martin Gellert) were used to infect SF21 insect cells. Each Mre11 complex component was His-eptiope tagged. Cell lysates were prepared 40 hr post-infection. Lysates were purified using nickel beads. Samples were run out using SDS-PAGE and stained with Coomassie Brillant Blue G.

B. Baculovirus-derived Mre11 complex is immunoblotted with antibodies recognizing Mre11, Rad50 and Nbs1 as indicated.

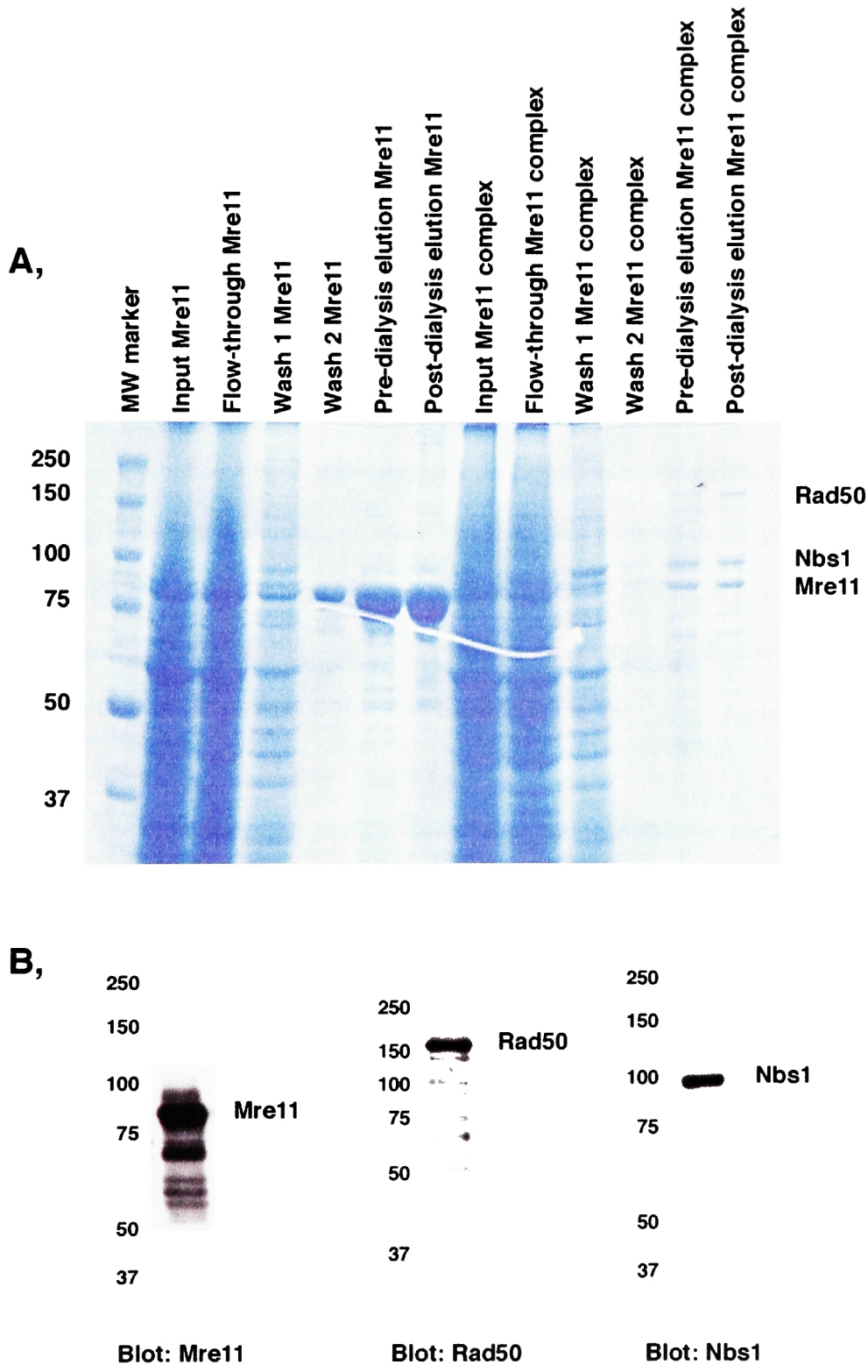
A,
MW marker
Input Mre11
Flow-through Mre11
Wash 1 Mre11
Wash 2 Mre11
Pre-dialysis elution Mre11
Post-dialysis elution Mre11
Input Mre11 complex
Flow-through Mre11 complex
Wash 1 Mre11 complex
Wash 2 Mre11 complex
Pre-dialysis elution Mre11 complex
Post-dialysis elution Mre11 complex
250
150
100
75
50
37
Rad50
Nbs1
Mre11
B,
250
150
100
75
50
37
Mre11
Blot: Mre11
250
150
100
75
50
37
Rad50
Blot: Rad50
250
150
100
75
50
37
Nbs1
Blot: Nbs1

The complex presented here looks the same as the purified Mre11/Nbs1/Rad50 complex (Carney et al. 1998).

In order to perform GST pulldown experiments, hRap1 was cloned into the pGEX-2TK plasmid by PCR to give a GST-hRap1 expression construct. E. coli (B21 strain) were transformed with this plasmid to produce GST-Rap1 protein (Figure 4-2A). Protein concentration was determined through the Bradford assay and comparing the GST-hRap1 fusion to known quantities of BSA on Coomassie-stained gels following SDS-PAGE (Figure 4-2A). Protein purity was determined by examining these gels and observing a prominent band at the correctly predicted molecular weight of 73 kD (Figure 4-2A). There are a number of other bands in this preparation (Figure 4-2A). An immunoblot of the GST-hRap1 fusion with an antibody that recognizes hRap1 reveals both that the 73 kD band indeed contains hRap1 and that the bands seen in Figure 4-2A also contain hRap1 (Figure 4-2B). Degradation is the most likely explanation for these smaller molecular weight bands (Figure 4-2B).

The first approach used involved attempts to pulldown baculovirus-derived Mre11 complex with a GST-Rap1 fusion protein. Early experiments gave an impression that GST-Rap1 could indeed pulldown the Mre11 complex (Figure 4-3). When the experiment was reproduced, there was some degree of binding of the Mre11 complex to GST alone. A number of different conditions were attempted, including the addition of baculovirus-derived TRF2 and the use of SDS / TritonX-100. TRF2 was added to possibly stabilize the complex and SDS / Triton X-100 was used to decrease the background binding of the Mre11 complex. Further attempts reveal that, while

Figure 4-2 Preparation of GST and GST-Rap1 proteins.

A. GST and GST-hRap1 was produced in BL21 strain *E. coli*. Cell lysates were made and proteins were purified using glutathione sepharose beads. Samples were run out using SDS-PAGE and stained with Coomassie Brilliant Blue G. The top and bottom gels shown are 7% and 9% SDS-PAGE, respectively.

B. Immunoblots of the GST and GST-hRap1 samples in A were probed with an antibody recognizing hRap1.

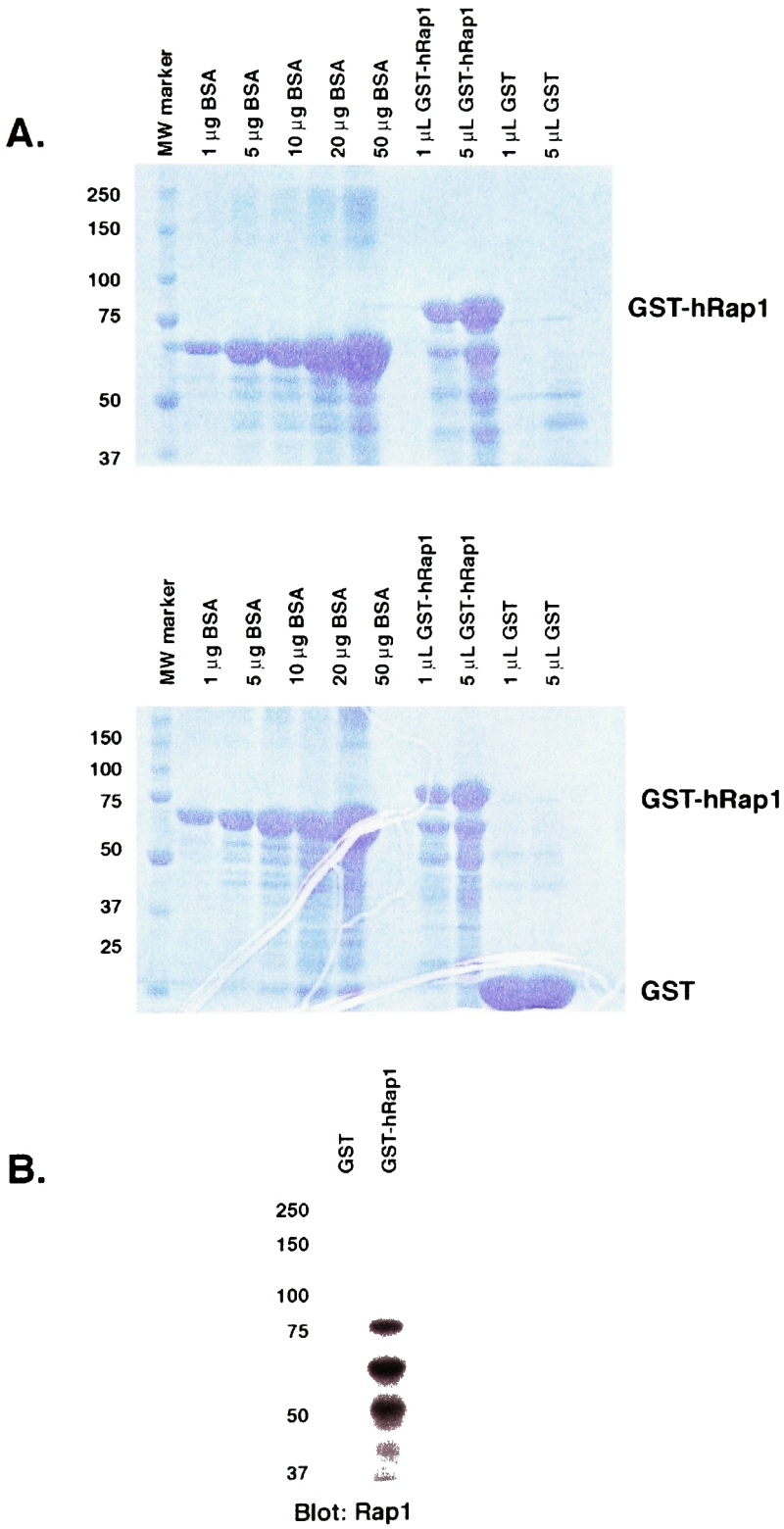
A.
MW marker
1 μg BSA
5 μg BSA
10 μg BSA
20 μg BSA
50 μg BSA
1 μL GST-hRap1
5 μL GST-hRap1
1 μL GST
5 μL GST
250
150
100
75
50
37
GST-hRap1
MW marker
1 μg BSA
5 μg BSA
10 μg BSA
20 μg BSA
50 μg BSA
1 μL GST-hRap1
5 μL GST-hRap1
1 μL GST
5 μL GST
150
100
75
50
37
25
GST-hRap1
GST
B.
GST
GST-hRap1
250
150
100
75
50
37
Blot: Rap1

Figure 4-3. GST-hRap1 pulldown of the Mre11 complex, TRF1 and TRF2.
GST and GST-hRap1 were used to pulldown baculovirus-derived Mre11 complex, TRF1 and TRF2. Mre11 complex was added in the top three blots, TRF1 in the lower left blot and TRF2 in the lower right blot. Immunoblots were performed on the samples using antibodies recognizing Mre11, Rad50, Nbs1, TRF1 and TRF2 as indicated. 1% input was loaded in lanes designated as input.

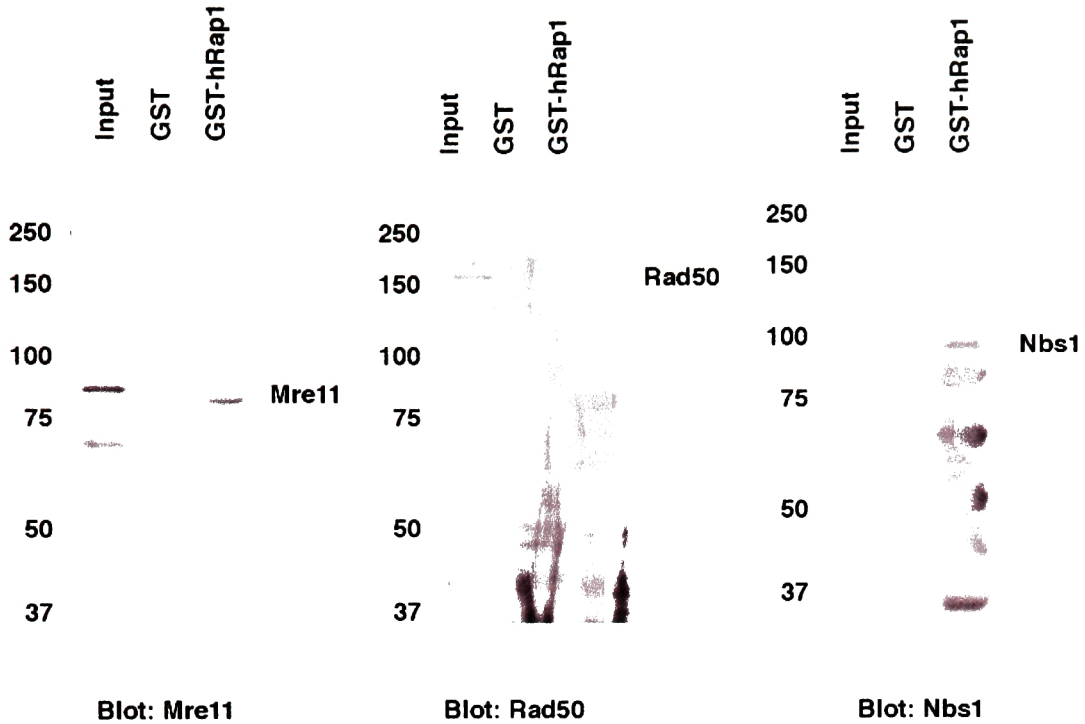
Input
GST
GST-hRap1
250
150
100
75
50
37
Mre11
Blot: Mre11
Rad50
Blot: Rad50
Nbs1
Blot: Nbs1

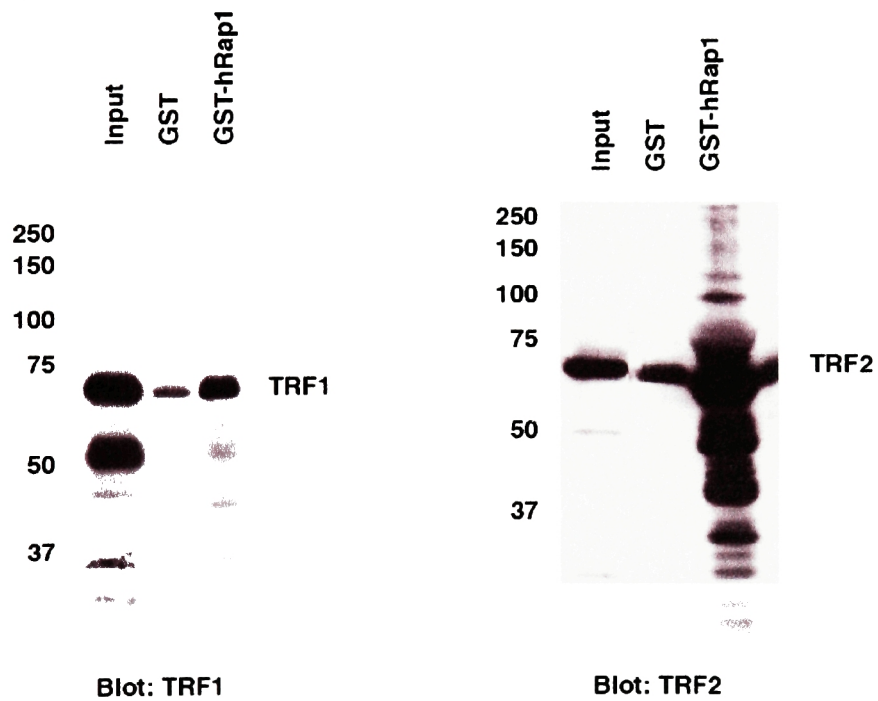
Input
GST
GST-hRap1
250
150
100
75
50
37
TRF1
Blot: TRF1
TRF2
Blot: TRF2

promising, the background binding of the Mre11 complex continued to be a problem. There is a strong enrichment of baculovirus-derived TRF2 in a pulldown with GST-hRap1 relative to a pulldown with GST alone (Figure 4-3). Although there is a bit of background binding with baculovirus-derived TRF1, there is a small enrichment in GST-hRap1 in comparison to GST alone pulldown (Figure 4-3). These controls demonstrate that GST-hRap1 behaves as expected in terms of its ability to bind to Rap1 and its inability to interact with TRF1. However, the amount of enrichment of TRF1 is not completely insignificant.

Another approach to understanding the binding interactions between the TRF2-hRap1 complex and the Mre11 complex is the use of electrophoretic mobility shift assay (EMSA), also known as gel-shift analysis. A labeled probe containing twelve TTAGGG double-stranded repeats corresponding to human telomeric DNA was used to assay the ability of the Mre11 complex to supershift or affect the mobility of TRF2-telomeric DNA or Rap1-TRF2-telomeric DNA complexes. This system was originally developed to assay the ability of TRF1 to bind telomeric DNA (Bianchi et al. 1997). is capable of binding telomeric DNA directly and producing an EMSA shift. Human Rap1, while unable to bind DNA directly, can supershift a TRF2-DNA complex (Broccoli et al. 1997a; Li et al. 2000). Initial attempts were performed to determine if baculovirus-derived Mre11 or Mre11 complex could supershift TRF2-DNA (Figure 4-4). The initial data was promising in that Mre11 complex appeared to shift the TRF2-DNA complex (Figure 4-A lanes 5 and 9). Although some of this data appeared promising, a technical problem involved the fact that the Mre11 complex was fairly dilute and a large amount of salt was added to the EMSA reactions along with Mre11 complex protein. The salt

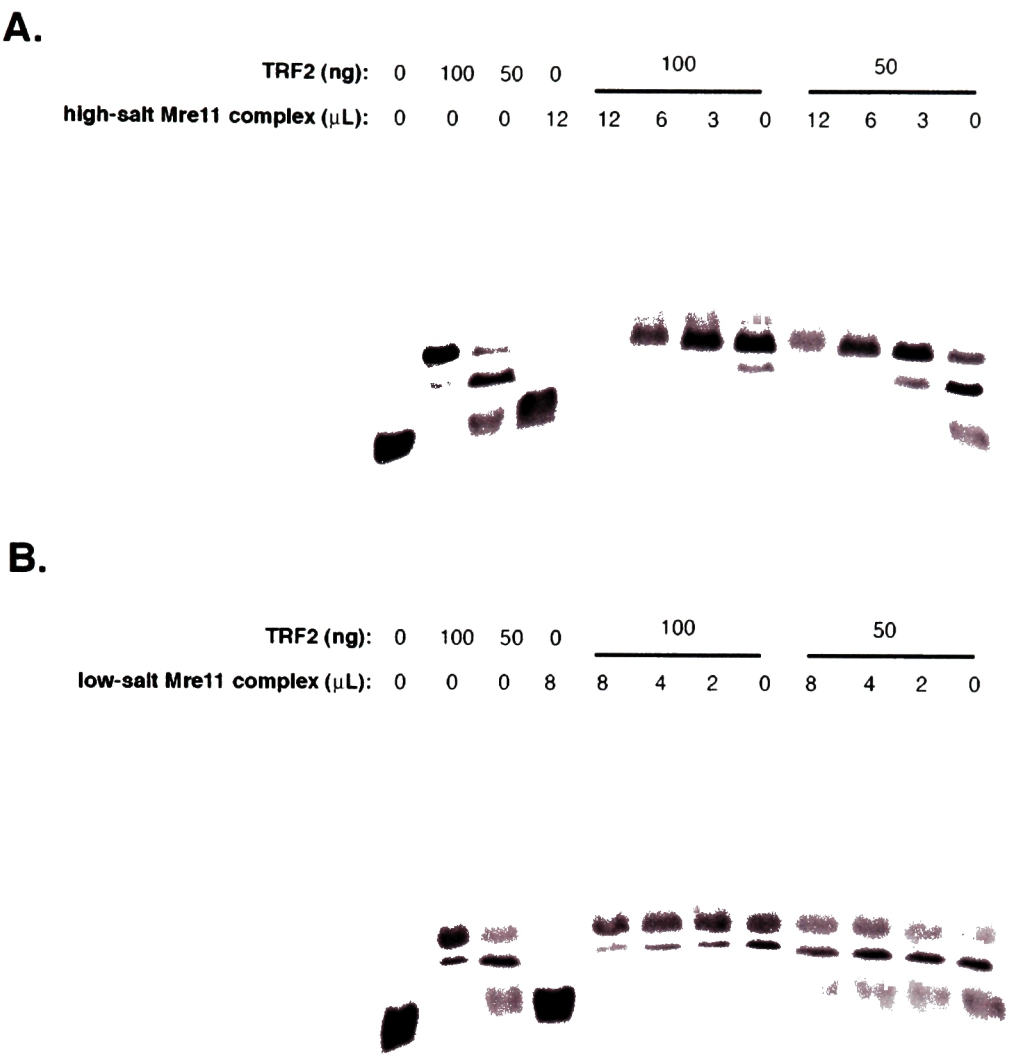

Figure 4-4. Gel shift analysis to determine if Mre11 complex can supershift a TRF2-DNA complex.

A. EMSA performed using the indicated quantities of baculovirus-derived TRF2 and/or Mre11 complex prepared with 450 mM KCl and a radiolabeled probe containing twelve TTAGGG telomeric duplex repeats.

B. Same as in A., except that Mre11 complex dialyzed against 150 mM KCl is used.

carried along with the Mre11 complex may affect the TRF2-DNA complex and give the appearance that Mre11 complex is able to supershift the TRF2-DNA complex. In order to solve this problem, Mre11 complex was prepared as previously, but was dialyzed against 150 mM KCl to lower the amount of salt. The EMSA experiments were then repeated (Figure 4-4B). Although these experiments were repeated numerous times under varying protein concentrations, no evidence exists that conclusively and reproducibly indicates that Mre11 complex is able to supershift the TRF2-DNA complex.

Mre11 complex may also be recruited to the telomere through Rap1. As a result, EMSA was performed to determine whether or not the Mre11 complex could supershift the Rap1-TRF2-DNA complex. Rap1 is able to supershift the TRF2-DNA complex ((Li et al. 2000), Figure 4-5). Baculovirus-derived Mre11 or Mre11 complex were added to the Rap1-TRF2-DNA complex (Figure 4-5A and 4-5B, respectively). Although there may be small effects on the shift, these are not reproducible. It is unclear whether this is due to the gel shift conditions used, the quality of the protein preparations, or reflects the biology of the Mre11 complex.

Figure 4-5. Gel shift analysis to determine if Mre11 complex can supershift a Rap1-TRF2-DNA complex.

A. EMSA performed using the indicated quantities of baculovirus-derived TRF2, Rap1, and/or Mre11 and a radiolabeled probe containing 11 TTAGGG telomeric duplex repeats. B. Same procedure as in A., except that Mre11 complex dialyzed against 150 mM KCl is used.

A.

TRF2 (ng):	0	100	50	25	50						0	0	0	0	0	50			
Rap1 (ng):	0	0	0	0	0	0	0	0	0	0	0	0	0	0	0	250	100	50	0
Mre11 (ng):	0	0	0	0	1K	500	250	100	50	0	1K	500	250	100	50	0	0	0	0

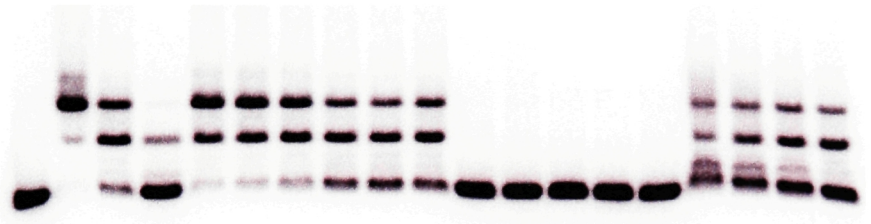

B.

TRF2 (ng):	0	50				100				0	100								0
Rap1 (ng):	0	100	50	25	0	100	50	25	0	100	50				0				0
Mre11complex (μL):	0										8	4	2	0	8	4	2	0	8

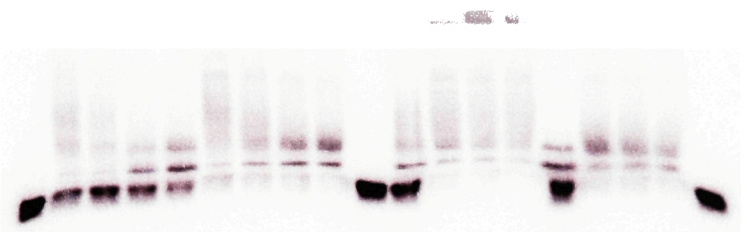

Materials and Methods

Yeast Two-Hybrid library-scale transformation

The library transformation of L40 yeast cells was performed as follows. A full-length human Rap1 fused to LexA or a carboxy-terminal human Rap1 fused to LexA were used to screen transformants from of a human fetal liver two-hybrid library (Clontech) created in pGAD10. An overnight culture of the yeast bait strain was grown at 30 °C in appropriate dropout media. A 50 ml culture was then inoculated with 0.25 ml of the overnight culture and grown overnight at 30 °C. 200 ml of YPD (prewarmed to 30 °C) was inoculated with enough culture to give OD600 of 0.3 and cells were grown for 3 hours at 30 °C (at least one doubling). Cells were pelleted at 2.5 K for 5 min at room temperature, resuspended in 100 ml TE (10 mM Tris-HCl pH 8.0 / 1mM EDTA), pelleted agan and resuspended in 4 ml 100 mM LiOAc / 0.5 X TE (10 mM Tris-HCl pH 8.0 / 1mM EDTA). 0.2 μL denatured carrier DNA (10 mg / ml) and 50 micrograms of library DNA was then added. Then, 28 ml 100 mM LiOAc / 40% polyethylene glycol / 1x TE (10 mM Tris-HCl pH 8.0 / 1mM EDTA) was added, mixed, and incubated 30 min at 30 °C with gentle shaking. 3.5 ml dimethyl sulfoxide was added with swirling to mix and cells were heat shocked at 42 °C for 6 min with occasional swirling. After heat shock, cells were immediately diluted with 80 ml YPD and cooled to room temperature in a water bath. The cells were pelleted at 2.5 K for 5 min at room temperature, washed with 100 ml YPD resuspended in 200 ml YPD (prewarmed to 30 °C) and incubated at 30 °C for 1 hr with gentle shaking. Cells were pelleted again at 2.5 K for 5 min at room temperature and resuspended in 100 ml SD –Trp, - Leu. 10 μL and 1 μL of this were plated on SD –Trp, -Leu to allow a determination of the number of transformants plated during the screen. The remaining cells were pelleted and resuspended in 200 ml SD –Trp, -Leu (prewarmed to 30 °C) and incubated at 30 °C with shaking between 4 hr and 16 hr. Cells are pelleted, washed twice with SD –Trp, -Leu, -His and resuspended in 10 ml SD –Trp, -Leu, -His. Plate 0.1 μL and 0.01 μL on SD –Trp, -Leu to assess number of tranformants plated and plate 10 ml on 50 SD –Trp, - Leu, -His plates and incubate at 30 °C.

Yeast transformation

Yeast transformation was performed as follows. The yeast strain to be transformed is grown to mid-log phase (OD600 = 0.6 - 0.8). Cells are harvested in a clinical centrifuge for 15 min at 10 K at 4 °C and resuspended in 1/2 total volume of 1 x YTB. Cells are centrifuged for 15 min at 10 K at 4 °C again and resuspended in 1ml of 1X YTB per 50 ml starting culture. For each transformation, 50 μL of cells are placed in an eppendorf tube. Add 5 μL of boiled carrier DNA at 5 mg/ml (eg herring sperm DNA) and the plasmid or library DNA (usually 1 to 5 μL). Shake gently to mix, add 0.5 ml of polyethylene glycol 40%/ LiAc / TE (10 mM Tris-HCl pH 8.0 / 1mM EDTA) solution, vortex and incubate at 30 °C for 30 min without shaking. Heat shock the cells at 42 °C for 20 min, spin tubes in microfuge for 2 min at setting 3, wash cells once with 0.5 ml of H_2O, resuspend cells in 0.3 ml of H_2O and plate on appropriate nutritional selection plates.

A "quick" method of yeast transformation was also used. In this method, a 2 x 2 cm patch of the yeast strain to be transformed was grown at 30 °C. The patch is collected with a sterile toothpick and placed in an eppendorf tube with H_2O. The cells are spun down, the H_2O is aspirated, and cells are resuspended in 0.7 ml 40% polyethylene glycol / 0.1 M LiOAc / TE (10 mM Tris-HCl pH 7.5 / 1mM EDTA). 5 μL of herring sperm DNA (5 mg/ml) and 3 μL of DNA are added and the tube is incubated at room temperature overnight. The following day, the tubes are heat shocked at 42 °C for 20 min, spun 2 min at speed 3, and the pellets are washed once with 0.5 ml H_2O. The cells are then resuspended in 300 μL H_2O and plated on appropriate nutritional selection plates.

Yeast protein extracts

Yeast protein extracts were prepared from 50 ml of yeast culture grown to mid-log phase (OD600 approximately 0.5) at 30 °C. The culture is then centrifuged at 2.5 K for 5 min at 4 °C and washed once with sterile, ice-cold H_2O. The pellet is resuspended

in 0.5 ml 2 X Laemelli buffer (125 mM Tris-HCl, 4% SDS, 20% glycerol, 10% mercaptoethanol, 0.004% bromophenol blue). The samples are then transfered to an Eppendorf tube containing 100 µl glass beads, vortexed 1 min, boiled 5 min, and placed on ice for 3 min. The vortex and ice steps are repeated three times and samples are centrifuged at 14 K for 1 min at 4 °C. Finally, transfer supernatant to new tube and store at –80 °C.

Yeast plasmid isolation

In order to isolate plasmid DNA from yeast, a 3 cm x 3 cm patch of the appropriate yeast strain was grown and collected with a toothpick into 0.5 ml H_2O in an Eppendorf tube. The cells are spun down at 3 K for 2 min at room temperature and the supernatant is aspirated. The cells are then resuspended in 100 µL STET (50 mM Tris-HCl pH 8.0, 50 mM EDTA, 8% sucrose, 5% Triton X-100) and then 0.2 g of glass beads area added. The tubes are vortexed at room temperature for 15 min, another 100 µL STET (50 mM Tris-HCl pH 8.0, 50 mM EDTA, 8% sucrose, 5% Triton X-100) are added and the tubes are vortexed for 10 min after which they are centrifuged at 14 K for 10 min at 4 °C. 100 µL of the supernatant is removed, combined with 100 µL 4 M ammonium acetate, and then stored at –20C for at least 1 hr. Tubes are spun at 14 K for 10 min at 4 °C and 150 µL of supernatant is transferred to new tube with 200 µL ice-cold EtOH and incubated for at least 15 min at –20 C. Tubes are spun again 14 K for 15 minutes at 4 °C. Aspirate the supernatant, speedvac to dry the DNA pellet and reuspend in 20 µL 0.1 x TE (10 mM Tris-HCl pH 8.0 / 1mM EDTA).

β-galactosidase filter lift assay

To perform the β-galactosidase filter lift assay, yeast strains are first grown on plates. A filter (VWR qualitative diameter 7.5 cm grade 410, cat. # 28321-055) is placed on top of the cells, removed and placed in liquid N_2 for 20-30 sec, allowed to warm to room temperature and then placed in liquid N_2 for another 20-30 sec and allowed to warm

to room temperature again. Another filter is placed in an empty Petri dish and covered with 1 ml of ZX solution (10 ml Z buffer, 27 μl beta-mercaptoethanol, and 500 μl X-gal stock (20 mg/ml in DMF) for final concentration of 1 mg/ml; Z buffer is 16.1 g/L Na_2HPO_4-$7H_20$, 5.5 g/L NaH_2PO_4-$7H_2O$, 0.75 g/L KCl and 0.246 g/L $MgSO_4$-7H2O. The original filter is placed, cell side up, on top of the wetted filter in the Petri dish and another 100-300 μl of ZX buffer is added. Eliminate bubbles and place in 37 °C incubator. The filters are observed and the time required for a given colony to turn blue is recorded.

Quantitative β-galactosidase assay

To perform the quantitative beta-galactosidase liquid culture assay, the appropriate yeast strains are grown to an OD_{600} between 0.5 and 0.8. The exact OD is recorded. Then, place 1.5 ml of culture in an Eppendorf tube, centrifuge 14 K for 30 sec at room temperature and aspirate the supernatant. Wash and resuspend pellet in 1.5 ml Z buffer, spin down cells, and resuspend in 300 lambda Z buffer. After pipetting 100 lambda into a new Eppendorf tube, place tubes in liquid N2 and then thaw cells at 37 C in water bath for 1 min. After also setting up blank tube with 100 lambda Z buffer, add 0.7 ml of Z buffer (16.1 g/L Na_2HPO_4-$7H_20$, 5.5 g/L NaH_2PO_4-$7H_2O$, 0.75 g/L KCl and 0.246 g/L $MgSO_4$-7H2O) and β-mercaptoethanol to the reaction and blank tubes. Start a timer as one adds 0.16 ml ONPG to reaction and blank tubes and places in 30 C incubator. To stop the reactions add 0.4 ml 1 M Na_2CO_3 to reaction and blank and record time. After spinning tubes at 14K at room temperature, the OD_{420}. Calculate the standard units by the following formula: beta-galactosidase units = (1000 x OD420) / (t x V x OD600) where t = elapsed time in minutes of incubation and V = 0.1 ml x concentration factor.

Yeast telomere blot

The isolation of genomic DNA from yeast is the first step in the yeast telomere blot. To perform this, 8-10 ml culures of appropriate yeast strains are grown on a roller.

The cultures are then centrifuged at 14 K for 10 minutes at 4 °C, the supernatants are aspirated and the pellets are resuspended in 1 ml H_2O and transferred to Eppendorf tubes. The samples are centrifuged 14 K for 5-10 sec and the supernatant is aspirated. The pellets are then resuspended in 0.6 ml of a sorbitol/EDTA/zymolase solution (For 10 ml of 0.9 M sorbitol / 0.1 M EDTA solution, add 3 mg of powdered zymolase 20,000 and 20 µl of beta-mercaptoethanol; 1 L of sorbitol / EDTA solution made by adding 550 ml H_2O to flask, then 163.98 g sorbitol, 200 ml 0.5 M EDTA, mix and bring up to 1 L) made fresh and incubated at 37 °C for 1 hr. The samples are centifrigued 14 K for 5 sec, the supernatants are aspirated and the pellets are resuspended in 0.6 ml TE (10 mM Tris-HCl pH 8.0 / 1mM EDTA). 120 µl EDTA/Tris/SDS solution (2 ml 0.5 M EDTA, 1 ml 2 M Tris base, 0.5 ml H_2O, and 0.5 ml 20% SDS) is added to each sample. The samples are mixed gently by inverting the tubes and then they are incubated at 65 °C for 30 min. Following this, 200 µl 5 M KOAc is added to each sample and the samples are mixed completely by inverting and incubated on ice for 1 hr. The samples are then spun down in a centrifuge 14 K for 15 min at 4 °C, the supernatants are poured off carefully into into fresh tubes containing 550 µl of isopropanol and the tubes are mixed immediately by inverting the tubes. The samples are centrifuged 14 K for 10 minutes at 4 °C, the supernatants are decanted and the pellets are washed with 1 ml 70% ethanol, centrifuged at 14 K for 2-5 minutes at 4 °C and the supernatants are carefully aspirated. The pellets are then dried for 5-10 min on a SpeedVac. After drying, the pellets are resuspended in 500 µl TE + 3 µl RNase and incubated at 37 °C for 1 hr (vortexing the tubes briefly at 30 min). The samples are then centrifuged 14 K for 15 min at 4 °C and the supernatant is transferred to a new tube. 20 µl of 5 M NaCl and 300 µl isopropanol is added to each sample and then the tubes are inverted to precipitate the DNA. The samples are centrifuged 14 K for 10 min at 4 °C, the supernatants are decanted, the pellets are washed with 70% ethanol. After the samples are again centrifuged 14 K for 10 min at 4 °C, the ethanol is aspirated and the pellets are dried in a speed-vac. Finally, the samples are resuspend in 20 µl TE (10 mM Tris-HCl pH 8.0 / 1mM EDTA) and vortexed well to resuspend the pellets.

The radiolabeled telomere probe is made according to the following protocol. To prepare poly(dA-dC)–poly(dG-dT) DNA (Pharmacia Biotech), resuspend at 1 U/ml TE (50 ng/μl) and then further dilute to a concentration of 10 ng/μl. The telomere probe is made via random priming using the Megaprime DNA labeling system kit (Amersham). First, 5 μl poly(dA-dC)–poly(dG-dT) DNA is aliquoted into an Eppendorf tube and then 15 μl H_2O is added to a final volume of 20 μl. The DNA is then dantured 95°C for 10 min, snap cooled on ice for 5 min. and briefly spun to collect contents. The following are then added in order: 5 μl primer solution, 5 μl reaction buffer, 4 μl cold dATP, 4 μl cold dTTP (from Amersham kit thus far), 5 μl radioactive dGTP, 5 μl radioactive dCTP, and 2 μl Klenow. The reaction mix is then incubated at 37°C for 30 min and the DNA is then precipitated by adding 50 μl TE (10 mM Tris-HCl pH 8.0 / 1mM EDTA), 1 μl glycogen, 50 μl 7.5 M ammonium acetate, and 300 μl 95% ethanol. The mixture is then left to stand at room temperature for 15 min. The supernatant is removed carefully with a pasteur pipet and dispensed into a clean eppendorf (save this). The pellet should be visible as a small white pellet (due to the glycogen). The pellet is washed with 300 μl 70% ethanol and mixed by inverting. The samples are then centrifuged 14 K for 2 min at 4°C and the supernatant if removed. The amount of radioactivity incorporated into the probe is then estimated by comparing the amount of signal from the tube of radioactive supernatant with the tube of the actual probe. The probe should have at least 30% of the radioactivity incorporated into the probe. The probe is then dried using a Speedvac for 5-10 min, and resuspend in 200 μl TE (10 mM Tris-HCl pH 8.0 / 1mM EDTA).

The telomere blot for *S. cerevisiae* samples is performed as follows. First, yeast genomic DNA samples are digested with XhoI. Approximatedly 5 to 8 μl of a standard yeast DNA prep (i.e. 8 to 10 ml of yeast prepped into 20 μl of DNA) is used and 1 to 2 μl of XhoI enzyme and appropriate buffer is added in a 20 μl total reaction volume. The DNA is digested at 37°C for a minimum of 4 hr. The samples and molecular weight markers are subjected to electrophoresis on a large agarose gel at 55 volts (for about 16-18 hr). Prior to transfer, a picture of the gel is taken with a ruler aligned with the molecular weight markers and the top marking the top of the well. The gel is then soaked in denaturation solution for 30 min (the solution is changed after 15 min). A Hybond N

membrane is cut and the gel is blotted overnight in 10 X SSC. The DNA is then crosslinked to the membrane using UV, the membrane is pre-hybridized in telomere hybridization solution (6 X SSC, 4 X Denhardt's reagent, 0.5 % SDS, 25 micrograms / ml E. coli DNA) at 60°C for 6 hr, and the blot is hybridized in telomere hyrbidization solution with telomeric probe prepared as above (and denatured 95°C for 5 min and quickly cooled on ice just prior to use) at 60°C for at least 16 hr. The blot is then washed four times in 4 X SSC, 0.1% SDS for 15 min each and three times in 0.1 X SSC, 0.1% SDS for 10 min each while monitoring with a Geiger counter. The blot was then exposed overnight on a phosphorimager.

Cell culture

Cells were passaged by treatment with trypsin and seeding at appropriate densities per cell line. Cell numbers were determined by using a Coulter Counter to assay a 1:20 dilution of cell suspension in diluent fluid. For cell freezing, cells were harvested, washed with media and resuspended in approximately 0.5 ml 2 x A freezing solution (40 ml FBS (Hyclone), 0.4 ml gentamycin stock solution [stock is 50 mg/ml gentamycin from Sigma], 4 ml HEPES stock solution [stock is 1 M HEPES pH 7.6], and 156 ml L15 media (Sigma) and is sterilized through a 0.2 micron filter] per 10 cm^2 plate. 0.5 ml of 2 x D freezing media (40 ml PVP stock solution [stock is 100 mg PVP (Sigma) per ml of HEPES-buffered saline, 30 ml DMSO (Sigma), 4 ml HEPES stock solution [stock is 1 M HEPES pH 7.6], and 126 ml L15 media (Sigma) and is sterilized through a 0.2 micron filter) is then added and 1 ml of each mixture is added per cryovial. The vials were placed in a room temperature Styrofoam box at –80°C overnight before being transferred to a liquid N_2 storage container several days later.

IMR90 primary human fibroblasts (ATCC), AG02496 and AG04405 primary A-T fibroblasts (Coriell Cell Repository), SV40-transformed NBS-1 LB1 cells ((Zdzienicka 1999); a gift from Margaret Zdziencka), and ATLD-3 and ATLD-4 cells (Stewart et al. 1999), a gift from John Petrini) were grown in DMEM, 15% fetal bovine serum. HeLa and 293T cells were grown in DMEM, 10% bovine calf serum. U2OS cells (ATCC) were

grown in McCoy's modified medium with 10% fetal bovine serum. HCC1937 cells (ATCC) and HCT-15 cells (ATCC) were grown in RPMI media with 10% fetal bovine serum and 1 mM sodium pyruvate. All media were supplemented with 2 mM L-glutamine, 0.1 mM non-essential amino acids, 100 units of penicillin per ml and 0.1 mg of streptomycin per ml.

For IR treatment, cells were exposed to γ-irradiation using a Cs^{137} source at a rate of 770 rad/min in 6 cm^2 dishes. For UV radiation, cells were washed with PBS and exposed to 25 J/m^2 UV radiation (265 nm) in a Stratalinker (Stratagene). The lid was removed from the dishes just prior to UV radiation and replaced immediately after this treatment. After UV radiation, cells were incubated in media until harvest. MMS and etoposide (0.01% w/v and 50 mg/ml, respectively) were added to the media and cells were incubated for 1 hr before harvesting. Caffeine and wortmannin (20 mM and 100 mM, respectively) were added to the media 2 hrs and 1 hr, respectively, before irradiation.

Antibodies

Antibodies 1025 and 1060 were affinity purified from rabbit serum immunized with keyhole limpet haemocyanin-conjugated Rif1 peptides (NSESDSSEAKEEG SRKKRSGKWKNK and EEGIIDANKTETNTEYSKSEEKLDN; both with an added C-terminal Cys residue). Peptides were obtained from Bio-synthesis Incorporated and rabbit serum obtained from Covance Research Products. KLH was obtained from Pierce. Serum obtained from mice immunized with the KLH-conjugated 1060 peptide was also used but without affinity purification. Antibodies 1066 and 1067 are crude serum from rabbits immunized with a GST fusion protein consisting of GST fused to a portion of Rif1 extending from amino acid 907 to amino acid 1327.

For other proteins, following antibodies were used: TRF1, 371 ((van Steensel and de Lange 1997)); TRF2, 647 ((Smogorzewska et al. 2000)); ATM 2C1 (GeneTex); phospho-ATM Ser 1981 ((Bakkenist and Kastan 2003); a gift from Mike Kastan); ATRIP-N ((Cortez et al. 2001); a gift from Steve Elledge); BRCA1 Ab-1 (Oncogene

Research Products); phospho-BRCA1 Ser1524 (Oncogene Research Products); phospho-Chk1 Ser317 (Cell Signaling); phospho-Chk1 Ser345 (Cell Signalling); FANCD2 (a gift from Arlene Auerbach); g-H2AX Ser139 (Upstate); phospho-Histone H3 Ser10 (Upstate); Nbs1 ((Maser et al. 2001); a gift from John Petrini); phospho-p53 Ser15 (Cell Signalling); p53, DO1 (Santa Cruz); phospho-Rad17 Ser 645 (Cell Signalling); 53BP1 ((Schultz et al. 2000); a gift from Thanos Halazonetis); a-tubulin clone B-5-1-2 (Sigma); and g-tubulin clone GTU-88 (Sigma).

To prepare whole cell lysates, cell were trypsinized, washed once with media, washed once with cold PBS, counted and resuspended at 1 x 10^4 cells/ml 4X Laemmli buffer (0.24 mM Tris-HCl, 4% SDS, 20% glycerol, 10% beta-mercaptoethanol, 0.004% bromophenol blue), boiled for 10 min and then sheared through a 28 gauge insulin syringe. To prepare buffer C extract, cells were trypsinized, washed once with media, twice with ice-cold PBS, and incubated in buffer C (van Steensel et al. 1998) on ice for 30 min. After centrifugation at 4°C for 10 min at 14 K, the supernatant was collected and the Bradford assay was used to determine protein concentration. The extract was then combined with Laemmli buffer and boiled for 10 min. Protein samples were separated by SDS-PAGE and blotted to either nitrocellulose or PVDF (for ATM) membranes. Membranes were blocked in 10% non-fat powdered milk/0.5% Tween-20 in PBS for 30 min at room temperature and incubated with primary antibodies in 0.1% non-fat powdered milk/0.1% Tween-20 in PBS (IB) at 4°C overnight. Membranes were washed three times in IB, incubated with secondary antibody in IB for 40 min at room temperature, washed three times with IB, twice with PBS, and once with H_2O. ECL (Amersham) was applied and membranes were exposed to film.

GST pulldowns

This protocol was obtained from the Amersham Pharmacia biotech manual and Edward Yang. Large scale bacterial sonicates were obtained by growing BL21 bacteria in 2 x YTA at 20-30°C with shaking until mid-log phase. 100 mM stock of IPTG was added to give a final concentration of 1 mM and cells were grown from 2-6 hr at 30°C.

Cells were spun down at 8 K for 10 min at 4°C, the supernatant was discarded, and the pellet was drained and placed on ice. The pellet was then resuspended in 1/20th volume of 1 x PBS with 1 mM PMSF and protease inhibitor cocktail, sonicated, and 20% Triton X-100 was added to give a final concentration of 1% Triton X-100. The samples were mixed gently for 30 min, centrifuged for 10 min at 10K in 4°C, and the supernatant containing the protein was transferred to a new tube. To purify the GST-fusion protein, 2 ml 50% glutathione bead slurry (prepared by spinning down beads, washing with PBS three times and resuspending beads in an equal volume of PBS) was added to each 100 ml of bacterial sonicate and incubated on nutator for 30 min at room temperature. The beads were then sedimented and washed with PBS three times.

GST pulldowns were performed at 4°C with 10 μg of GST fusion protein which was added to 1 ml of BC x buffer (20 mM Tris-HCl pH 8.0, 20% glycerol, x mM KCl where x depends on require salt (i.e. BC150 implies 150 mM KCl), 0.1 mM EDTA pH 8.0, 0.1% NP-40, 1 mM PMSF, 1 mM DTT and protease inhibitors and given quantities of baculovirus-derived proteins. After 6 hr nutation in cold room, cells were spun down and pellets where washed with BC buffer (usually BC300 or BC400) three times. Pellets were resuspended in 2 x Laemelli buffer, boiled for 10 min, and then stored at -20°C until used for immunoblotting.

Electromobility shift assays

Electromobility shift assays (EMSA) were performed using a radiolabeled pTH12 probe containing human telomeric TTAGGG repeats. The 142 bp HindIII / Asp718 fragment was isolated from pTH12 $[TTAGGG]_{12}$ and gel purified using the QIAEXII gel purification kit. The isolated fragment was then diluted to a concentration of 75 ng/μl. In order to label this fragment, the following mix was made: 2 μl 10x OLB (0.5M Tris-HCl pH 6.8, 0.1 M MgOAc, 1 mM DTT, 0.5 mg/ml BSA; aliquots stored at –80°C) with fresh dG, dA, and dT (for 100 μl working buffer, add 0.6 μl each dGTP, dATP, and dTTP (Pharmacia)), 2 μl 75 ng/μl 142 bp pTH12 fragment, 5 μl ^{32}P-a-dCTP (3000 Ci/mmol), 10 μl H2O, and 1 μl Klenow (2 U/μl). This mix is then incubated for 1

hr at RT, add 80 µl TENS (Tris-HCl pH 7.5, 10 mM EDTA pH 8.0, 100 mM NaCl, 0.1% SDS) and mix, add 5 µl sheared *E. coli* DNA and mix. This was purified over a Sepadex G50 column as follows: G50 column equilibrated in a 3 ml syringe with TENS, probe is added and allowed to settle, 1 ml TENS is added and collected, 0.8 ml TENS is added and collected to be used as probe. The 0.8 ml is divided into two eppendorf tubes, extracted once with phenol/CIAA and once with chloroform. 40 phenol/CIAA 2 M NaOAc pH 5.5 and 2 X volumes ethanol are then added to precipitate probe. The probe is then mixed and incubated at –20 C for at least one hour, centrifuged 14K for 15 min at 4°C, washed once with 70% ethanol, spun again and resuspended in 10 mM Tris-HCl pH 7.5.

For EMSA under TRF2 conditions, samples are run on a 0.8% agarose gel made with 0.1 x TBE. The following mix is then made: 1 µl 80% glycerol, 0.5 µl 1 µg/µl sheared *E. coli* DNA, 2 µl 150 mM TRIS-HCl pH 7.5, 0.5 µl 100 ng/µl beta-casein, and 0.5 µl labeled pTH12 probe. This mix is combined with the appropriate amounts of H_2O and quantities of protein in a total reaction volume of 20 µl. The samples are mixed gently and incubated at room temperature for 20 minutes and then subjected to gel electrophoresis at 200V for 30 minutes. The gel is then dried onto DE81/Whatmann paper at 80°C on a gel dryer and exposed to phosphorimager cassette overnight.

Calcium phosphate transfection of 293T cells

Twenty-four hours before transfection, plate 4-5x10^6 cells per 10 cm^2 plate so that cells are 30-40% confluent at the time of transfection. 15–20 micrograms of DNA is transfected per plate. First, the following mix for two plates if prepared (in this order): 856 µl H_2O, 124 µl 2 M $CaCl_2$, 20 1 µg/µl DNA and vortex this mix. Then, 1 ml of 2 x HBSS (50 mM HEPES pH 7.05, 10 mM KCl, 12 mM dextrose, 280 mM NaCl, 1.5 mM Na_2PO_4) is added dropwise while bubbling the mix with a 1 ml pipette. 1 ml of the final mix is added slowly and evenly onto a plate of the appropriate cells. 12-16 hr later, the media is aspirated and 10 ml fresh media is added to the plates. Cells are typically harvested 24 hr later.

Co-immunoprecipitation in 293T cells

To perform co-immunoprecipitation from 293T cells, transfected 293T cells are harvested by flushing the cells off with ice-cold PBS and the cells are transferred to a Falcon tube. The cells are collected and the PBS is aspirated. The cells are then lysed by resuspending them in 0.5 ml lysis buffer (50 mM Tris-HCl pH 7.4, 1% Triton X-100, 0.1% SDS, 150 mM NaCl, 1 mM EDTA, 1 mM DTT, 1 mM PMSF, 1 μg/μl aprotinin, 10 μg/μl pepstatin, 1 μg/μl leupeptin) and gently resuspending the cells with a pippet. The lysate is then transferred to an Eppendorf tube, vortexed 3-5 sec and kept on ice. 25 μl 5 M NaCl (raising the sodium concentration to 400 mM) is added to each tube. The samples are then vortexed, incubated on ice for 5 minutes, 0.5 ml ice-old H_2O (sodium concentration is now 200 mM) is added. The samples are then mixed well after adding H_2O and samples are centrifuged 14K for 10 min at 4°C. The resulting supernatant is then transferred to a new tube and a aliquot is saved fot the input sample.

To begin the immunoprecipitation from these prepare lysates, antibody is added to the remaining supernatant and the samples are nutated in cold room for 5 hr. Then, 60 μl 50% slurry pre-blocked protein A or protein G beads is added to each tube and the samples are nutated in the cold room for another hour. In order to block protein A/G beads, 3-4 ml of beads are placed into a Falcon tube, spun down down 1 K for 1 min at 4°C, and washed with PBS twice. The beads are resuspended in 10 ml of 5% BSA in PBS and keep on ice for 30 minutes, washed three times with PBS and stored with an equal volume of PBS containing 0.02% sodium azide at 4°C. Then, the tubes are centrifuged 4 K for 5 sec at 4°C to collect the beads which are then washed three or four times with 1 ml cold lysis buffer. The final centrifugation is performed at 14K for 10 sec at 4°C. The buffer is removed and 45-60 μl pre-boiled 2 x Laemelli buffer is added to each pellet. The pellets are resuspend, boiled for 10 min and stored at –20°C.

Multiple Tissue Northern Blots

Multiple tissue northern blots (Clontech) were pre-hybridized in Church's buffer (0.5M $NaPO_4$ pH 7.2, 1 mM EDTA pH 8.0, 7% (w/v) SDS, 1% (w/v) BSA) at 55°C for 1 hr. A radiolabeled probe was then denatured at 95°C for 5 min. The blots were hybridized in Church's buffer at overnight at 55°C and washed with Church's wash (40 mM $NaPO_4$ pH 7.2, 1 mM EDTA pH 8.0, 1% (w/v) SDS) and exposed to a phosphorimager overnight.

In vitro transcription / translation

The in vitro transciption / translation system (Promega TNT coupled reticulocyte system) is performed using RNase-free reagents. The following reagents are combined: 12.5 µl reticulocyte lysate, 1 µl TNT buffer, 0.5 µl polymerase (T7 or T3), 0.5 µl amino acids – methionine, 2 µl S^{35}-labeled methionine, 0.5 µl RNasin, 5.5 µl H_2O, 2.5 µl of 0.2 µg /µl DNA. The mix is then incubated for 1 hr. Samples are immediately processed by laoding 3 µl undiluted sample with 2 x Laemelli buffer on SDS-PAGE. One must make sure that the dye front is off of the gel to prevent background. The gel is then incubated with Amplify (Amersham) for 15 min, transferred to Whatmann paper, dried on a gel dryer at 80°C for 30 min, and exposed to film.

Transient transfection by electroporation

Exponentially growing cells are harvested by trypsinization, washed once with media, washed once with PBS and resuspended at a density of 1 $x10^6$ cells per µl of transfection buffer (21 mM HEPES pH 7.05, 137 mM NaCl, 0.7 mM Na_2HPO_4, 5 mM KCl, 6 mM glucose). 800 µl of suspension is then combined with 15 µg of plasmid DNA in an electroporation cuvette and electroporated at 300 mV with a capacitance setting of 960 µF. The cell debris at the top of the cuvette was removed with a pipette tip and cells are then plated. One-third of the volume is plated onto a 10 cm^2 dish with additional media and coverslips for immunofluorescence and two-thirds of the volume was plated

on a 10 cm^2 dish with media for protein extracts. Cells were processed 24 hr after electroporation.

Immunofluorescence

To stain cells for immunofluorescence, tissue culture cells plated on dished with coverslips are washed twice with PBS, fixed with 2% paraformaldehyde in PBS (stored at –20°C) for 10 min at room temperature, washed twice with PBS and permeabilized with 0.5% NP-40 in PBS for 10 min at room temperature and washed three times with PBS. Cells can be stored at 4°C wrapped in PBS with sodium azide. Coverslips are placed on parafilm in a humidified tray and blocked with PBG (0.2% (w/v) cold water fish gelatin (Sigma), 0.5% (w/v) BSA (Sigma) in PBS; stored at –20°C) for 30 minutes at room temperature. Cells are then incubated with primary antibody diluted in PBG for 3 hr at room temperature, washed three times with PBG for 5 minutes at room temperature, incubated with secondary antibody diluted 1:100 in PBG for 40 min at room temperature, washed three times with PBG for 5 minutes at room temperature (with the last wash containing 4,6-diamidino-2-phenylindole (DAPI)). Coverslips are then washed twice with PBS and mounted on glass slides. This is done by draining the excess PBS and placing coverslip with cells down onto a drop of embedding media (dissolve 20 mg p-phenylene diamine (Sigma) in 2 ml 10x PBS by vortexing and immediately add 10 ml glycerol, mixing carefully to avoid air bubbles and store in 1 ml aliquots at –70°C; should be colorless and not used if yellow or brown). The excess is removed with a tissue and the coverslip is sealed with clear nail polish.

Alternatively, cells can be pre-extracted with Triton X-100 or treated with a cytoskeleton pre-extraction protocol. For Triton X-100 extraction, cells grown on coverslips are rinsed twice with PBS and extracted with Triton X-100 extraction buffer (0.5% Triton X-100, 20 mM HEPES-KOH pH 7.9, 50 mM NaCl, 3 mM $MgCl_2$, and 300 mM sucrose) at either room temperature or 4°C for 1-5 min. Cells are then rinsed twice with PBS and fixed in 3% paraformaldehyde/ 2% sucrose for 10 min at room temperature, washed twice with PBS, permeabilized in Triton X-100 buffer for 10

minutes at room temperature, rinsed twice with PBS and stored in PBS with sodium azide.

Images were captured using an Axioplan2 Zeis microscope with a Hamamatsu digital camera using OpenLab software and images were processed using Adobe Photoshop and Adobe Illustrator.

RNAi

The following sequences were used as Rif1 siRNAs:
#1, AACAGCAAGAAAUAGCACCUAdTdT; #2,
AAUGAGACUUACGUGUUAAAAdTdT; #3,
AAGAGAAACCAGGUUCUGAAGdTdT; #4,
AAGAAUGAGCCCCUAGGGAAAdTdT; #5,
AAGAGGAAAAGUCUACUGACUdTdT; #6,
AAGAGCAUCUCAGGGUUUGCUdTdT; #7,
AAGAGAGAACCAAAACUGGUAdTdT; #8,
AAGAUGAAAUCUCAUCACCUGdTdT.

53BP1 siRNAs 1 and 2 (Wang et al. 2002); ATRIP siRNAs 1 and 2 (Cortez et al. 2001); BRCA1 (Ganesan et al. 2002); GFP (Novina et al. 2002); lamin A/C and luciferase GL2 (Elbashir et al. 2001); and scrambled (Dharmacon, Scramble I duplex) were used. All siRNAs were obtained from Dharmacon. HeLa2 or U2OS cells were transfected using OligofectamineTM (Invitrogen) according to the manufacturer's instructions. Briefly, 2.0 x 10^5 of HeLa2 or 1.0 x 10^5 of U2OS cells per well of a 6-well plate were plated 18-24 hr prior to transfection. Transfections were done twice with a 24 hr interval. Cells were processed 48-72 hr after the first transfection as indicated. As a control, cells were mock treated or treated with lamin, GFP, scrambled, or luciferase siRNAs.

Clonogenic survival assay

Cells transfected with Rif1 and control siRNAs were harvested and counted in parallel 72 hr after transfection. The cells diluted to the same cell density (5 x 10^4 cells/ml), irradiated, and subsequently plated in triplicate at a range of cell densities. After 10 to 14 days, plates were gently washed with PBS and stained with 50% MeOH/7% glacial acetic acid/43% H_2O/0.1% Coomassie Brilliant Blue G for 10 min, rinsed with water and air-dried. Colonies were counted for the various treatments on plates with similar numbers of colonies.

References

Abraham, R.T. 2001. Cell cycle checkpoint signaling through the ATM and ATR kinases. *Genes Dev* **15**: 2177-96.

Adams, I.R. and A. McLaren. 2004. Identification and characterisation of mRif1: a mouse telomere-associated protein highly expressed in germ cells and embryo-derived pluripotent stem cells. *Dev Dyn* **229**: 733-44.

Agami, R. and R. Bernards. 2000. Distinct initiation and maintenance mechanisms cooperate to induce G1 cell cycle arrest in response to DNA damage. *Cell* **102**: 55-66.

Agarwal, S.S., D.Q. Brown, E.J. Katz, and L.A. Loeb. 1977. Screening for deficits in DNA repair by the response of irradiated human lymphocytes to phytohemagglutinin. *Cancer Res* **37**: 3594-8.

Anderson, L., C. Henderson, and Y. Adachi. 2001. Phosphorylation and rapid relocalization of 53BP1 to nuclear foci upon DNA damage. *Mol Cell Biol* **21**: 1719-29.

Anderson, S.F., B.P. Schlegel, T. Nakajima, E.S. Wolpin, and J.D. Parvin. 1998. BRCA1 protein is linked to the RNA polymerase II holoenzyme complex via RNA helicase A. *Nat Genet* **19**: 254-6.

Athma, P., R. Rappaport, and M. Swift. 1996. Molecular genotyping shows that ataxia-telangiectasia heterozygotes are predisposed to breast cancer. *Cancer Genet Cytogenet* **92**: 130-4.

Aurias, A., B. Dutrillaux, D. Buriot, and J. Lejeune. 1980. High frequencies of inversions and translocations of chromosomes 7 and 14 in ataxia telangiectasia. *Mutat Res* **69**: 369-74.

Bakkenist, C.J. and M.B. Kastan. 2003. DNA damage activates ATM through intermolecular autophosphorylation and dimer dissociation. *Nature* **421**: 499-506.

Banin, S., L. Moyal, S. Shieh, Y. Taya, C.W. Anderson, L. Chessa, N.I. Smorodinsky, C. Prives, Y. Reiss, Y. Shiloh, and Y. Ziv. 1998. Enhanced phosphorylation of p53 by ATM in response to DNA damage. *Science* **281**: 1674-7.

Baumann, P. and T.R. Cech. 2000. Protection of telomeres by the Ku protein in fission yeast. *Mol Biol Cell* **11**: 3265-75.

-. 2001. Pot1, the putative telomere end-binding protein in fission yeast and humans. *Science* **292**: 1171-5.

Baumann, P., E. Podell, and T.R. Cech. 2002. Human pot1 (protection of telomeres) protein: cytolocalization, gene structure, and alternative splicing. *Mol Cell Biol* **22**: 8079-87.

Becker-Catania, S.G. and R.A. Gatti. 2001. Ataxia-telangiectasia. *Adv Exp Med Biol* **495**: 191-8.

Bender, C.F., M.L. Sikes, R. Sullivan, L.E. Huye, M.M. Le Beau, D.B. Roth, O.K. Mirzoeva, E.M. Oltz, and J.H. Petrini. 2002. Cancer predisposition and hematopoietic failure in Rad50(S/S) mice. *Genes Dev* **16**: 2237-51.

Berman, J., C.Y. Tachibana, and B.K. Tye. 1986. Identification of a telomere-binding activity from yeast. *Proc Natl Acad Sci U S A* **83**: 3713-7.

Bermudez, V.P., L.A. Lindsey-Boltz, A.J. Cesare, Y. Maniwa, J.D. Griffith, J. Hurwitz, and A. Sancar. 2003. Loading of the human 9-1-1 checkpoint complex onto DNA by the checkpoint clamp loader hRad17-replication factor C complex in vitro. *Proc Natl Acad Sci U S A* **100**: 1633-8.

Bianchi, A., S. Smith, L. Chong, P. Elias, and T. de Lange. 1997. TRF1 is a dimer and bends telomeric DNA. *Embo J* **16**: 1785-94.

Bianchi, A., R.M. Stansel, L. Fairall, J.D. Griffith, D. Rhodes, and T. de Lange. 1999. TRF1 binds a bipartite telomeric site with extreme spatial flexibility. *Embo J* **18**: 5735-44.

Bodnar, A.G., M. Ouellette, M. Frolkis, S.E. Holt, C.P. Chiu, G.B. Morin, C.B. Harley, J.W. Shay, S. Lichtsteiner, and W.E. Wright. 1998. Extension of life-span by introduction of telomerase into normal human cells *Science* **279**: 349-52.

Bork, P., K. Hofmann, P. Bucher, A.F. Neuwald, S.F. Altschul, and E.V. Koonin. 1997. A superfamily of conserved domains in DNA damage-responsive cell cycle checkpoint proteins. *Faseb J* **11**: 68-76.

Boulton, S.J. and S.P. Jackson. 1998. Components of the Ku-dependent non-homologous end-joining pathway are involved in telomeric length maintenance and telomeric silencing. *Embo J* **17**: 1819-28.

Bourns, B.D., M.K. Alexander, A.M. Smith, and V.A. Zakian. 1998. Sir proteins, Rif proteins, and Cdc13p bind Saccharomyces telomeres in vivo. *Mol Cell Biol* **18**: 5600-8.

Broccoli, D., L. Chong, S. Oelmann, A.A. Fernald, N. Marziliano, B. van Steensel, D. Kipling, M.M. Le Beau, and T. de Lange. 1997a. Comparison of the human and mouse genes encoding the telomeric protein, TRF1: chromosomal localization, expression and conserved protein domains. *Hum Mol Genet* **6**: 69-76.

Broccoli, D., A. Smogorzewska, L. Chong, and T. de Lange. 1997b. Human telomeres contain two distinct Myb-related proteins, TRF1 and TRF2. *Nat Genet* **17**: 231-5.

Bryan, T.M., A. Englezou, L. Dalla-Pozza, M.A. Dunham, and R.R. Reddel. 1997a. Evidence for an alternative mechanism for maintaining telomere length in human tumors and tumor-derived cell lines *Nat Med* **3**: 1271-4.

Bryan, T.M., A. Englezou, J. Gupta, S. Bacchetti, and R.R. Reddel. 1995. Telomere elongation in immortal human cells without detectable telomerase activity. *Embo J* **14**: 4240-8.

Bryan, T.M., L. Marusic, S. Bacchetti, M. Namba, and R.R. Reddel. 1997b. The telomere lengthening mechanism in telomerase-negative immortal human cells does not involve the telomerase RNA subunit. *Hum Mol Genet* **6**: 921-6.

Bryan, T.M. and R.R. Reddel. 1997. Telomere dynamics and telomerase activity in in vitro immortalised human cells. *Eur J Cancer* **33**: 767-73.

Buchman, A.R., W.J. Kimmerly, J. Rine, and R.D. Kornberg. 1988. Two DNA-binding factors recognize specific sequences at silencers, upstream activating sequences, autonomously replicating sequences, and telomeres in Saccharomyces cerevisiae. *Mol Cell Biol* **8**: 210-25.

Buck, S.W. and D. Shore. 1995. Action of a RAP1 carboxy-terminal silencing domain reveals an underlying competition between HMR and telomeres in yeast. *Genes Dev* **9**: 370-84.

Burma, S., B.P. Chen, M. Murphy, A. Kurimasa, and D.J. Chen. 2001. ATM phosphorylates histone H2AX in response to DNA double-strand breaks. *J Biol Chem* **276**: 42462-7.

Callebaut, I. and J.P. Mornon. 1997. From BRCA1 to RAP1: a widespread BRCT module closely associated with DNA repair. *FEBS Lett* **400**: 25-30.

Canman, C.E., D.S. Lim, K.A. Cimprich, Y. Taya, K. Tamai, K. Sakaguchi, E. Appella, M.B. Kastan, and J.D. Siliciano. 1998. Activation of the ATM kinase by ionizing radiation and phosphorylation of p53. *Science* **281**: 1677-9.

Canman, C.E., A.C. Wolff, C.Y. Chen, A.J. Fornace, Jr., and M.B. Kastan. 1994. The p53-dependent G1 cell cycle checkpoint pathway and ataxia-telangiectasia. *Cancer Res* **54**: 5054-8.

Carney, J.P., R.S. Maser, H. Olivares, E.M. Davis, M. Le Beau, J.R. Yates, 3rd, L. Hays, W.F. Morgan, and J.H. Petrini. 1998. The hMre11/hRad50 protein complex and Nijmegen breakage syndrome: linkage of double-strand break repair to the cellular DNA damage response. *Cell* **93**: 477-86.

Carr, A.M. 2003. Molecular biology. Beginning at the end. *Science* **300**: 1512-3.

Carson, C.T., R.A. Schwartz, T.H. Stracker, C.E. Lilley, D.V. Lee, and M.D. Weitzman. 2003. The Mre11 complex is required for ATM activation and the G2/M checkpoint. *Embo J* **22**: 6610-20.

Cenci, G., R.B. Rawson, G. Belloni, D.H. Castrillon, M. Tudor, R. Petrucci, M.L. Goldberg, S.A. Wasserman, and M. Gatti. 1997. UbcD1, a Drosophila ubiquitin-conjugating enzyme required for proper telomere behavior. *Genes Dev* **11**: 863-75.

Chambers, A., J.S. Tsang, C. Stanway, A.J. Kingsman, and S.M. Kingsman. 1989. Transcriptional control of the Saccharomyces cerevisiae PGK gene by RAP1. *Mol Cell Biol* **9**: 5516-24.

Chan, S.W., J. Chang, J. Prescott, and E.H. Blackburn. 2001. Altering telomere structure allows telomerase to act in yeast lacking ATM kinases. *Curr Biol* **11**: 1240-50.

Chandra, A., T.R. Hughes, C.I. Nugent, and V. Lundblad. 2001. Cdc13 both positively and negatively regulates telomere replication. *Genes Dev* **15**: 404-14.

Chehab, N.H., A. Malikzay, M. Appel, and T.D. Halazonetis. 2000. Chk2/hCds1 functions as a DNA damage checkpoint in G(1) by stabilizing p53. *Genes Dev* **14**: 278-88.

Chen, J., D.P. Silver, D. Walpita, S.B. Cantor, A.F. Gazdar, G. Tomlinson, F.J. Couch, B.L. Weber, T. Ashley, D.M. Livingston, and R. Scully. 1998. Stable interaction between the products of the BRCA1 and BRCA2 tumor suppressor genes in mitotic and meiotic cells. *Mol Cell* **2**: 317-28.

Chen, M.J., Y.T. Lin, H.B. Lieberman, G. Chen, and E.Y. Lee. 2001. ATM-dependent phosphorylation of human Rad9 is required for ionizing radiation-induced checkpoint activation. *J Biol Chem* **276**: 16580-6.

Chikashige, Y. and Y. Hiraoka. 2001. Telomere binding of the Rap1 protein is required for meiosis in fission yeast. *Curr Biol* **11**: 1618-23.

Chong, L., B. van Steensel, D. Broccoli, H. Erdjument-Bromage, J. Hanish, P. Tempst, and T. de Lange. 1995. A human telomeric protein. *Science* **270**: 1663-7.

Cliby, W.A., C.J. Roberts, K.A. Cimprich, C.M. Stringer, J.R. Lamb, S.L. Schreiber, and S.H. Friend. 1998. Overexpression of a kinase-inactive ATR protein causes sensitivity to DNA-damaging agents and defects in cell cycle checkpoints. *Embo J* **17**: 159-69.

Cockell, M., F. Palladino, T. Laroche, G. Kyrion, C. Liu, A.J. Lustig, and S.M. Gasser. 1995. The carboxy termini of Sir4 and Rap1 affect Sir3 localization: evidence for a multicomponent complex required for yeast telomeric silencing. *J Cell Biol* **129**: 909-24.

Cong, Y.S., W.E. Wright, and J.W. Shay. 2002. Human telomerase and its regulation. *Microbiol Mol Biol Rev* **66**: 407-25.

Connelly, J.C., E.S. de Leau, and D.R. Leach. 1999. DNA cleavage and degradation by the SbcCD protein complex from Escherichia coli. *Nucleic Acids Res* **27**: 1039-46.

Conrad, M.N., J.H. Wright, A.J. Wolf, and V.A. Zakian. 1990. RAP1 protein interacts with yeast telomeres in vivo: overproduction alters telomere structure and decreases chromosome stability. *Cell* **63**: 739-50.

Conti, E., M. Uy, L. Leighton, G. Blobel, and J. Kuriyan. 1998. Crystallographic analysis of the recognition of a nuclear localization signal by the nuclear import factor karyopherin alpha. *Cell* **94**: 193-204.

Cook, B.D., J.N. Dynek, W. Chang, G. Shostak, and S. Smith. 2002. Role for the related poly(ADP-Ribose) polymerases tankyrase 1 and 2 at human telomeres. *Mol Cell Biol* **22**: 332-42.

Cooper, J.P., E.R. Nimmo, R.C. Allshire, and T.R. Cech. 1997. Regulation of telomere length and function by a Myb-domain protein in fission yeast *Nature* **385**: 744-7.

Cortez, D., S. Guntuku, J. Qin, and S.J. Elledge. 2001. ATR and ATRIP: partners in checkpoint signaling. *Science* **294**: 1713-6.

Cortez, D., Y. Wang, J. Qin, and S.J. Elledge. 1999. Requirement of ATM-dependent phosphorylation of brca1 in the DNA damage response to double-strand breaks. *Science* **286**: 1162-6.

Craven, R.J. and T.D. Petes. 1999. Dependence of the regulation of telomere length on the type of subtelomeric repeat in the yeast Saccharomyces cerevisiae. *Genetics* **152**: 1531-41.

Crawford, T.O. 1998. Ataxia telangiectasia. *Semin Pediatr Neurol* **5**: 287-94.

d'Adda di Fagagna, F., M.P. Hande, W.M. Tong, P.M. Lansdorp, Z.Q. Wang, and S.P. Jackson. 1999. Functions of poly(ADP-ribose) polymerase in controlling telomere length and chromosomal stability. *Nat Genet* **23**: 76-80.

d'Adda di Fagagna, F., M.P. Hande, W.M. Tong, D. Roth, P.M. Lansdorp, Z.Q. Wang, and S.P. Jackson. 2001. Effects of DNA nonhomologous end-joining factors on telomere length and chromosomal stability in mammalian cells. *Curr Biol* **11**: 1192-6.

D'Andrea, A.D. and M. Grompe. 2003. The Fanconi anaemia/BRCA pathway. *Nat Rev Cancer* **3**: 23-34.

Dahlen, M., T. Olsson, G. Kanter-Smoler, A. Ramne, and P. Sunnerhagen. 1998. Regulation of telomere length by checkpoint genes in Schizosaccharomyces pombe. *Mol Biol Cell* **9**: 611-21.

Danilevskaya, O.N., K. Lowenhaupt, and M.L. Pardue. 1998. Conserved subfamilies of the Drosophila HeT-A telomere-specific retrotransposon. *Genetics* **148**: 233-42.

Danilevskaya, O.N., F. Slot, K.L. Traverse, N.C. Hogan, and M.L. Pardue. 1994. Drosophila telomere transposon HeT-A produces a transcript with tightly bound protein. *Proc Natl Acad Sci U S A* **91**: 6679-82.

de Lange, T. 2002. Protection of mammalian telomeres. *Oncogene* **21**: 532-40.

-. 2003. Protection and Maintenance of Human Telomeres. *Encyclopedia of the Human Genome*: 1-7.

Deng, C., P. Zhang, J.W. Harper, S.J. Elledge, and P. Leder. 1995. Mice lacking p21CIP1/WAF1 undergo normal development, but are defective in G1 checkpoint control. *Cell* **82**: 675-84.

Diede, S.J. and D.E. Gottschling. 1999. Telomerase-mediated telomere addition in vivo requires DNA primase and DNA polymerases alpha and delta. *Cell* **99**: 723-33.

Diffley, J.F. and B. Stillman. 1989. Similarity between the transcriptional silencer binding proteins ABF1 and RAP1. *Science* **246**: 1034-8.

DiTullio, R.A., Jr., T.A. Mochan, M. Venere, J. Bartkova, M. Sehested, J. Bartek, and T.D. Halazonetis. 2002. 53BP1 functions in an ATM-dependent checkpoint pathway that is constitutively activated in human cancer. *Nat Cell Biol* **4**: 998-1002.

Dolganov, G.M., R.S. Maser, A. Novikov, L. Tosto, S. Chong, D.A. Bressan, and J.H. Petrini. 1996. Human Rad50 is physically associated with human Mre11: identification of a conserved multiprotein complex implicated in recombinational DNA repair. *Mol Cell Biol* **16**: 4832-41.

Dong, Z., Q. Zhong, and P.L. Chen. 1999. The Nijmegen breakage syndrome protein is essential for Mre11 phosphorylation upon DNA damage. *J Biol Chem* **274**: 19513-6.

Dulic, V., W.K. Kaufmann, S.J. Wilson, T.D. Tlsty, E. Lees, J.W. Harper, S.J. Elledge, and S.I. Reed. 1994. p53-dependent inhibition of cyclin-dependent kinase activities in human fibroblasts during radiation-induced G1 arrest. *Cell* **76**: 1013-23.

Dumaz, N. and D.W. Meek. 1999. Serine15 phosphorylation stimulates p53 transactivation but does not directly influence interaction with HDM2. *Embo J* **18**: 7002-10.

el-Deiry, W.S., T. Tokino, V.E. Velculescu, D.B. Levy, R. Parsons, J.M. Trent, D. Lin, W.E. Mercer, K.W. Kinzler, and B. Vogelstein. 1993. WAF1, a potential mediator of p53 tumor suppression. *Cell* **75**: 817-25.

Elbashir, S.M., J. Harborth, W. Lendeckel, A. Yalcin, K. Weber, and T. Tuschl. 2001. Duplexes of 21-nucleotide RNAs mediate RNA interference in cultured mammalian cells. *Nature* **411**: 494-8.

Elledge, S.J. and A. Amon. 2002. The BRCA1 suppressor hypothesis: an explanation for the tissue-specific tumor development in BRCA1 patients. *Cancer Cell* **1**: 129-32.

Espejel, S., S. Franco, A. Sgura, D. Gae, S.M. Bailey, G.E. Taccioli, and M.A. Blasco. 2002. Functional interaction between DNA-PKcs and telomerase in telomere length maintenance. *Embo J* **21**: 6275-87.

Evans, S.K. and V. Lundblad. 1999. Est1 and Cdc13 as comediators of telomerase access. *Science* **286**: 117-20.

Fairall, L., L. Chapman, H. Moss, T. de Lange, and D. Rhodes. 2001. Structure of the TRFH dimerization domain of the human telomeric proteins TRF1 and TRF2. *Molecular Cell* **8**: 351-61.

Falck, J., N. Mailand, R.G. Syljuasen, J. Bartek, and J. Lukas. 2001. The ATM-Chk2-Cdc25A checkpoint pathway guards against radioresistant DNA synthesis. *Nature* **410**: 842-7.

Falck, J., J.H. Petrini, B.R. Williams, J. Lukas, and J. Bartek. 2002. The DNA damage-dependent intra-S phase checkpoint is regulated by parallel pathways. *Nat Genet* **30**: 290-4.

Feng, J., W.D. Funk, S.S. Wang, S.L. Weinrich, A.A. Avilion, C.P. Chiu, R.R. Adams, E. Chang, R.C. Allsopp, J. Yu, and et al. 1995. The RNA component of human telomerase. *Science* **269**: 1236-41.

Foray, N., D. Marot, A. Gabriel, V. Randrianarison, A.M. Carr, M. Perricaudet, A. Ashworth, and P. Jeggo. 2003. A subset of ATM- and ATR-dependent phosphorylation events requires the BRCA1 protein. *Embo J* **22**: 2860-71.

Friedberg, E.C. 2003. DNA damage and repair. *Nature* **421**: 436-40.

Galloway, S.M. 1977. Ataxia telangiectasia: the effects of chemical mutagens and x-rays on sister chromatid exchanges in blood lymphocytes. *Mutat Res* **45**: 343-9.

Galloway, S.M. and H.J. Evans. 1975. Sister chromatid exchange in human chromosomes from normal individuals and patients with ataxia telangiectasia. *Cytogenet Cell Genet* **15**: 17-29.

Ganesan, S., D.P. Silver, R.A. Greenberg, D. Avni, R. Drapkin, A. Miron, S.C. Mok, V. Randrianarison, S. Brodie, J. Salstrom, T.P. Rasmussen, A. Klimke, C. Marrese, Y. Marahrens, C.X. Deng, J. Feunteun, and D.M. Livingston. 2002. BRCA1 supports XIST RNA concentration on the inactive X chromosome. *Cell* **111**: 393-405.

Garvik, B., M. Carson, and L. Hartwell. 1995. Single-stranded DNA arising at telomeres in cdc13 mutants may constitute a specific signal for the RAD9 checkpoint. *Mol Cell Biol* **15**: 6128-38.

Gatei, M., S.P. Scott, I. Filippovitch, N. Soronika, M.F. Lavin, B. Weber, and K.K. Khanna. 2000a. Role for ATM in DNA damage-induced phosphorylation of BRCA1. *Cancer Res* **60**: 3299-304.

Gatei, M., K. Sloper, C. Sorensen, R. Syljuasen, J. Falck, K. Hobson, K. Savage, J. Lukas, B.B. Zhou, J. Bartek, and K.K. Khanna. 2003. Ataxia-telangiectasia-mutated (ATM) and NBS1-dependent phosphorylation of Chk1 on Ser-317 in response to ionizing radiation. *J Biol Chem* **278**: 14806-11.

Gatei, M., D. Young, K.M. Cerosaletti, A. Desai-Mehta, K. Spring, S. Kozlov, M.F. Lavin, R.A. Gatti, P. Concannon, and K. Khanna. 2000b. ATM-dependent phosphorylation of nibrin in response to radiation exposure. *Nat Genet* **25**: 115-9.

Gatei, M., B.B. Zhou, K. Hobson, S. Scott, D. Young, and K.K. Khanna. 2001. Ataxia telangiectasia mutated (ATM) kinase and ATM and Rad3 related

kinase mediate phosphorylation of Brca1 at distinct and overlapping sites. In vivo assessment using phospho-specific antibodies. *J Biol Chem* **276**: 17276-80.

Gilson, E., M. Roberge, R. Giraldo, D. Rhodes, and S.M. Gasser. 1993. Distortion of the DNA double helix by RAP1 at silencers and multiple telomeric binding sites. *J Mol Biol* **231**: 293-310.

Goldberg, M., M. Stucki, J. Falck, D. D'Amours, D. Rahman, D. Pappin, J. Bartek, and S.P. Jackson. 2003. MDC1 is required for the intra-S-phase DNA damage checkpoint. *Nature* **421**: 952-6.

Goodman, M.F. 2002. Error-prone repair DNA polymerases in prokaryotes and eukaryotes. *Annu Rev Biochem* **71**: 17-50.

Gotoff, S.P., E. Amirmokri, and E.J. Liebner. 1967. Ataxia telangiectasia. Neoplasia, untoward response to x-irradiation, and tuberous sclerosis. *Am J Dis Child* **114**: 617-25.

Gotta, M. and S.M. Gasser. 1996. Nuclear organization and transcriptional silencing in yeast. *Experientia* **52**: 1136-47.

Gotta, M., T. Laroche, A. Formenton, L. Maillet, H. Scherthan, and S.M. Gasser. 1996. The clustering of telomeres and colocalization with Rap1, Sir3, and Sir4 proteins in wild-type Saccharomyces cerevisiae. *J Cell Biol* **134**: 1349-63.

Goytisolo, F.A., E. Samper, S. Edmonson, G.E. Taccioli, and M.A. Blasco. 2001. The absence of the DNA-dependent protein kinase catalytic subunit in mice results in anaphase bridges and in increased telomeric fusions with normal telomere length and G-strand overhang. *Mol Cell Biol* **21**: 3642-51.

Grandin, N., C. Damon, and M. Charbonneau. 2001. Ten1 functions in telomere end protection and length regulation in association with Stn1 and Cdc13. *Embo J* **20**: 1173-83.

Grant, P.A., D. Schieltz, M.G. Pray-Grant, J.R. Yates, 3rd, and J.L. Workman. 1998. The ATM-related cofactor Tra1 is a component of the purified SAGA complex. *Mol Cell* **2**: 863-7.

Gravel, S., M. Larrivee, P. Labrecque, and R.J. Wellinger. 1998. Yeast Ku as a regulator of chromosomal DNA end structure. *Science* **280**: 741-4.

Green, C.M., H. Erdjument-Bromage, P. Tempst, and N.F. Lowndes. 2000. A novel Rad24 checkpoint protein complex closely related to replication factor C. *Curr Biol* **10**: 39-42.

Greenwell, P.W., S.L. Kronmal, S.E. Porter, J. Gassenhuber, B. Obermaier, and T.D. Petes. 1995. TEL1, a gene involved in controlling telomere length in S. cerevisiae, is homologous to the human ataxia telangiectasia gene. *Cell* **82**: 823-9.

Greider, C.W. and E.H. Blackburn. 1985. Identification of a specific telomere terminal transferase activity in Tetrahymena extracts. *Cell* **43**: 405-13.
-. 1989. A telomeric sequence in the RNA of Tetrahymena telomerase required for telomere repeat synthesis. *Nature* **337**: 331-7.
Griffith, J.D., L. Comeau, S. Rosenfield, R.M. Stansel, A. Bianchi, H. Moss, and T. de Lange. 1999. Mammalian telomeres end in a large duplex loop. *Cell* **97**: 503-14.
Haber, J.E. 1995. In vivo biochemistry: physical monitoring of recombination induced by site-specific endonucleases. *Bioessays* **17**: 609-20.
-. 1998. The many interfaces of Mre11. *Cell* **95**: 583-6.
Hahn, W.C., C.M. Counter, A.S. Lundberg, R.L. Beijersbergen, M.W. Brooks, and R.A. Weinberg. 1999. Creation of human tumour cells with defined genetic elements. *Nature* **400**: 464-8.
Hahn, W.C., S.K. Dessain, M.W. Brooks, J.E. King, B. Elenbaas, D.M. Sabatini, J.A. DeCaprio, and R.A. Weinberg. 2002. Enumeration of the simian virus 40 early region elements necessary for human cell transformation. *Mol Cell Biol* **22**: 2111-23.
Hande, M.P., A.S. Balajee, A. Tchirkov, A. Wynshaw-Boris, and P.M. Lansdorp. 2001. Extra-chromosomal telomeric DNA in cells from Atm(-/-) mice and patients with ataxia-telangiectasia. *Hum Mol Genet* **10**: 519-28.
Hande, P., P. Slijepcevic, A. Silver, S. Bouffler, P. van Buul, P. Bryant, and P. Lansdorp. 1999. Elongated telomeres in scid mice. *Genomics* **56**: 221-3.
Hardy, C.F., L. Sussel, and D. Shore. 1992. A RAP1-interacting protein involved in transcriptional silencing and telomere length regulation. *Genes Dev* **6**: 801-14.
Hartwell, L.H. and T.A. Weinert. 1989. Checkpoints: controls that ensure the order of cell cycle events. *Science* **246**: 629-34.
Hayflick, L. 1998. How and why we age. *Exp Gerontol* **33**: 639-53.
Henry, Y.A., A. Chambers, J.S. Tsang, A.J. Kingsman, and S.M. Kingsman. 1990. Characterisation of the DNA binding domain of the yeast RAP1 protein. *Nucleic Acids Res* **18**: 2617-23.
Henson, J.D., A.A. Neumann, T.R. Yeager, and R.R. Reddel. 2002. Alternative lengthening of telomeres in mammalian cells. *Oncogene* **21**: 598-610.
Hirao, A., Y.Y. Kong, S. Matsuoka, A. Wakeham, J. Ruland, H. Yoshida, D. Liu, S.J. Elledge, and T.W. Mak. 2000. DNA damage-induced activation of p53 by the checkpoint kinase Chk2. *Science* **287**: 1824-7.
Hiyama, E., K. Hiyama, T. Yokoyama, Y. Matsuura, M.A. Piatyszek, and J.W. Shay. 1995. Correlating telomerase activity levels with human neuroblastoma outcomes *Nat Med* **1**: 249-55.
Hoeijmakers, J.H. 2001. Genome maintenance mechanisms for preventing cancer. *Nature* **411**: 366-74.

Hopfner, K.P., L. Craig, G. Moncalian, R.A. Zinkel, T. Usui, B.A. Owen, A. Karcher, B. Henderson, J.L. Bodmer, C.T. McMurray, J.P. Carney, J.H. Petrini, and J.A. Tainer. 2002. The Rad50 zinc-hook is a structure joining Mre11 complexes in DNA recombination and repair. *Nature* **418**: 562-6.

Hsieh, C.L., C.F. Arlett, and M.R. Lieber. 1993. V(D)J recombination in ataxia telangiectasia, Bloom's syndrome, and a DNA ligase I-associated immunodeficiency disorder. *J Biol Chem* **268**: 20105-9.

Huber, A.H., W.J. Nelson, and W.I. Weis. 1997. Three-dimensional structure of the armadillo repeat region of beta-catenin. *Cell* **90**: 871-82.

Hughes, T.R., S.K. Evans, R.G. Weilbaecher, and V. Lundblad. 2000. The Est3 protein is a subunit of yeast telomerase. *Curr Biol* **10**: 809-12.

Imai, Y., T. Kimura, A. Murakami, N. Yajima, K. Sakamaki, and S. Yonehara. 1999. The CED-4-homologous protein FLASH is involved in Fas-mediated activation of caspase-8 during apoptosis. *Nature* **398**: 777-85.

Inskip, H.M., L.J. Kinlen, A.M. Taylor, C.G. Woods, and C.F. Arlett. 1999. Risk of breast cancer and other cancers in heterozygotes for ataxia-telangiectasia. *Br J Cancer* **79**: 1304-7.

Iwabuchi, K., P.L. Bartel, B. Li, R. Marraccino, and S. Fields. 1994. Two cellular proteins that bind to wild-type but not mutant p53. *Proc Natl Acad Sci U S A* **91**: 6098-102.

Iwabuchi, K., B. Li, H.F. Massa, B.J. Trask, T. Date, and S. Fields. 1998. Stimulation of p53-mediated transcriptional activation by the p53-binding proteins, 53BP1 and 53BP2. *J Biol Chem* **273**: 26061-8.

Jackson, S.P. 2002. Sensing and repairing DNA double-strand breaks. *Carcinogenesis* **23**: 687-96.

Jasin, M. 2002. Homologous repair of DNA damage and tumorigenesis: the BRCA connection. *Oncogene* **21**: 8981-93.

Jimenez, G.S., F. Bryntesson, M.I. Torres-Arzayus, A. Priestley, M. Beeche, S. Saito, K. Sakaguchi, E. Appella, P.A. Jeggo, G.E. Taccioli, G.M. Wahl, and M. Hubank. 1999. DNA-dependent protein kinase is not required for the p53-dependent response to DNA damage. *Nature* **400**: 81-3.

Johnson, F.B., R.A. Marciniak, M. McVey, S.A. Stewart, W.C. Hahn, and L. Guarente. 2001. The Saccharomyces cerevisiae WRN homolog Sgs1p participates in telomere maintenance in cells lacking telomerase. *Embo J* **20**: 905-13.

Jullien, D., P. Vagnarelli, W.C. Earnshaw, and Y. Adachi. 2002. Kinetochore localisation of the DNA damage response component 53BP1 during mitosis. *J Cell Sci* **115**: 71-9.

Kaminker, P.G., S.H. Kim, R.D. Taylor, Y. Zebarjadian, W.D. Funk, G.B. Morin, P. Yaswen, and J. Campisi. 2001. TANK2, a new TRF1-associated PARP,

causes rapid induction of cell death upon overexpression. *J Biol Chem* **276**: 35891-99.

Kanoh, J. and F. Ishikawa. 2001. spRap1 and spRif1, recruited to telomeres by Taz1, are essential for telomere function in fission yeast. *Curr Biol* **11**: 1624-30.

Karlseder, J., D. Broccoli, Y. Dai, S. Hardy, and T. de Lange. 1999. p53- and ATM-dependent apoptosis induced by telomeres lacking TRF2. *Science* **283**: 1321-5.

Kastan, M.B. and D.S. Lim. 2000. The many substrates and functions of ATM. *Nat Rev Mol Cell Biol* **1**: 179-86.

Kastan, M.B., Q. Zhan, W.S. el-Deiry, F. Carrier, T. Jacks, W.V. Walsh, B.S. Plunkett, B. Vogelstein, and A.J. Fornace, Jr. 1992. A mammalian cell cycle checkpoint pathway utilizing p53 and GADD45 is defective in ataxia-telangiectasia. *Cell* **71**: 587-97.

Khanna, K.K. and S.P. Jackson. 2001. DNA double-strand breaks: signaling, repair and the cancer connection. *Nat Genet* **27**: 247-54.

Khanna, K.K., K.E. Keating, S. Kozlov, S. Scott, M. Gatei, K. Hobson, Y. Taya, B. Gabrielli, D. Chan, S.P. Lees-Miller, and M.F. Lavin. 1998. ATM associates with and phosphorylates p53: mapping the region of interaction. *Nat Genet* **20**: 398-400.

Kim, N.W., M.A. Piatyszek, K.R. Prowse, C.B. Harley, M.D. West, P.L. Ho, G.M. Coviello, W.E. Wright, S.L. Weinrich, and J.W. Shay. 1994. Specific association of human telomerase activity with immortal cells and cancer. *Science* **266**: 2011-5.

Kim, S.T., D.S. Lim, C.E. Canman, and M.B. Kastan. 1999. Substrate specificities and identification of putative substrates of ATM kinase family members. *J Biol Chem* **274**: 37538-43.

Klein, F., T. Laroche, M.E. Cardenas, J.F. Hofmann, D. Schweizer, and S.M. Gasser. 1992. Localization of RAP1 and topoisomerase II in nuclei and meiotic chromosomes of yeast. *J Cell Biol* **117**: 935-48.

Kojis, T.L., R.A. Gatti, and R.S. Sparkes. 1991. The cytogenetics of ataxia telangiectasia. *Cancer Genet Cytogenet* **56**: 143-56.

Kolodner, R.D., C.D. Putnam, and K. Myung. 2002. Maintenance of genome stability in Saccharomyces cerevisiae. *Science* **297**: 552-7.

Konig, P., R. Giraldo, L. Chapman, and D. Rhodes. 1996. The crystal structure of the DNA-binding domain of yeast RAP1 in complex with telomeric DNA. *Cell* **85**: 125-36.

Kyrion, G., K.A. Boakye, and A.J. Lustig. 1992. C-terminal truncation of RAP1 results in the deregulation of telomere size, stability, and function in Saccharomyces cerevisiae. *Mol Cell Biol* **12**: 5159-73.

Kyrion, G., K. Liu, C. Liu, and A.J. Lustig. 1993. RAP1 and telomere structure regulate telomere position effects in Saccharomyces cerevisiae. *Genes Dev* **7**: 1146-59.

Lakin, N.D., B.C. Hann, and S.P. Jackson. 1999. The ataxia-telangiectasia related protein ATR mediates DNA-dependent phosphorylation of p53. *Oncogene* **18**: 3989-95.

Larson, G.P., D. Castanotto, J.J. Rossi, and M.P. Malafa. 1994. Isolation and functional analysis of a Kluyveromyces lactis RAP1 homologue. *Gene* **150**: 35-41.

Lavin, M.F. and Y. Shiloh. 1997. The genetic defect in ataxia-telangiectasia. *Annu Rev Immunol* **15**: 177-202.

Lee, J.S., K.M. Collins, A.L. Brown, C.H. Lee, and J.H. Chung. 2000. hCds1-mediated phosphorylation of BRCA1 regulates the DNA damage response. *Nature* **404**: 201-4.

Lei, M., P. Baumann, and T.R. Cech. 2002. Cooperative Binding of Single-Stranded Telomeric DNA by the Pot1 Protein of Schizosaccharomyces pombe. *Biochemistry* **41**: 14560-8.

Lendvay, T.S., D.K. Morris, J. Sah, B. Balasubramanian, and V. Lundblad. 1996. Senescence mutants of Saccharomyces cerevisiae with a defect in telomere replication identify three additional EST genes. *Genetics* **144**: 1399-412.

Levis, R.W. 1989. Viable deletions of a telomere from a Drosophila chromosome. *Cell* **58**: 791-801.

Li, B. and T. De Lange. 2003. Rap1 affects the length and heterogeneity of human telomeres. *Mol Biol Cell.*

Li, B., S. Oestreich, and T. de Lange. 2000. Identification of human Rap1: implications for telomere evolution. *Cell* **101**: 471-83.

Lieber, M.R., Y. Ma, U. Pannicke, and K. Schwarz. 2003. Mechanism and regulation of human non-homologous DNA end-joining. *Nat Rev Mol Cell Biol* **4**: 712-20.

Lim, D.S., S.T. Kim, B. Xu, R.S. Maser, J. Lin, J.H. Petrini, and M.B. Kastan. 2000. ATM phosphorylates p95/nbs1 in an S-phase checkpoint pathway. *Nature* **404**: 613-7.

Lin, S.Y. and S.J. Elledge. 2003. Multiple tumor suppressor pathways negatively regulate telomerase. *Cell* **113**: 881-9.

Lingner, J., T.R. Hughes, A. Shevchenko, M. Mann, V. Lundblad, and T.R. Cech. 1997. Reverse transcriptase motifs in the catalytic subunit of telomerase *Science* **276**: 561-7.

Lipkowitz, S., M.H. Stern, and I.R. Kirsch. 1990. Hybrid T cell receptor genes formed by interlocus recombination in normal and ataxia-telangiectasis lymphocytes. *J Exp Med* **172**: 409-18.

Liu, C. and A.J. Lustig. 1996. Genetic analysis of Rap1p/Sir3p interactions in telomeric and HML silencing in Saccharomyces cerevisiae. *Genetics* **143**: 81-93.

Loayza, D. and T. De Lange. 2003. POT1 as a terminal transducer of TRF1 telomere length control. *Nature* **424**: 1013-8.

Loayza, D., H. Parsons, J. Donigian, K. Hoke, and T. De Lange. 2004. DNA binding features of human POT1: A nonamer 5'-TAGGGTTAG-3' minimal binding site, sequence specificity, and internal binding to multimeric sites. *J Biol Chem* **279**: 13241-8.

Longhese, M.P., V. Paciotti, H. Neecke, and G. Lucchini. 2000. Checkpoint proteins influence telomeric silencing and length maintenance in budding yeast. *Genetics* **155**: 1577-91.

Longtine, M.S., N.M. Wilson, M.E. Petracek, and J. Berman. 1989. A yeast telomere binding activity binds to two related telomere sequence motifs and is indistinguishable from RAP1. *Curr Genet* **16**: 225-39.

Lou, Z., C.C. Chini, K. Minter-Dykhouse, and J. Chen. 2003a. Mediator of DNA damage checkpoint protein 1 regulates BRCA1 localization and phosphorylation in DNA damage checkpoint control. *J Biol Chem* **278**: 13599-602.

Lou, Z., K. Minter-Dykhouse, X. Wu, and J. Chen. 2003b. MDC1 is coupled to activated CHK2 in mammalian DNA damage response pathways. *Nature* **421**: 957-61.

Lundblad, V. and E.H. Blackburn. 1993. An alternative pathway for yeast telomere maintenance rescues est1- senescence. *Cell* **73**: 347-60.

Lundblad, V. and J.W. Szostak. 1989. A mutant with a defect in telomere elongation leads to senescence in yeast. *Cell* **57**: 633-43.

Luo, C.M., W. Tang, K.L. Mekeel, J.S. DeFrank, P.R. Anne, and S.N. Powell. 1996. High frequency and error-prone DNA recombination in ataxia telangiectasia cell lines. *J Biol Chem* **271**: 4497-503.

Lustig, A.J., S. Kurtz, and D. Shore. 1990. Involvement of the silencer and UAS binding protein RAP1 in regulation of telomere length. *Science* **250**: 549-53.

Makiniemi, M., T. Hillukkala, J. Tuusa, K. Reini, M. Vaara, D. Huang, H. Pospiech, I. Majuri, T. Westerling, T.P. Makela, and J.E. Syvaoja. 2001. BRCT domain-containing protein TopBP1 functions in DNA replication and damage response. *J Biol Chem* **276**: 30399-406.

Mallory, J.C. and T.D. Petes. 2000. Protein kinase activity of Tel1p and Mec1p, two Saccharomyces cerevisiae proteins related to the human ATM protein kinase. *Proc Natl Acad Sci U S A* **97**: 13749-54.

Maser, R.S., K.J. Monsen, B.E. Nelms, and J.H. Petrini. 1997. hMre11 and hRad50 nuclear foci are induced during the normal cellular response to DNA double-strand breaks. *Mol Cell Biol* **17**: 6087-96.

Maser, R.S., R. Zinkel, and J.H. Petrini. 2001. An alternative mode of translation permits production of a variant NBS1 protein from the common Nijmegen breakage syndrome allele. *Nat Genet* **27**: 417-21.

Matsuoka, S., M. Huang, and S.J. Elledge. 1998. Linkage of ATM to cell cycle regulation by the Chk2 protein kinase. *Science* **282**: 1893-7.

Maya, R., M. Balass, S.T. Kim, D. Shkedy, J.F. Leal, O. Shifman, M. Moas, T. Buschmann, Z. Ronai, Y. Shiloh, M.B. Kastan, E. Katzir, and M. Oren. 2001. ATM-dependent phosphorylation of Mdm2 on serine 395: role in p53 activation by DNA damage. *Genes Dev* **15**: 1067-77.

McClintock, B. 1941. The stability of broken ends of chromosomes in Zea mays. *Genetics* **26**: 234-282.

McEachern, M.J. and E.H. Blackburn. 1995. Runaway telomere elongation caused by telomerase RNA gene mutations. *Nature* **376**: 403-9.

McMahon, S.B., H.A. Van Buskirk, K.A. Dugan, T.D. Copeland, and M.D. Cole. 1998. The novel ATM-related protein TRRAP is an essential cofactor for the c-Myc and E2F oncoproteins. *Cell* **94**: 363-74.

Metcalfe, J.A., J. Parkhill, L. Campbell, M. Stacey, P. Biggs, P.J. Byrd, and A.M. Taylor. 1996. Accelerated telomere shortening in ataxia telangiectasia. *Nat Genet* **13**: 350-3.

Meyerson, M., C.M. Counter, E.N. Eaton, L.W. Ellisen, P. Steiner, S.D. Caddle, L. Ziaugra, R.L. Beijersbergen, M.J. Davidoff, Q. Liu, S. Bacchetti, D.A. Haber, and R.A. Weinberg. 1997. hEST2, the putative human telomerase catalytic subunit gene, is up- regulated in tumor cells and during immortalization. *Cell* **90**: 785-95.

Meyn, M.S. 1993. High spontaneous intrachromosomal recombination rates in ataxia-telangiectasia. *Science* **260**: 1327-30.

Miki, Y., J. Swensen, D. Shattuck-Eidens, P.A. Futreal, K. Harshman, S. Tavtigian, Q. Liu, C. Cochran, L.M. Bennett, W. Ding, and et al. 1994. A strong candidate for the breast and ovarian cancer susceptibility gene BRCA1. *Science* **266**: 66-71.

Mirzoeva, O.K. and J.H. Petrini. 2001. DNA damage-dependent nuclear dynamics of the Mre11 complex. *Mol Cell Biol* **21**: 281-8.

Mishra, K. and D. Shore. 1999. Yeast Ku protein plays a direct role in telomeric silencing and counteracts inhibition by rif proteins. *Curr Biol* **9**: 1123-6.

Mitchell, J.R., J. Cheng, and K. Collins. 1999a. A box H/ACA small nucleolar RNA-like domain at the human telomerase RNA 3' end. *Mol Cell Biol* **19**: 567-76.

Mitchell, J.R., E. Wood, and K. Collins. 1999b. A telomerase component is defective in the human disease dyskeratosis congenita. *Nature* **402**: 551-5.

Mitton-Fry, R.M., E.M. Anderson, T.R. Hughes, V. Lundblad, and D.S. Wuttke. 2002. Conserved structure for single-stranded telomeric DNA recognition. *Science* **296**: 145-7.

Morales, C.P., S.E. Holt, M. Ouellette, K.J. Kaur, Y. Yan, K.S. Wilson, M.A. White, W.E. Wright, and J.W. Shay. 1999. Absence of cancer-associated changes in human fibroblasts immortalized with telomerase. *Nat Genet* **21**: 115-8.

Moretti, P., K. Freeman, L. Coodly, and D. Shore. 1994. Evidence that a complex of SIR proteins interacts with the silencer and telomere-binding protein RAP1. *Genes Dev* **8**: 2257-69.

Morgan, J.L., T.M. Holcomb, and R.W. Morrissey. 1968. Radiation reaction in ataxia telangiectasia. *Am J Dis Child* **116**: 557-8.

Morris, D.K. and V. Lundblad. 1997. Programmed translational frameshifting in a gene required for yeast telomere replication. *Curr Biol* **7**: 969-76.

Morrison, C., E. Sonoda, N. Takao, A. Shinohara, K. Yamamoto, and S. Takeda. 2000. The controlling role of ATM in homologous recombinational repair of DNA damage. *Embo J* **19**: 463-71.

Moynahan, M.E. 2002. The cancer connection: BRCA1 and BRCA2 tumor suppression in mice and humans. *Oncogene* **21**: 8994-9007.

Muller, H.J. 1938. The remaking of chromosomes. *The Collecting Net, Woods Hole* **8**: 182-195.

Munoz-Jordan, J.L., G.A. Cross, T. de Lange, and J.D. Griffith. 2001. t-loops at trypanosome telomeres. *Embo J* **20**: 579-88.

Murti, K.G. and D.M. Prescott. 1999. Telomeres of polytene chromosomes in a ciliated protozoan terminate in duplex DNA loops. *Proc Natl Acad Sci U S A* **96**: 14436-9.

Myung, K., C. Chen, and R.D. Kolodner. 2001. Multiple pathways cooperate in the suppression of genome instability in Saccharomyces cerevisiae. *Nature* **411**: 1073-6.

Naito, T., A. Matsuura, and F. Ishikawa. 1998. Circular chromosome formation in a fission yeast mutant defective in two ATM homologues. *Nat Genet* **20**: 203-6.

Nakamura, T.M., G.B. Morin, K.B. Chapman, S.L. Weinrich, W.H. Andrews, J. Lingner, C.B. Harley, and T.R. Cech. 1997. Telomerase catalytic subunit homologs from fission yeast and human *Science* **277**: 955-9.

Nakamura, T.M., B.A. Moser, and P. Russell. 2002. Telomere binding of checkpoint sensor and DNA repair proteins contributes to maintenance of functional fission yeast telomeres. *Genetics* **161**: 1437-52.

Nelms, B.E., R.S. Maser, J.F. MacKay, M.G. Lagally, and J.H. Petrini. 1998. In situ visualization of DNA double-strand break repair in human fibroblasts. *Science* **280**: 590-2.

Novina, C.D., M.F. Murray, D.M. Dykxhoorn, P.J. Beresford, J. Riess, S.K. Lee, R.G. Collman, J. Lieberman, P. Shankar, and P.A. Sharp. 2002. siRNA-directed inhibition of HIV-1 infection. *Nat Med* **8**: 681-6.

Nugent, C.I., G. Bosco, L.O. Ross, S.K. Evans, A.P. Salinger, J.K. Moore, J.E. Haber, and V. Lundblad. 1998. Telomere maintenance is dependent on activities required for end repair of double-strand breaks. *Curr Biol* **8**: 657-60.

Nugent, C.I., T.R. Hughes, N.F. Lue, and V. Lundblad. 1996. Cdc13p: a single-strand telomeric DNA-binding protein with a dual role in yeast telomere maintenance. *Science* **274**: 249-52.

O'Neill, T., A.J. Dwyer, Y. Ziv, D.W. Chan, S.P. Lees-Miller, R.H. Abraham, J.H. Lai, D. Hill, Y. Shiloh, L.C. Cantley, and G.A. Rathbun. 2000. Utilization of oriented peptide libraries to identify substrate motifs selected by ATM. *J Biol Chem* **275**: 22719-27.

Olovnikov, A.M. 1973. A theory of marginotomy. The incomplete copying of template margin in enzymic synthesis of polynucleotides and biological significance of the phenomenon. *J Theor Biol* **41**: 181-90.

Olsen, J.H., J.M. Hahnemann, A.L. Borresen-Dale, K. Brondum-Nielsen, L. Hammarstrom, R. Kleinerman, H. Kaariainen, T. Lonnqvist, R. Sankila, N. Seersholm, S. Tretli, J. Yuen, J.D. Boice, Jr., and M. Tucker. 2001. Cancer in patients with ataxia-telangiectasia and in their relatives in the nordic countries. *J Natl Cancer Inst* **93**: 121-7.

Painter, R.B. and B.R. Young. 1980. Radiosensitivity in ataxia-telangiectasia: a new explanation. *Proc Natl Acad Sci U S A* **77**: 7315-7.

Paules, R.S., E.N. Levedakou, S.J. Wilson, C.L. Innes, N. Rhodes, T.D. Tlsty, D.A. Galloway, L.A. Donehower, M.A. Tainsky, and W.K. Kaufmann. 1995. Defective G2 checkpoint function in cells from individuals with familial cancer syndromes. *Cancer Res* **55**: 1763-73.

Paull, T.T. and M. Gellert. 1998. The 3' to 5' exonuclease activity of Mre 11 facilitates repair of DNA double-strand breaks. *Mol Cell* **1**: 969-79.

-. 1999. Nbs1 potentiates ATP-driven DNA unwinding and endonuclease cleavage by the Mre11/Rad50 complex. *Genes Dev* **13**: 1276-88.

Pennock, E., K. Buckley, and V. Lundblad. 2001. Cdc13 delivers separate complexes to the telomere for end protection and replication. *Cell* **104**: 387-96.

Perry, J. and N. Kleckner. 2003. The ATRs, ATMs, and TORs are giant HEAT repeat proteins. *Cell* **112**: 151-5.

Petrini, J. and T. Stracker. 2003. The cellular response to DNA double strand breaks: defining the sensors and mediators. *Trends Cell Biol* **13**: 458-62.

Petrini, J.H. 2000. The Mre11 complex and ATM: collaborating to navigate S phase. *Curr Opin Cell Biol* **12**: 293-6.

Petrini, J.H., M.E. Walsh, C. DiMare, X.N. Chen, J.R. Korenberg, and D.T. Weaver. 1995. Isolation and characterization of the human MRE11 homologue. *Genomics* **29**: 80-6.

Polotnianka, R.M., J. Li, and A.J. Lustig. 1998. The yeast Ku heterodimer is essential for protection of the telomere against nucleolytic and recombinational activities. *Curr Biol* **8**: 831-4.

Porter, S.E., P.W. Greenwell, K.B. Ritchie, and T.D. Petes. 1996. The DNA-binding protein Hdf1p (a putative Ku homologue) is required for maintaining normal telomere length in Saccharomyces cerevisiae. *Nucleic Acids Res* **24**: 582-5.

Price, C.M. and T.R. Cech. 1987. Telomeric DNA-protein interactions of Oxytricha macronuclear DNA. *Genes Dev* **1**: 783-93.

Ramboarina, S., N. Morellet, M.C. Fournie-Zaluski, B.P. Roques, and N. Moreller. 1999. Structural investigation on the requirement of CCHH zinc finger type in nucleocapsid protein of human immunodeficiency virus 1. *Biochemistry* **38**: 9600-7.

Ramirez, R.D., C.P. Morales, B.S. Herbert, J.M. Rohde, C. Passons, J.W. Shay, and W.E. Wright. 2001. Putative telomere-independent mechanisms of replicative aging reflect inadequate growth conditions. *Genes Dev* **15**: 398-403.

Rappold, I., K. Iwabuchi, T. Date, and J. Chen. 2001. Tumor suppressor p53 binding protein 1 (53BP1) is involved in DNA damage-signaling pathways. *J Cell Biol* **153**: 613-20.

Reichenbach, P., M. Hoss, C.M. Azzalin, M. Nabholz, P. Bucher, and J. Lingner. 2003. A human homolog of yeast est1 associates with telomerase and uncaps chromosome ends when overexpressed. *Curr Biol* **13**: 568-74.

Ritchie, K.B., J.C. Mallory, and T.D. Petes. 1999. Interactions of TLC1 (which encodes the RNA subunit of telomerase), TEL1, and MEC1 in regulating telomere length in the yeast Saccharomyces cerevisiae. *Mol Cell Biol* **19**: 6065-75.

Ritchie, K.B. and T.D. Petes. 2000. The Mre11p/Rad50p/Xrs2p complex and the Tel1p function in a single pathway for telomere maintenance in yeast. *Genetics* **155**: 475-9.

Rogakou, E.P., C. Boon, C. Redon, and W.M. Bonner. 1999. Megabase chromatin domains involved in DNA double-strand breaks in vivo. *J Cell Biol* **146**: 905-16.

Rogakou, E.P., D.R. Pilch, A.H. Orr, V.S. Ivanova, and W.M. Bonner. 1998. DNA double-stranded breaks induce histone H2AX phosphorylation on serine 139. *J Biol Chem* **273**: 5858-68.

Samper, E., F.A. Goytisolo, J. Menissier-de Murcia, E. Gonzalez-Suarez, J.C. Cigudosa, G. de Murcia, and M.A. Blasco. 2001. Normal telomere length and chromosomal end capping in poly(ADP-ribose) polymerase-deficient mice and primary cells despite increased chromosomal instability. *J Cell Biol* **154**: 49-60.

Samper, E., F.A. Goytisolo, P. Slijepcevic, P.P. van Buul, and M.A. Blasco. 2000. Mammalian Ku86 protein prevents telomeric fusions independently of the length of TTAGGG repeats and the G-strand overhang. *EMBO Rep* **1**: 244-52.

Santoro, C., N. Mermod, P.C. Andrews, and R. Tjian. 1988. A family of human CCAAT-box-binding proteins active in transcription and DNA replication: cloning and expression of multiple cDNAs. *Nature* **334**: 218-24.

Savitsky, K., A. Bar-Shira, S. Gilad, G. Rotman, Y. Ziv, L. Vanagaite, D.A. Tagle, S. Smith, T. Uziel, S. Sfez, and et al. 1995. A single ataxia telangiectasia gene with a product similar to PI-3 kinase. *Science* **268**: 1749-53.

Sbodio, J.I., H.F. Lodish, and N.W. Chi. 2002. Tankyrase-2 oligomerizes with tankyrase-1 and binds to both TRF1 (telomere-repeat-binding factor 1) and IRAP (insulin-responsive aminopeptidase). *Biochem J* **361**: 451-9.

Schmelzle, T. and M.N. Hall. 2000. TOR, a central controller of cell growth. *Cell* **103**: 253-62.

Schultz, L.B., N.H. Chehab, A. Malikzay, and T.D. Halazonetis. 2000. p53 binding protein 1 (53BP1) is an early participant in the cellular response to DNA double-strand breaks. *J Cell Biol* **151**: 1381-90.

Scully, R., S.F. Anderson, D.M. Chao, W. Wei, L. Ye, R.A. Young, D.M. Livingston, and J.D. Parvin. 1997a. BRCA1 is a component of the RNA polymerase II holoenzyme. *Proc Natl Acad Sci U S A* **94**: 5605-10.

Scully, R., J. Chen, R.L. Ochs, K. Keegan, M. Hoekstra, J. Feunteun, and D.M. Livingston. 1997b. Dynamic changes of BRCA1 subnuclear location and phosphorylation state are initiated by DNA damage. *Cell* **90**: 425-35.

Scully, R., S. Ganesan, K. Vlasakova, J. Chen, M. Socolovsky, and D.M. Livingston. 1999. Genetic analysis of BRCA1 function in a defined tumor cell line. *Mol Cell* **4**: 1093-9.

Seger, Y.R., M. Garcia-Cao, S. Piccinin, C.L. Cunsolo, C. Doglioni, M.A. Blasco, G.J. Hannon, and R. Maestro. 2002. Transformation of normal human cells in the absence of telomerase activation. *Cancer Cell* **2**: 401-13.

Seimiya, H. and S. Smith. 2002. The telomeric poly(ADP-ribose) polymerase, tankyrase 1, contains multiple binding sites for telomeric repeat binding

factor 1 (TRF1) and a novel acceptor, 182-kDa tankyrase-binding protein (TAB182). *J Biol Chem* **277**: 14116-26.
Seto, A.G., A.J. Zaug, S.G. Sobel, S.L. Wolin, and T.R. Cech. 1999. Saccharomyces cerevisiae telomerase is an Sm small nuclear ribonucleoprotein particle. *Nature* **401**: 177-80.
Sharples, G.J. and D.R. Leach. 1995. Structural and functional similarities between the SbcCD proteins of Escherichia coli and the RAD50 and MRE11 (RAD32) recombination and repair proteins of yeast *Mol Microbiol* **17**: 1215-7.
Shay, J.W. 1997. Telomerase in human development and cancer. *J Cell Physiol* **173**: 266-70.
Shieh, S.Y., J. Ahn, K. Tamai, Y. Taya, and C. Prives. 2000. The human homologs of checkpoint kinases Chk1 and Cds1 (Chk2) phosphorylate p53 at multiple DNA damage-inducible sites. *Genes Dev* **14**: 289-300.
Shiloh, Y. 1995. Ataxia-telangiectasia: closer to unraveling the mystery. *Eur J Hum Genet* **3**: 116-38.
-. 2003. ATM and related protein kinases: safeguarding genome integrity. *Nat Rev Cancer* **3**: 155-68.
Shippen-Lentz, D. and E.H. Blackburn. 1990. Functional evidence for an RNA template in telomerase. *Science* **247**: 546-52.
Shore, D. and K. Nasmyth. 1987. Purification and cloning of a DNA binding protein from yeast that binds to both silencer and activator elements. *Cell* **51**: 721-32.
Siliciano, J.D., C.E. Canman, Y. Taya, K. Sakaguchi, E. Appella, and M.B. Kastan. 1997. DNA damage induces phosphorylation of the amino terminus of p53. *Genes Dev* **11**: 3471-81.
Singer, M.S. and D.E. Gottschling. 1994. TLC1: template RNA component of Saccharomyces cerevisiae telomerase *Science* **266**: 404-9.
Smith, S. and T. de Lange. 2000. Tankyrase promotes telomere elongation in human cells. *Curr Biol* **10**: 1299-302.
Smith, S., I. Giriat, A. Schmitt, and T. de Lange. 1998. Tankyrase, a poly(ADP-ribose) polymerase at human telomeres *Science* **282**: 1484-7.
Smogorzewska, A. and T. de Lange. 2002. Different telomere damage signaling pathways in human and mouse cells. *Embo J* **21**: 4338-48.
Smogorzewska, A., J. Karlseder, H. Holtgreve-Grez, A. Jauch, and T. de Lange. 2002. DNA Ligase IV-Dependent NHEJ of Deprotected Mammalian Telomeres in G1 and G2. *Curr Biol* **12**: 1635.
Smogorzewska, A., B. van Steensel, A. Bianchi, S. Oelmann, M.R. Schaefer, G. Schnapp, and T. de Lange. 2000. Control of human telomere length by TRF1 and TRF2. *Mol Cell Biol* **20**: 1659-68.

Snow, B.E., N. Erdmann, J. Cruickshank, H. Goldman, R.M. Gill, M.O. Robinson, and L. Harrington. 2003. Functional conservation of the telomerase protein est1p in humans. *Curr Biol* **13**: 698-704.

Sonoda, E., M.S. Sasaki, C. Morrison, Y. Yamaguchi-Iwai, M. Takata, and S. Takeda. 1999. Sister chromatid exchanges are mediated by homologous recombination in vertebrate cells. *Mol Cell Biol* **19**: 5166-9.

Spring, K., F. Ahangari, S.P. Scott, P. Waring, D.M. Purdie, P.C. Chen, K. Hourigan, J. Ramsay, P.J. McKinnon, M. Swift, and M.F. Lavin. 2002. Mice heterozygous for mutation in Atm, the gene involved in ataxia-telangiectasia, have heightened susceptibility to cancer. *Nat Genet* **32**: 185-90.

Stewart, G.S., R.S. Maser, T. Stankovic, D.A. Bressan, M.I. Kaplan, N.G. Jaspers, A. Raams, P.J. Byrd, J.H. Petrini, and A.M. Taylor. 1999. The DNA double-strand break repair gene hMRE11 is mutated in individuals with an ataxia-telangiectasia-like disorder. *Cell* **99**: 577-87.

Stewart, G.S., B. Wang, C.R. Bignell, A.M. Taylor, and S.J. Elledge. 2003. MDC1 is a mediator of the mammalian DNA damage checkpoint. *Nature* **421**: 961-6.

Summers, M.F. 1991. Zinc finger motif for single-stranded nucleic acids? Investigations by nuclear magnetic resonance. *J Cell Biochem* **45**: 41-8.

Swift, M., D. Morrell, R.B. Massey, and C.L. Chase. 1991. Incidence of cancer in 161 families affected by ataxia-telangiectasia. *N Engl J Med* **325**: 1831-6.

Taggart, A.K., S.C. Teng, and V.A. Zakian. 2002. Est1p as a cell cycle-regulated activator of telomere-bound telomerase. *Science* **297**: 1023-6.

Takai, H., A. Smogorzewska, and T. de Lange. 2003. DNA damage foci at dysfunctional telomeres. *Curr Biol* **13**: 1549-56.

Takao, N., H. Kato, R. Mori, C. Morrison, E. Sonada, X. Sun, H. Shimizu, K. Yoshioka, S. Takeda, and K. Yamamoto. 1999. Disruption of ATM in p53-null cells causes multiple functional abnormalities in cellular response to ionizing radiation. *Oncogene* **18**: 7002-9.

Takata, M., M.S. Sasaki, E. Sonoda, C. Morrison, M. Hashimoto, H. Utsumi, Y. Yamaguchi-Iwai, A. Shinohara, and S. Takeda. 1998. Homologous recombination and non-homologous end-joining pathways of DNA double-strand break repair have overlapping roles in the maintenance of chromosomal integrity in vertebrate cells. *Embo J* **17**: 5497-508.

Taylor, A.M., D.G. Harnden, C.F. Arlett, S.A. Harcourt, A.R. Lehmann, S. Stevens, and B.A. Bridges. 1975. Ataxia telangiectasia: a human mutation with abnormal radiation sensitivity. *Nature* **258**: 427-9.

Teng, S.C., J. Chang, B. McCowan, and V.A. Zakian. 2000. Telomerase-independent lengthening of yeast telomeres occurs by an abrupt Rad50p-dependent, Rif-inhibited recombinational process. *Mol Cell* **6**: 947-52.

Teng, S.C. and V.A. Zakian. 1999. Telomere-telomere recombination is an efficient bypass pathway for telomere maintenance in Saccharomyces cerevisiae. *Mol Cell Biol* **19**: 8083-93.

Thelen, M.P., C. Venclovas, and K. Fidelis. 1999. A sliding clamp model for the Rad1 family of cell cycle checkpoint proteins. *Cell* **96**: 769-70.

Tibbetts, R.S., K.M. Brumbaugh, J.M. Williams, J.N. Sarkaria, W.A. Cliby, S.Y. Shieh, Y. Taya, C. Prives, and R.T. Abraham. 1999. A role for ATR in the DNA damage-induced phosphorylation of p53. *Genes Dev* **13**: 152-7.

Tibbetts, R.S., D. Cortez, K.M. Brumbaugh, R. Scully, D. Livingston, S.J. Elledge, and R.T. Abraham. 2000. Functional interactions between BRCA1 and the checkpoint kinase ATR during genotoxic stress. *Genes Dev* **14**: 2989-3002.

Tomlinson, G.E., T.T. Chen, V.A. Stastny, A.K. Virmani, M.A. Spillman, V. Tonk, J.L. Blum, N.R. Schneider, Wistuba, II, J.W. Shay, J.D. Minna, and A.F. Gazdar. 1998. Characterization of a breast cancer cell line derived from a germ-line BRCA1 mutation carrier. *Cancer Res* **58**: 3237-42.

Trujillo, K.M., S.S. Yuan, E.Y. Lee, and P. Sung. 1998. Nuclease activities in a complex of human recombination and DNA repair factors Rad50, Mre11, and p95. *J Biol Chem* **273**: 21447-50.

Uziel, T., Y. Lerenthal, L. Moyal, Y. Andegeko, L. Mittelman, and Y. Shiloh. 2003. Requirement of the MRN complex for ATM activation by DNA damage. *Embo J* **22**: 5612-21.

van Gent, D.C., J.H. Hoeijmakers, and R. Kanaar. 2001. Chromosomal stability and the DNA double-stranded break connection. *Nat Rev Genet* **2**: 196-206.

van Steensel, B. and T. de Lange. 1997. Control of telomere length by the human telomeric protein TRF1 *Nature* **385**: 740-3.

van Steensel, B., A. Smogorzewska, and T. de Lange. 1998. TRF2 protects human telomeres from end-to-end fusions. *Cell* **92**: 401-13.

Varon, R., C. Vissinga, M. Platzer, K.M. Cerosaletti, K.H. Chrzanowska, K. Saar, G. Beckmann, E. Seemanova, P.R. Cooper, N.J. Nowak, M. Stumm, C.M. Weemaes, R.A. Gatti, R.K. Wilson, M. Digweed, A. Rosenthal, K. Sperling, P. Concannon, and A. Reis. 1998. Nibrin, a novel DNA double-strand break repair protein, is mutated in Nijmegen breakage syndrome. *Cell* **93**: 467-76.

Vaziri, H. and S. Benchimol. 1998. Reconstitution of telomerase activity in normal human cells leads to elongation of telomeres and extended replicative life span. *Curr Biol* **8**: 279-82.

Vignais, M.L., L.P. Woudt, G.M. Wassenaar, W.H. Mager, A. Sentenac, and R.J. Planta. 1987. Specific binding of TUF factor to upstream activation sites of yeast ribosomal protein genes. *Embo J* **6**: 1451-7.

Walter, J. and J. Newport. 2000. Initiation of eukaryotic DNA replication: origin unwinding and sequential chromatin association of Cdc45, RPA, and DNA polymerase alpha. *Mol Cell* **5**: 617-27.

Wang, B., S. Matsuoka, P.B. Carpenter, and S.J. Elledge. 2002. 53BP1, a mediator of the DNA damage checkpoint. *Science* **298**: 1435-8.

Wang, Y., D. Cortez, P. Yazdi, N. Neff, S.J. Elledge, and J. Qin. 2000. BASC, a super complex of BRCA1-associated proteins involved in the recognition and repair of aberrant DNA structures. *Genes Dev* **14**: 927-39.

Wang, Z.Q., B. Auer, L. Stingl, H. Berghammer, D. Haidacher, M. Schweiger, and E.F. Wagner. 1995. Mice lacking ADPRT and poly(ADP-ribosyl)ation develop normally but are susceptible to skin disease. *Genes Dev* **9**: 509-20.

Watson, J.D. 1972. Origin of concatemeric T7 DNA. *Nat New Biol* **239**: 197-201.

Weiffenbach, B. and J.E. Haber. 1981. Homothallic mating type switching generates lethal chromosome breaks in rad52 strains of Saccharomyces cerevisiae. *Mol Cell Biol* **1**: 522-34.

Wotton, D. and D. Shore. 1997. A novel Rap1p-interacting factor, Rif2p, cooperates with Rif1p to regulate telomere length in Saccharomyces cerevisiae. *Genes Dev* **11**: 748-60.

Wu, L.C., Z.W. Wang, J.T. Tsan, M.A. Spillman, A. Phung, X.L. Xu, M.C. Yang, L.Y. Hwang, A.M. Bowcock, and R. Baer. 1996. Identification of a RING protein that can interact in vivo with the BRCA1 gene product. *Nat Genet* **14**: 430-40.

Xu, B., S.T. Kim, D.S. Lim, and M.B. Kastan. 2002a. Two molecularly distinct G(2)/M checkpoints are induced by ionizing irradiation. *Mol Cell Biol* **22**: 1049-59.

Xu, B., A.H. O'Donnell, S.T. Kim, and M.B. Kastan. 2002b. Phosphorylation of serine 1387 in Brca1 is specifically required for the Atm-mediated S-phase checkpoint after ionizing irradiation. *Cancer Res* **62**: 4588-91.

Xu, X. and D.F. Stern. 2003. NFBD1/KIAA0170 is a chromatin-associated protein involved in DNA damage signaling pathways. *J Biol Chem* **278**: 8795-803.

Yamane, K., X. Wu, and J. Chen. 2002. A DNA Damage-Regulated BRCT-Containing Protein, TopBP1, Is Required for Cell Survival. *Mol Cell Biol* **22**: 555-66.

Yarden, R.I. and L.C. Brody. 1999. BRCA1 interacts with components of the histone deacetylase complex. *Proc Natl Acad Sci U S A* **96**: 4983-8.

Yeager, T.R., A.A. Neumann, A. Englezou, L.I. Huschtscha, J.R. Noble, and R.R. Reddel. 1999. Telomerase-negative immortalized human cells contain a novel type of promyelocytic leukemia (PML) body. *Cancer Res* **59**: 4175-9.

Yu, G.L., J.D. Bradley, L.D. Attardi, and E.H. Blackburn. 1990. In vivo alteration of telomere sequences and senescence caused by mutated Tetrahymena telomerase RNAs. *Nature* **344**: 126-32.

Zdzienicka, M.Z. 1999. Mammalian X-ray-sensitive mutants which are defective in non-homologous (illegitimate) DNA double-strand break repair. *Biochimie* **81**: 107-16.

Zhang, N., P. Chen, K.K. Khanna, S. Scott, M. Gatei, S. Kozlov, D. Watters, K. Spring, T. Yen, and M.F. Lavin. 1997. Isolation of full-length ATM cDNA and correction of the ataxia-telangiectasia cellular phenotype. *Proc Natl Acad Sci U S A* **94**: 8021-6.

Zhao, S., Y.C. Weng, S.S. Yuan, Y.T. Lin, H.C. Hsu, S.C. Lin, E. Gerbino, M.H. Song, M.Z. Zdzienicka, R.A. Gatti, J.W. Shay, Y. Ziv, Y. Shiloh, and E.Y. Lee. 2000. Functional link between ataxia-telangiectasia and Nijmegen breakage syndrome gene products. *Nature* **405**: 473-7.

Zhong, Q., C.F. Chen, S. Li, Y. Chen, C.C. Wang, J. Xiao, P.L. Chen, Z.D. Sharp, and W.H. Lee. 1999. Association of BRCA1 with the hRad50-hMre11-p95 complex and the DNA damage response *Science* **285**: 747-50.

Zhou, B.B. and S.J. Elledge. 2000. The DNA damage response: putting checkpoints in perspective. *Nature* **408**: 433-9.

Zhou, X.Z. and K.P. Lu. 2001. The Pin2/TRF1-Interacting Protein PinX1 Is a Potent Telomerase Inhibitor. *Cell* **107**: 347-59.

Zhu, X.D., B. Kuster, M. Mann, J.H. Petrini, and T. de Lange. 2000. Cell-cycle-regulated association of RAD50/MRE11/NBS1 with TRF2 and human telomeres. *Nat Genet* **25**: 347-52.

Ziv, Y., A. Bar-Shira, I. Pecker, P. Russell, T.J. Jorgensen, I. Tsarfati, and Y. Shiloh. 1997. Recombinant ATM protein complements the cellular A-T phenotype. *Oncogene* **15**: 159-67.

Zou, L. and S.J. Elledge. 2003. Sensing DNA damage through ATRIP recognition of RPA-ssDNA complexes. *Science* **300**: 1542-8.